

THESIS

INVESTIGATION OF TEMPERATURE EFFECTS ON SUBSURFACE ATTENUATION  
OF NITROAROMATIC COMPOUNDS

Submitted by

Zoe Elizabeth Bezold

Department of Civil and Environmental Engineering

In partial fulfillment of the requirements

For the Degree of Master of Science

Colorado State University

Fort Collins, Colorado

Spring 2015

Master's Committee:

Advisor: Jens Blotevogel

Co-advisor: Susan De Long

Michael Ronayne

Copyright by Zoe Elizabeth Bezold 2015

All Rights Reserved

## ABSTRACT

### INVESTIGATION OF TEMPERATURE EFFECTS ON SUBSURFACE ATTENUATION OF NITROAROMATIC COMPOUNDS

Inadvertent releases of nitroaromatic compounds (NACs) during the production of dyes, explosives, and pesticides have led to soil and groundwater contamination at a chemical production facility in New Jersey. Elevated carbon dioxide fluxes and depleted  $^{14}\text{C}$  content were observed in the contaminated area compared to a background area, indicating that anthropogenic organic contaminants were degrading under natural site conditions. Recent research at Colorado State University has shown that maintaining soil temperatures  $\sim 5^\circ\text{C}$  above natural site conditions substantially increases rates of anaerobic petroleum hydrocarbon degradation. The overarching goal of this research is to determine whether thermal enhancement might increase attenuation rates of NACs under otherwise natural conditions at the contaminated site.

Detailed depth-resolved site characterization was performed to elucidate current biogeochemical processes. While nitronaphthalene dominated the nonaqueous phase contamination at concentrations up to 47,500 mg/kg, major aqueous contaminants were the more water-soluble 1,3-dinitrobenzene (up to 216 mg/L), 2,4-dinitrotoluene (up to 163 mg/L), and 1,2-chloronitrobenzene (up to 91 mg/L). Comparison of organic carbon in detected contaminants with total organic carbon revealed that there were no other organic contaminants at relevant concentrations in the contaminated area, indicating that the increased  $\text{CO}_2$  fluxes were due to mineralization of NACs under natural conditions. The presence of nitroaniline and chloroaniline throughout the entire depth of the shallow aquifer ( $\sim 3\text{-}24$  ft bgs) in aqueous samples suggested

partial degradation of NACs through reduction of the nitro group, given there are no upstream sources for the anilines. For nitronaphthalene and nitrated toluenes, no degradation products were detected.

Microbial diversity analysis revealed that the contaminated transmissive zone was dominated by *Pseudomonas stutzeri*, a facultative aerobe that has been shown to degrade a variety of monoaromatic compounds including chloronitrobenzene and chlorobenzene. At abundances of up to 83%, it appears likely that *P. stutzeri* plays a key role in the biodegradation of NACs at the site. The dominance of a nitrate-reducing microbial species, *P. stutzeri*, and depleted nitrate concentrations suggested that natural degradation processes at the site are limited by electron acceptor availability. Further degradation and mineralization of aniline intermediates, however, may require aerobic conditions. Thus, the aniline compounds may persist under natural conditions or irreversibly sorb to natural organic matter as long as sorption sites are available.

To determine the effect of temperature on biodegradation rates, anaerobic microcosms containing homogenized site soil were held at temperatures between 10-30 °C for 350 days. Concentrations of the minor contaminants toluene, xylene, ethylbenzene, and chlorobenzene were significantly depleted. The extent of their degradation along with generated gas volumes suggested a temperature maximum of stimulation around 18-22 °C. In contrast to field observations, reduced organic intermediates of NAC degradation were not detected. However, a slight increase in ammonia was observed, potentially due to slow degradation of NACs. The inability to recreate field degradation rates may likely be attributed to soil sampling and/or homogenization, eliminating favorable biogeochemical zones for site microorganisms.

In summary, degradation of select organic contaminants at the site is occurring under natural anaerobic conditions, and may be stimulated by a slight increase in temperature to ~20 °C. However, complete NAC mineralization will likely require oxygen delivery. As a path forward, an aerobic microcosm study is proposed to assess the potential for biodegradation. A subsequent biosparging pilot test, in which subsurface temperatures can be passively raised using gas-permeable surface insulation, may prove the feasibility of this technology for site remediation. Furthermore, consideration should be given to further analysis of subsurface temperature data to resolve natural rates of contaminant degradation in source zones.

## ACKNOWLEDGEMENTS

I would especially like to thank Dr. Jens Blotevogel, Dr. Susan De Long, and Dr. Tom Sale for their advice and support throughout this study. I was lucky to have the opportunity to work with such knowledgeable and experienced individuals, and I am grateful to have learned so much from them. I would also like to thank Dr. Mike Ronayne for acting as an outside committee member and providing additional insight and feedback into this study. I would like to thank URS Corporation, especially Kathy West and Don Layman for collecting field samples. Maria Irianni Renno, Saeed Kiaalhosseini, and Gary Dick provided a great deal of help in the lab and field. I cannot thank them enough for their patience and willingness to share their knowledge. Thank you to all the members of the Center for Contaminant Hydrology. I am blessed to have gotten to work with such a great group of people.

I would also like to acknowledge the support of my family and friends throughout this process. I would like to thank my parents and brother for helping and encouraging me in all of my endeavors. I would also like to thank Kayla Ranney, Jill Vandegrift, and Sarah Eberhart for their friendship and support throughout graduate school.

This research was supported by E. I. du Pont de Nemours and Company as well as by the University Consortium for Field-Focused Groundwater Contamination Research. Thank you to Ed Lutz and Ed Seger for their insight and support.

## TABLE OF CONTENTS

Abstract .....	ii
Acknowledgements .....	v
Table of Contents .....	vi
List of Tables .....	x
List of Figures .....	xii
1. Literature Review .....	1
1.1 Background and Motivation .....	1
1.2 Objectives .....	1
1.3 Organization and Content .....	2
2. Literature Review .....	3
2.1 Definition of Nitroaromatic Compounds .....	3
2.2 Fate and Transport in Subsurface .....	4
2.3 Biotic Degradation .....	7
2.3.1 Nitrobenzene Degraders and Pathways .....	8
2.3.2 Nitrotoluene Degraders and Pathways .....	10
2.3.3 Dinitrotoluene Degraders and Pathways .....	11
2.3.4 Chlorinated Nitroaromatic Compound Degraders and Pathways .....	12
2.3.5 Biodegradation Kinetics .....	14

2.3.6 Effect of Temperature on Biodegradation Rates .....	15
2.4 Sorption.....	16
2.4.1 Sorption Behavior of Nitroaromatic Compounds .....	17
2.4.2 Sorption Behavior of Aromatic Amines .....	18
2.5 Remediation Approaches .....	18
2.5.1 Ex situ Treatment Techniques .....	19
2.5.2 In situ Treatment Techniques.....	19
2.5.3 Proposed Treatment: Thermal Enhancement.....	22
3. Field Studies.....	23
3.1 Introduction.....	23
3.2 Methods.....	23
3.2.1 Site Description.....	24
3.2.2 Estimating Carbon Fluxes .....	27
3.2.3 Macrocore Sampling .....	29
3.2.4 Multilevel Sampling.....	33
3.3 Results.....	38
3.3.1 Estimated Carbon Fluxes .....	38
3.3.2 Water Table Measurements .....	39
3.3.3 Macrocore Sampling .....	39
3.3.4 Multilevel Sampling.....	47

3.4 Discussion .....	54
3.4.1 Estimated CO <sub>2</sub> Fluxes .....	54
3.4.2 Biogeochemical Characterization with Depth .....	54
3.4.3 Impedance with Depth .....	64
4. Anaerobic Microcosm Study .....	66
4.1 Introduction.....	66
4.2 Methods.....	66
4.2.1 Microcosm Set-up.....	66
4.2.2 Contaminant Concentration Analysis .....	68
4.2.3 Microbial Analysis.....	69
4.2.4 Gas Sampling Procedures .....	69
4.2.5 Soil Analyses .....	70
4.3 Results.....	71
4.4 Discussion.....	78
5. Summary and Conclusions .....	83
6. Site Conceptual Model.....	88
7. Future work .....	91
7.1 Additional Site Characterization.....	91
7.2 Effect of Aerobic Conditions .....	93
7.2.1 Aerobic Microcosm Studies.....	94

7.2.2 Biosparging .....	94
7.3 Temperature Modeling & Enhancement.....	96
7.3.1 Thermal Signature Modeling.....	96
7.3.2 Temperature Enhancement with Gas Permeable Insulation .....	96
8. References.....	98
Appendix A: Calibration.....	109
A.1 Contaminant Calibration Curves.....	109
A.2 Determining Limit of Detection and Quantification.....	115
Appendix B: Field Studies Supplementary Information.....	117
B.1 Soil Core Recovery .....	117
B.2 Aqueous Contaminant Concentrations.....	118
B.3 Water Quality Analysis .....	125
B.4 Average Monthly Temperature .....	129
Appendix C: Microcosm Study Supplementary Information .....	130
C.1 Microcosm Soil Analysis .....	130
C.2 Microcosm Concentrations .....	131
Appendix D: Microbial Analysis Methodology .....	133

LIST OF TABLES

Table 1- Chemical formulae, molecular structures, and properties of major NACs found at the investigated site..... 3

Table 2- First order biodegradation rate constants ..... 14

Table 3- CO<sub>2</sub> fluxes ..... 38

Table 4- Water table fluctuations..... 39

Table 5- Contaminants detected in the soil core, their maximum concentrations, and depths of maximum concentrations..... 42

Table 6- Detected dissolved contaminants in groundwater samples, their maximum concentrations, and depths of maximum concentration..... 48

Table 7- Geology, temperature, contaminant concentrations, and possible degradation byproducts with depth..... 56

Table 8- Electron acceptors and microbial characterization with depth..... 57

Table 9- Average concentrations of detected contaminants in the soil core used for the microcosm study..... 72

Table 10- Limits of detection and quantification..... 116

Table 11- Recovery from macrocore sampling ..... 117

Table 12- Water quality analysis of samples taken on January 15, 2014..... 125

Table 13- Cation concentrations in water samples taken on January 15, 2014 ..... 125

Table 14- Anion concentrations in water samples taken on January 14, 2014..... 126

Table 15- Water quality analysis of samples taken on April 8, 2014 ..... 126

Table 16- Cation concentrations in water samples taken on April 8, 2014 ..... 127

Table 17- Anion concentrations in water samples taken on April 8, 2014.....	127
Table 18- Water quality analysis of samples taken on August 6, 2014.....	128
Table 19- Cation concentrations in water samples taken on August 6, 2014.....	128
Table 20- Anion concentrations in water samples taken on August 6, 2014.....	129
Table 21- Microcosm soil analysis .....	130
Table 22- Percent carbon and nitrogen of soil microcosm .....	130

LIST OF FIGURES

Figure 1 – DNAPL spill in the subsurface modified from Parkow and Cherry (1996)..... 5

Figure 2 – Aerobic degradation pathway of nitrobenzene by *Pseudomonas pseudoalcaligenes* JS45 adapted from Ju & Parales (2010)..... 9

Figure 3 – Degradation pathway of nitrobenzene by *Acidovorax* sp. strain JS42 adapted from Ju & Parales (2010). ..... 11

Figure 4 – Degradation pathway of 2-chloronitrobenzene by *Pseudomonas stutzeri* ZWLR2-1 adapted from Liu et al. (2011). ..... 13

Figure 5 – Aniline and nitrobenzene biodegradation rates (Liu et al., 2013) ..... 16

Figure 6 – Aerial view of the contaminated area (URS, 2013). ..... 24

Figure 7 – Chlorobenzene total mass (Stone Environmental Inc., 2011) ..... 25

Figure 8 – Chlorobenzene concentrations and observed NAPL along Transect 5 (Stone Environmental Inc., 2011) ..... 26

Figure 9 – Site stratigraphy (Stone Environmental Inc., 2011) ..... 27

Figure 10 – Water quality sampling port and thermocouple. .... 34

Figure 11 – Electrode for impedance measurements. .... 34

Figure 12 – Schematic of multilevel sampler. .... 36

Figure 13 – Geology with depth ..... 40

Figure 14 – Contaminant concentration in the soil core as a function of depth. .... 43

Figure 15 – Abundance of bacterial 16S rRNA genes and bacterial diversity analysis ..... 44

Figure 16 – Abundance of archaeal 16S rRNA genes and archaeal diversity analysis ..... 45

Figure 17 – Aqueous contaminant concentrations sampled on August 6, 2014. .... 49

Figure 18 – pH and ORP (SHE) measurements with depth.....	50
Figure 19 – Concentrations of electron acceptors with depth.....	51
Figure 20 – Groundwater temperature with depth over 9 months.....	52
Figure 21 – Impedance measurements with depth .....	53
Figure 22 – Microcosm set up modeled after Zeman et al. (2012).....	67
Figure 23 – Contaminant concentrations of ethylbenzene, 2-xylene, toluene and chlorobenzene before and after treatment.....	73
Figure 24 – Contaminant concentrations before and after treatment of 1,4-dichlorobenzene, naphthalene, 2,4-dinitrotoluene, and nitronaphthalene. ....	74
Figure 25 –Contaminant concentrations of 1,3-dinitrobenzene and 1,4-chloronitrobenzene before and after treatment.....	75
Figure 26 – Ammonia, nitrate, and sulfate concentrations in microcosms.....	76
Figure 27 – Total average cumulative gas volume produced by soil microcosms over the duration of the experiment.....	77
Figure 28 – Initial microbial analysis of the homogenized soil core used in microcosms. ....	78
Figure 29 – Site conceptual model.....	90
Figure 30 – Calibration curves for nitrobenzene 1,2-dinitrobenzene, 1,3-dinitrobenzene, and 1,3- chloronitrobenzene .....	109
Figure 31 – Calibration curves for 1,4-chloronitrobenzene, chlorobenzene, 1,2-dichlorobenzene, and 1,4-dichlorobenzene .....	110
Figure 32 – Calibration curves for 2-nitrotoluene, 3-nitrotoluene, 4-nitrotoluene, and 2,4- dinitrotoluene.....	111
Figure 33 – Calibration curves for 2,6-dinitrotoluene, toluene, ethylbenzene, and 2-xylene.....	112

Figure 34 – Calibration curves for naphthalene, nitronaphthalene, aniline, and 3-nitroaniline .	113
Figure 35 – Calibration curves for 2-chloroaniline and 4-chloroaniline .....	114
Figure 36 – Aqueous concentrations of nitrobenzene, 1,2-dinitrobenzene, 1,3-dinitrobenzene, and 1,2-chloronitrobenzene.....	118
Figure 37 – Aqueous concentrations of 1,4-chloronitrobenzene, chlorobenzene, 1,2- dichlorobenzene, and 1,4-dichlorobenzene .....	119
Figure 38 – Aqueous concentrations of 2-nitrotoluene, 3-nitrotoluene, 4-nitrotoluene, and 2,4- dinitrotoluene.....	120
Figure 39 – Aqueous concentrations of 2,6-dinitrotoluene, toluene, aniline, 3-nitroaniline .....	121
Figure 40 – Aqueous concentrations of 2-chloroaniline, 4-chloroaniline, naphthalene, and nitronaphthalene .....	122
Figure 41 – Aqueous contaminant concentrations on January 15, 2014. ....	123
Figure 42 – Aqueous contaminant concentrations April 8, 2014. ....	124
Figure 43 – Average monthly temperature with depth. ....	129
Figure 44 – Contaminant concentrations of nitrobenzene, 1,2-dinitrobenzene, 1,2- dichlorobenzene, and 1,2-chloronitrobenzene before and after treatment. ....	131
Figure 45 – Contaminant concentrations before and after treatment of 2-nitrotoluene, 3- nitrotoluene, 4-nitrotoluene, and 2,6-dinitrotoluene. ....	132

# 1. LITERATURE REVIEW

## 1.1 Background and Motivation

Historical industrial practices have led to inadvertent releases of chemical contaminants into shallow subsurface media. Due to human health and ecological risks associated with many of these contaminants, active remediation may be needed to mitigate risks when natural attenuation processes alone are insufficient. After subsurface contamination has occurred, *in situ* remediation strategies are often the most cost-effective options. Bioremediation has emerged as an effective remediation strategy for many types of contaminants (Kang, 2014). Bioremediation uses techniques such as bioaugmentation and/or delivery of electron acceptors or donors to stimulate microbial activity and increase degradation rates (Caliman et al., 2011).

Zeman et al. (2012) and McCoy et al. (2014) showed that petroleum hydrocarbon biodegradation rates increased above temperatures of 22°C (i.e., 5°C above natural site conditions) and that a shift in microbial communities occurred. Based on this research, Colorado State University has developed a bioremediation technology, Sustainable Thermally Enhanced LNAPL Attenuation (STELA) that involves placing heating elements into the subsurface to elevate temperature and stimulate biodegradation. While the treatment has been successful with petroleum hydrocarbons in laboratory studies, it is unclear whether the treatment would be effective for other contaminants such as nitroaromatic compounds (NACs) or chlorinated solvents.

## 1.2 Objectives

The overarching goal of this study is to determine if thermal enhancement would be an appropriate remediation strategy for a chemical manufacturing facility, at which accidental

release of NACs and other aromatic compounds have occurred. The specific objectives of this study are the following: (1) to develop a depth-resolved characterization of contaminant concentrations and biogeochemical parameters to provide a baseline for a potential field pilot test and (2) to determine whether thermal enhancement is a viable treatment approach for the organic contaminants present at the site.

### **1.3 Organization and Content**

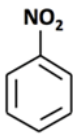
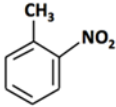
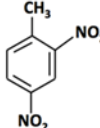
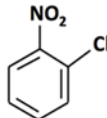
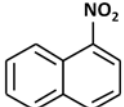
The following document is divided into six chapters. Chapter 2 presents previous research on nitroaromatic compounds focusing on their transport and fate within the subsurface and current remediation techniques. Chapter 3 contains a detailed description of field methods, results, and discussion of important findings. Chapter 4 describes methods, results, and conclusions from the microcosm experiment. Chapter 5 includes conclusions from the field and laboratory studies. Suggestions for future studies are outlined in detail in Chapter 6. The appendices include calibration data and supplemental results from laboratory and field studies.

## 2. LITERATURE REVIEW

### 2.1 Definition of Nitroaromatic Compounds

Nitroaromatic compounds consist of one or more nitro (-NO<sub>2</sub>) groups attached to one or more aromatic rings (Ju & Parales, 2010). These compounds are used primarily in the production of dyes, pesticides, pharmaceuticals, and explosives (Ye et al., 2004). Examples of NACs relevant to the study, their structure, and physical/chemical properties are provided in Table 1 (HDSB, 2014).

Table 1- Chemical formulae, molecular structures, and properties of major NACs found at the investigated site.

Compound	Formula	Structure	Physical/Chemical Properties
Nitrobenzene	C <sub>6</sub> H <sub>5</sub> NO <sub>2</sub>		Molecular Weight: 123.11 g/mol Water Solubility: 2.09 g/L @ 25°C Vapor Pressure: 0.245 mm Hg @ 25°C K <sub>oc</sub> : 30.6-370 L/kg K <sub>H</sub> =2.40(10 <sup>-5</sup> ) atm·m <sup>3</sup> /mol @ 25°C
2-Nitrotoluene	C <sub>7</sub> H <sub>7</sub> NO <sub>2</sub>		Molecular Weight: 137.14 g/mol Water Solubility: 609 mg/L @ 20°C Vapor Pressure: 0.185 mmHg @ 25°C K <sub>oc</sub> : 370 L/kg K <sub>H</sub> =1.25(10 <sup>-5</sup> ) atm·m <sup>3</sup> /mole @ 25°C
2,4-Dinitrotoluene	C <sub>7</sub> H <sub>6</sub> N <sub>2</sub> O <sub>4</sub>		Molecular Weight: 182.14 g/mol Water Solubility: 270 mg/L @ 22°C Vapor Pressure: 0.000147 mm Hg @ 22°C K <sub>oc</sub> : 57-2000 L/kg K <sub>H</sub> =5.40(10 <sup>-8</sup> ) atm·m <sup>3</sup> /mole @ 25°C
1-Chloro-2-nitrobenzene	C <sub>6</sub> H <sub>4</sub> ClNO <sub>2</sub>		Molecular Weight: 157.55 g/mol Water Solubility: 441 mg/L @ 25°C Vapor Pressure: 0.018 mm Hg @ 25°C K <sub>oc</sub> : 316 L/kg K <sub>H</sub> =9.3(10 <sup>-6</sup> ) atm·m <sup>3</sup> /mole @ 25°C
1-Nitronaphthalene	C <sub>10</sub> H <sub>7</sub> NO <sub>2</sub>		Molecular Weight: 173.17 g/mol Water Solubility: 9.81 mg/L @ 25°C Vapor Pressure: 0.00048 mm Hg @ 25°C K <sub>oc</sub> : 1295 L/kg K <sub>H</sub> = 1.76(10 <sup>-6</sup> ) atm·m <sup>3</sup> /mole @ 25°C

Accidental releases of NACs from industry and munitions storage as well as the application of pesticides have led to the presence of NACs in the subsurface (Ju & Parales, 2010). NACs may pose human health risks because of their toxicity and mutagenicity (Mason et al., 1985; Gong et al., 2001). Nitrobenzene and dinitrotoluene are included on the EPA's list of priority pollutants (EPA, 1999). Due to their potential human health risks, it is important to understand their transport and fate within the subsurface. Furthermore, knowledge of compound specific transport and fate is central to design and implementation of treatment remedies.

## **2.2 Fate and Transport in Subsurface**

Liquid NACs are denser than water and therefore are classified as dense nonaqueous phase liquids (DNAPLs). When DNAPLs enter the subsurface, they are driven downwards by gravity until they reach a capillary barrier such as clay or bedrock, where they may form pools. Regions around DNAPL bodies are often anaerobic due to the low solubility of oxygen and the oxygen demand exerted by released contaminants (Field et al., 1995). A conceptual diagram of a DNAPL release is provided in Figure 1.

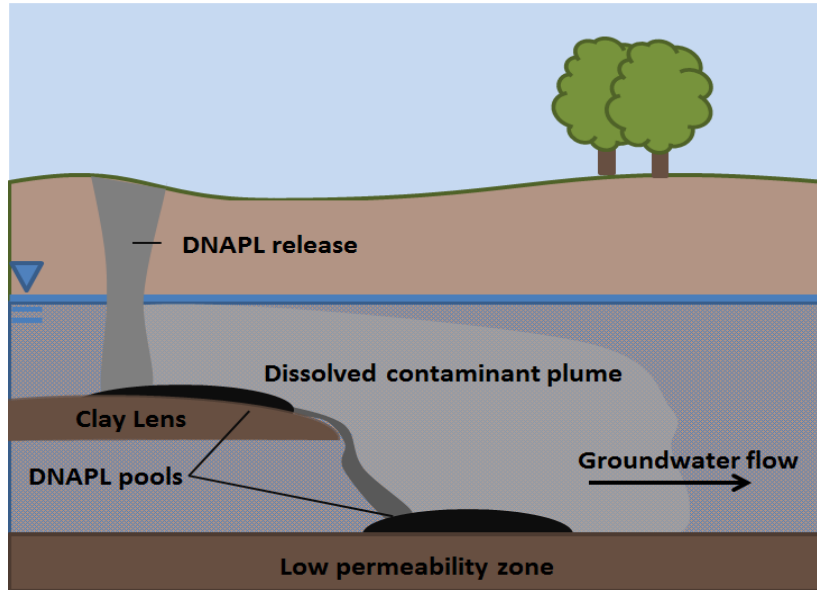


Figure 1 – DNAPL spill in the subsurface modified from Pankow and Cherry (1996).

In the subsurface, contaminants partition between aqueous, gaseous, sorbed, and NAPL phases. The following physical relationships describe partitioning processes. In all cases, the activity of aqueous and gas phase constituents is assumed to be 1. The conceptual model employed is that water is the wetting phase on the solids, DNAPL is either an intermediate wetting phase (when gases are present) or non-wetting, and gases are always a non-wetting phase. Given this arrangement, NAPL can directly partition into the aqueous and gaseous phases. If the NAPL contains several different contaminants, the aqueous concentration of one compound can be determined using a modified form of Raoult's law,

$$C_{aq_i} = C_{aq_i}^{\circ} x_i \quad [\text{Eq. 1}]$$

where  $C_{aq_i}$  is the aqueous concentration of a compound (mg/L),  $C_{aq_i}^{\circ}$  is the solubility of the pure compound (mg/L), and  $x_i$  is the mole fraction of the contaminant present in the NAPL.

Partitioning of NAPL into the gaseous phase also is described by Raoult's Law and can be expressed as

$$C_{gas_i} = \frac{P_v}{RT} x_i \quad [\text{Eq. 2}]$$

where  $C_{gas_i}$  is the contaminant concentration in the gaseous phase (mg/L),  $P_v$  is the vapor pressure of the contaminant (Pa),  $R$  is the universal gas constant (J/mol·°K), and  $T$  is temperature (°K). Contaminants also can enter the gaseous phase by partitioning from the aqueous phase. Henry's Law (Eq. 3) describes partitioning between the gaseous and aqueous phases and can be written as

$$C_{gas_i} = K_H C_{aq_i} \quad [\text{Eq. 3}]$$

where  $K_H$  is the dimensionless Henry's constant.

From the aqueous phase, compounds may sorb to the soil matrix. The amount sorbed can be described by a linear sorption isotherm equation such as

$$\omega_{sorbed_i} = f_{oc} K_{oc} C_{aq_i} \quad [\text{Eq. 4}]$$

where  $\omega_{sorbed_i}$  is the concentration of sorbed contaminant (mg/kg),  $f_{oc}$  is the fraction of organic carbon, and  $K_{oc}$  is the organic carbon-water partition coefficient (L/kg).

Understanding how compounds partition between DNAPL, water, air, and solids is needed when designing remediation system. Depending on the chemical properties of the compound, the contaminant may be more concentrated in one phase and could require different treatments to effectively limit contaminant concentration. Volatile compounds with high Henry's constants

partition into the gaseous phase and may cause vapor intrusion in buildings at grade. Singly nitrated compounds such as nitrobenzene, 2-nitrotoluene, 1,2-chloronitrobenzene, and nitronaphthalene would not be expected to volatilize based on their low Henry's constant. Soluble compounds like nitrobenzene partition into the aqueous phase where biodegradation or transport may occur. However, less soluble compounds like nitronaphthalene may be difficult to degrade since a limited amount is available in the aqueous phase. Sorption may provide a contaminant sink and prevent contaminants from impacting groundwater sources. Nitronaphthalene has a high  $K_{oc}$  value, which would limit mobility by binding the contaminant to the soil matrix. However, if reversible sorption occurs, contaminants may desorb back into the aqueous phase if aqueous concentrations are lower than equilibrium concentrations.

### **2.3 Biotic Degradation**

Evolution has led to microorganisms developing a wide variety of enzymes capable of degrading organic contaminants through numerous catalytic mechanisms (Dua et al., 2002). Organic compounds can provide a carbon source (electron donor) or assist in respiration by acting as an electron acceptor under anoxic conditions. Biodegradation pathways vary in the degree of transformation of the parent compound. Mineralization occurs when the microorganisms completely transform an organic compound into carbon dioxide, methane, or other inorganic products. If microbial processes simply transform an organic compound into another organic compound, (incomplete) biotransformation has occurred. Biotransformation may result in the formation of less or more toxic degradation products. The toxicity of reaction intermediates is an important concern when designing bioremediation treatments. Bioremediation may not be an effective remediation strategy if biotransformation leads to the accumulation of toxic products.

Several microorganisms have been observed to degrade NACs under a variety of subsurface conditions. However, because of the electron withdrawing (electronegative) nature of the nitro group, NACs and their amine daughter products can be very recalcitrant (Ye et al., 2004). Electron withdrawing groups (ie nitro, azo, and chloro) are resistant to electrophilic attack by oxygenases, but reduction of the nitro group is favorable under anaerobic conditions (Rieger & Knackmuss, 1995). The reduced compound is resistant to further reductive attack due to the electron donating nature of the amine group (McCormick et al., 1976). In many cases, complete mineralization of NACs has been observed under aerobic conditions (reviewed by Ye et al., 2004). The following section identifies specific microbial degraders of different types of NACs. Their degradation pathways and mechanisms are discussed.

### ***2.3.1 Nitrobenzene Degraders and Pathways***

Under anaerobic conditions, nitrobenzene is reduced to aniline (Hallas & Alexander, 1983; Dickel et al., 1993; Peres et al., 1998; Wang et al., 2009). A few microorganisms have been discovered to degrade aniline in anaerobic and aerobic environments. Under sulfate-reducing conditions, *Desulfobacterium anilini* degrades aniline by a carboxylation step followed by deamination to form benzoyl-CoA (Schnell & Schink, 1991). Benzoyl-CoA is further degraded to acetyl-CoA. Degradation of aniline has been observed under denitrifying conditions as well (Swindoll et al., 1993; De et al., 1994; Kahng et al., 2000). However, microorganisms that degrade aniline under anaerobic conditions are not prevalent (Nishino et al., 2000b). If the reduced product is transported into an aerobic zone, it may be further degraded by a dioxygenase attack leading to deamination and release of ammonia (Aoki et al., 1983; Bachofer et al., 1974). Several species of different genera including *Achromobacter*, *Comamomas*, *Pseudomonas*, and *Rhodococcus*, have been identified to degrade aniline under aerobic conditions and are more

abundant than anaerobic aniline degraders (Aoki et al., 1983; Bachofer et al., 1974; Boon et al., 2000; Kahng et al., 2000; Nishino et al., 2000b; Tanaka et al., 2009).

Under aerobic conditions, *Pseudomonas pseudoalcaligenes* JS45 has been found to mineralize nitrobenzene and follow a partially reductive pathway as shown in Figure 2 (Nishino & Spain, 1993). JS45 initially uses nitrobenzene reductase to reduce nitrobenzene to hydroxylaminobenzene (Nishino & Spain, 1993). A mutase then repositions the hydroxyl groups to form 2-aminophenol (Davis et al., 2000). The benzene ring is broken by 2-aminophenol-1,6-dioxygenase, and 2-aminomuconic semialdehyde is formed. 2-aminomuconic semialdehyde is oxidized and deaminated to form 4-oxalocrotonate. The degradation product undergoes decarboxylation and hydrolysis to become 4-hydroxy-2-oxovalerate. An aldolase cleaves 4-hydroxy-2-oxovalerate into acetaldehyde and pyruvate (He & Spain, 1997; He et al., 1998; He & Spain, 1998). These products are further oxidized in the tricarboxylic acid cycle (TCA cycle) and used to generate ATP (Ju & Parales, 2010).

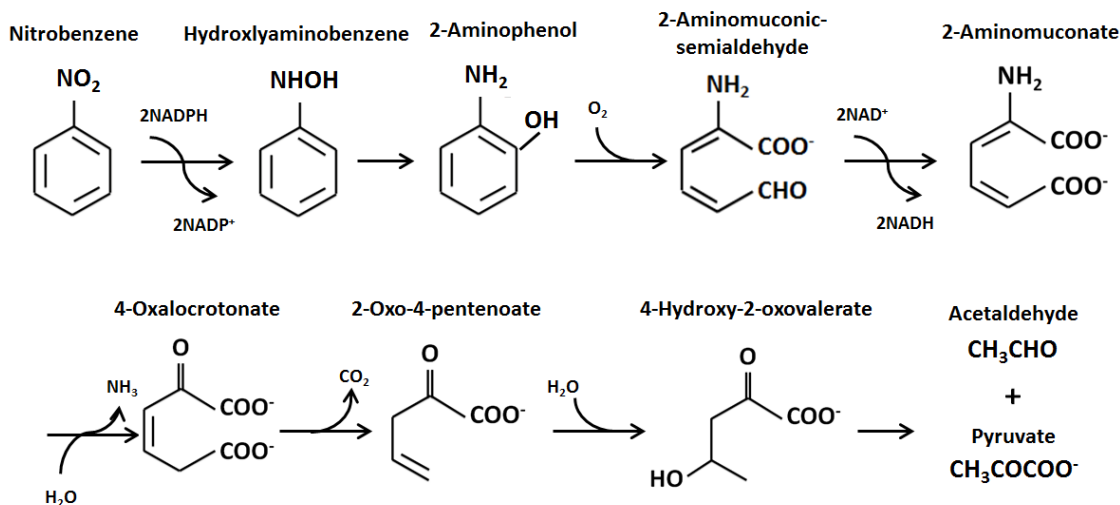


Figure 2 – Aerobic degradation pathway of nitrobenzene by *Pseudomonas pseudoalcaligenes* JS45 adapted from Ju & Parales (2010).

*Pseudomonas* sp. strain HS12 (Park et al., 1999; Park & Kim, 2000), *Pseudomonas* sp. strain AP-3 (Takenaka et al., 1997), and *Comamonas* sp. strain CNB-1 (Wu et al., 2006) are also known nitrobenzene degraders which follow degradation pathways similar to the pathway for JS45 (Ju & Parales, 2010). For the AP-3 strain, when 2-oxo-4-pentenoate is formed, deamination occurs before decarboxylation. *Streptomyces* sp. strain Z2 has also been found to degrade nitrobenzene as well as 2-aminophenol through a reductive pathway (Zheng et al., 2007). *Comamonas* sp. strain JS765 uses a fully oxidative pathway (Nishino & Spain, 1995), in which nitrobenzene dioxygenase oxidizes nitrobenzene leading to the formation of catechol and the release of nitrite (Lessner et al., 2002). Catechol then undergoes *meta* ring cleavage to form acetaldehyde and pyruvate (Nishino & Spain, 1995).

### ***2.3.2 Nitrotoluene Degradation Pathways***

*Acidovorax* sp. strain JS42 is the only known strain capable of mineralizing 2-nitrotoluene (Haigler et al., 1994). As shown in Figure 3, JS42 follows an oxidative pathway where 2-nitrotoluene dioxygenase transforms 2-nitrotoluene into nitrohydrodiol by oxidizing the 2 and 3 positions (Parales et al., 1996; Parales et al., 1998; Parales et al., 2005). Due to the instability of nitrohydrodiol, it spontaneously transforms into 3-methylcatechol, and nitrite is released. A standard *meta*-cleavage then occurs breaking the compounds into TCA cycle intermediates (Haigler & Spain, 1994).

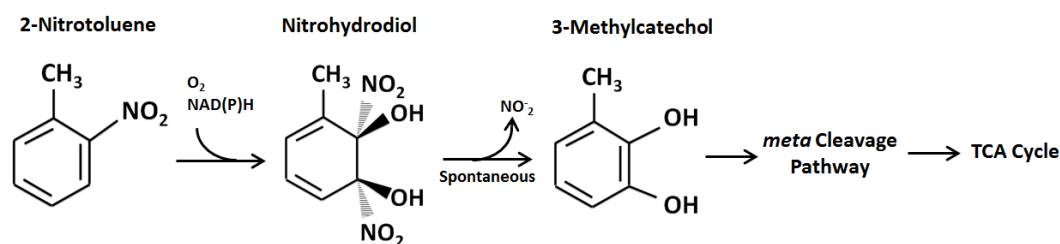


Figure 3 – Degradation pathway of nitrobenzene by *Acidovorax* sp. strain JS42 adapted from Ju & Parales (2010).

*Comamonas* sp. strain JS765 can mineralize 3-nitrotoluene in addition to nitrobenzene (Lessner et al., 2002). In the degradation pathway for JS765, nitrobenzenedioxygenase oxidizes 3-nitrotoluene into 4-methylcatechol. Methylcatechol then is degraded through a standard *meta*-cleavage pathway. Although JS765 is the only known species capable of mineralizing 3-nitrotoluene, other organisms have been identified which degrade 3-nitrotoluene into intermediate products. *Pseudomonas putida* OU3 has been observed transforming 3-nitrotoluene into 3-nitrophenol and then removing the nitro group (Alid-Sadat et al., 1995).

*Mycobacterium* sp. strain HL 4-NT-1 degraded 4-nitrotoluene to hydroxylaminotoluene by reducing the nitro group (Spiess et al., 1998). The intermediates are further degraded by *meta* ring cleavage and release of the amino group (He & Spain, 2000). *Pseudomonas* sp. strain 4NT and *Pseudomonas putida* TW3 oxidize the methyl group to form 4-nitrobenzoate which is then reduced to hydroxylaminobenzoate. Deamination of hydroxylaminobenzoate leads to the formation of protocatechuate. The ring structure of protocatechuate can then be broken into tricarboxylic acid cycle intermediates (Haigler & Spain, 1993; Rhys-Williams et al., 1993).

### 2.3.3 Dinitrotoluene Degraders and Pathways

Under anaerobic conditions, dinitrotoluene is reduced to aminonitrotoluene and nitrosonitrotoluene (Liu et al. 1984). Ring cleavage and further transformation of byproducts is

unlikely (Nishino et al. 2000a). Under aerobic conditions, known dinitrotoluene degraders utilize a dioxygenase to add oxygen to the aromatic ring and transform the compound into methylnitrocatechol while releasing nitrite (Ju & Parales, 2010). *Buckholderia* sp. strain DNT (Spanggord et al., 1991; Suen & Spain, 1993; Haigler et al., 1994) and *Buckholderia cepacia* R34 (Nishino et al., 2000a, Johnson et al., 2002) degrade 4-methyl-5-nitrocatechol by oxidizing the remaining nitro group with a monooxygenase. The oxidation product, 2,4,5-trihydroxytoluene, then undergoes *meta* cleavage (Johnson et al., 2002). Alternatively, *B. cepacia* JS850 and *Hydrogenophaga palleronii* JS863 degrade 2,6-dinitrotoluene into 3-methyl-4-nitrocatechol prior to *meta* ring cleavage, then the second nitro group is removed (Nishino et al., 2000a).

#### ***2.3.4 Chlorinated Nitroaromatic Compound Degradation Pathways***

*Pseudomonas stutzeri* ZWLR2-1, a 1,2-chloronitrobenzene (CNB) degrader, releases nitrite to form 3-chlorocatechol (Liu et al., 2005). The intermediate is then further degraded following the *ortho* ring cleavage pathway to 3-oxoadipate (Liu et al., 2011). The degradation pathway is provided in Figure 4.

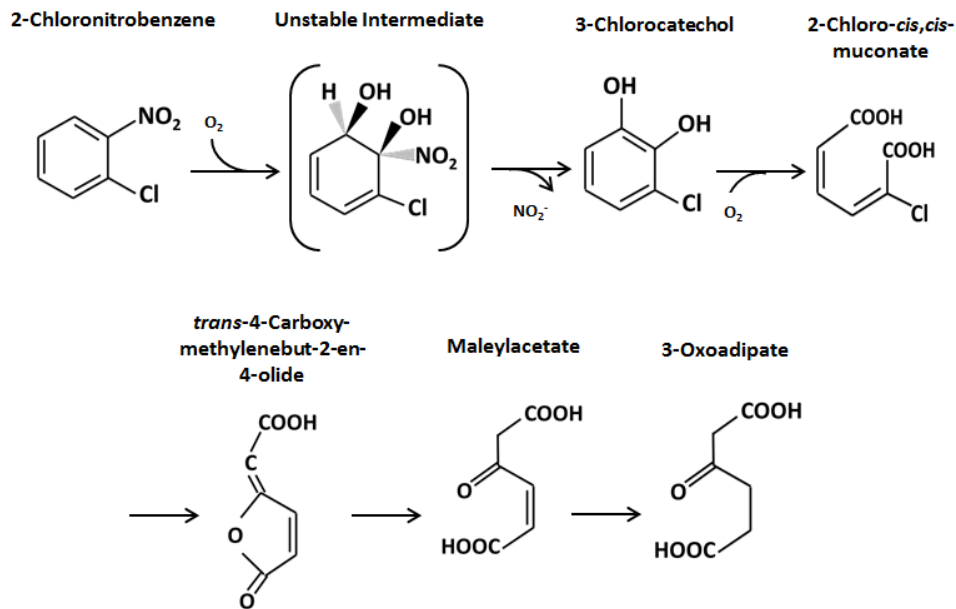


Figure 4 – Degradation pathway of 2-chloronitrobenzene by *Pseudomonas stutzeri* ZWLR2-1 adapted from Liu et al. (2011).

*Pseudomonas putida* OCNB-1 grows solely on 2-CNB and forms the intermediates 2-chloroaniline, 3-chlorocatechol, and 3-chloromuconic acid (Wu et al., 2009). The primary enzymes used in degradation were aniline dioxygenase, nitrobenzene reductase, and catechol-1,2 dioxygenase.

*Comamonas* sp. strain CNB, *Pseudomonas putida* ZWL73, and *Comamonas* sp. strain LW1 use chloronitrobenzene nitroreductase (CnbA) to reduce 4-CNB to 1-chloro-4-hydroxylaminobenzene (Katsivela et al., 1999; Ma et al., 2007; Wu et al., 2006; Zhen et al., 2006). Further degradation by either hydroxylaminobenzene mutase (CnbB) or a Bamberger rearrangement changes 1-chloro-4-hydroxylyaminobenzene into 2-amino-5-chlorophenol (Xiao et al., 2006). Ring cleavage by 2-aminophenol-1,6-dioxygenase leads to the formation of 2-amino-5-chloromuconate (Wu et al., 2005). Multiple other enzymatic steps occur until TCA cycle intermediates are formed (Wu et al., 2006).

Park et al. (1999) reported mineralization of 3-CNB and 4-CNB by a co-culture of *P. putida* HS12 and *Rhodococcus* sp. HS51. HS12 reduced and acetylated 3-CNB and 4-CNB to form chlorohydroxyacetanilides, which could then be degraded by *Rhodococcus* sp. HS51. Ammonia and chloride byproducts were observed.

### 2.3.5 Biodegradation Kinetics

First order anaerobic biodegradation rates of organic compounds from field and laboratory studies were reviewed by Aronson & Howard (1997), and ranges of rates are provided in Table 2. The lower limit of the range was the lowest rate constant found in the literature, and the upper limit was the mean of the rate constants in the reviewed literature. Rate constants show degradation of the parent compound and do not represent mineralization. While the rate constant is for anaerobic conditions, the redox conditions do vary between studies. Studies occurred under nitrate-, iron-, sulfate-reducing or methanogenic conditions. Changes in redox along with other site characteristics could account for the large range in measured rates, and biodegradation rates may be difficult to generalize from site to site.

Table 2- First order biodegradation rate constants (reviewed by Aronson & Howard 1997). The lower limit of the range is the lowest rate constant reported in the literature. The upper limit is the mean of the rate constants reported.

Compound	First-order Rate Constant (day <sup>-1</sup> )
Nitrobenzene	0.0037-0.032
Naphthalene	0-0.0072
Benzene	0-0.0036
Toluene	0.00099-0.059
Ethylbenzene	0.00060-0.015
<i>m</i> -Xylene	0.0012-0.016
<i>o</i> -Xylene	0.00082-0.021
<i>p</i> -Xylene	0.00085-0.015

Rates are generally higher in aerobic zones or at anoxic/oxic interfaces where oxygen acts as the electron acceptor. At anoxic/oxic sediment interfaces, Kurt et al. (2012) found site microorganisms were able to degrade nitrobenzene ( $6.5 \text{ g}\cdot\text{m}^{-2}\cdot\text{d}^{-1}$ ) at slightly higher rates than chlorobenzene ( $2\text{-}4.2 \text{ g}\cdot\text{m}^{-2}\cdot\text{d}^{-1}$ ), suggesting under aerobic conditions nitrobenzene degradation kinetics are slightly faster than chlorobenzene.

### ***2.3.6 Effect of Temperature on Biodegradation Rates***

Temperature has been shown to highly influence microbial metabolism rates (Nedwell, 1999). Studies have revealed the existence of temperature optima for petroleum hydrocarbon biodegradation under both aerobic and anaerobic conditions (Filler et al., 2001, Mohn & Stewart, 2000; Zeman et al., 2014). Maintaining subsurface temperatures near the optimum by insulating the ground surface has been found to keep biodegradation activity occurring during arctic winter conditions (Filler et al., 2001). Increases of  $2^{\circ}\text{C}$  have been found to increase biodegradation in arctic climates (Delille et al., 2004). Temperature optima are dependent on site conditions, indigenous microbial consortia, contaminants present, and active degradation processes (Mohn & Stewart, 2000). Temperature optima have ranged from  $10^{\circ}\text{C}$  to  $35^{\circ}\text{C}$  (Coulon et al. 2005; Higashioka et al., 2011; Walworth et al., 1999; Zeman et al., 2014).

Few studies have investigated how temperature affects biodegradation rates of NACs. Most studies have looked at degradation of NACs at temperatures ranging from  $30^{\circ}\text{C}$  to  $37^{\circ}\text{C}$ , which are dissimilar to actual groundwater temperatures (Nishino & Spain, 1993; Gheewala & Annachhatre, 1997; Tanaka et al., 2009; Zheng et al., 2007). One study, Liu et al. (2013), investigated nitrobenzene degradation at temperatures similar to subsurface conditions. They

developed a cold-tolerant aerobic consortium capable of mineralizing nitrobenzene and aniline at similar rates to microbial communities held at 20°C and 30°C (Figure 5).

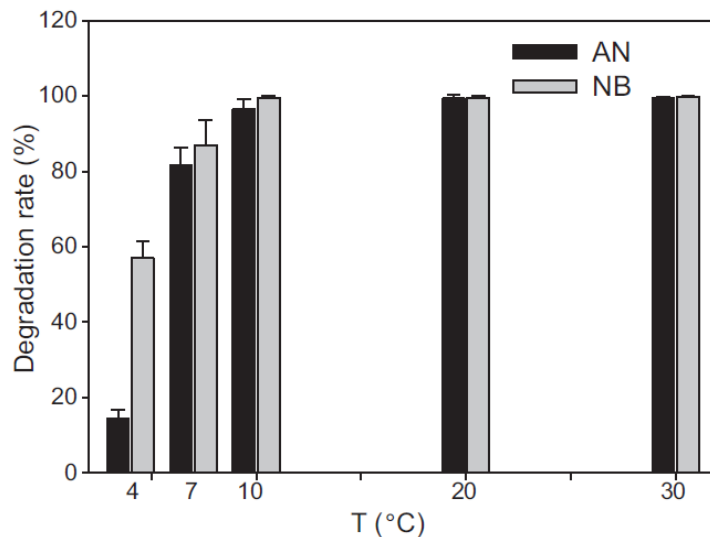


Figure 5 – Aniline (AN) and nitrobenzene (NB) biodegradation rates (Liu et al., 2013)

Microbial diversity analysis revealed 98% of the microbial species were classified under the *Pseudomonas* genus. The most prevalent species, *Pseudomonas maderi* and *Pseudomonas syringae*, are known to be cold tolerant species (Nemecek-Marshall et al., 1993; Jang et al., 2012). However, this study investigated degradation rates at 4°C, 7°C, 10°C, 20°C, and 30°C. The study did not elucidate how degradation rates change within the 10°C to 20°C range. Furthermore, these studies investigated only aerobic systems. Therefore, research is needed on how microbial NAC degraders respond to typical groundwater temperatures in anaerobic systems.

## 2.4 Sorption

Sorption is an important process in determining the fate and transport of organic compounds in the subsurface. Contaminant sorption to the soil matrix can control the transport and

bioavailability of contaminants in ground and surface water systems (Zhang et al., 2014).

Irreversible sorption may provide a permanent sink for organic contaminants.

#### ***2.4.1 Sorption Behavior of Nitroaromatic Compounds***

For polar compounds like nitrobenzene and 2,4-dinitrotoluene, non-hydrophobic sorbate/sorbent interactions such as charge transfer, hydrogen bonding, and electron donor-acceptor interactions are the primary sorption mechanisms (Brusseau & Rao, 1991; Zhu et al., 2004). These reactions are reversible, and irreversible sorption mechanisms have not been described in the literature (Haderlein et al., 1996). The electron withdrawing nature of the nitro group allows NACs to form electron donor-acceptor interactions with electron-rich moieties such as siloxanes present on aluminosilicate clay surfaces and soil organic matter (SOM) (Schwarzenbach et al., 2003; Zhu et al., 2005; Zhu & Pignatello, 2005). Therefore, sorption processes are highly dependent on both the availability of sorption sites on clay minerals and the fraction of SOM (Chiou & Kile, 1998; Schwarzenbach et al., 2003; Charles et al., 2006). Sheng et al. (2001) found smectite clays sorbed larger amounts of NACs than SOM. However, other studies have shown humin and humic acids are important in sorption processes for polar compounds like nitrobenzene and 2,4-dinitrotoluene (Shi et al., 2010; Zhang et al., 2014). With the removal of SOM, Shi et al. (2010) observed decreases in sorption of 34-54% for 1,3,5-trinitrobenzene. The remaining 46%-66% of sorption can be attributed to interactions with inorganics such as clay minerals. Since interactions with clay mineral and SOM are reversible, desorption from the soil matrix may occur if subsurface conditions change.

### ***2.4.2 Sorption Behavior of Aromatic Amines***

In addition to determining the sorption mechanisms of NACs, it is critical to fully understand how potential degradation byproducts sorb. Under reducing conditions, NACs may be reduced to aromatic amines, such as aniline, which are also toxic (HSDB, 2014). Aromatic amines have displayed biphasic sorption kinetics most likely due to different sorption mechanisms dominating at early and late stages of sorption (Hsu & Bartha, 1974, Graveel et al., 1985; Li & Lee, 1999). Cation-exchange and covalent bonding (i.e., chemisorption) are the primary mechanisms for aniline sorption (Weber et al., 2001). At early time periods, rapid, reversible cation-exchange sorption occurs (Parris 1980; Weber et al., 2001). However, as time progresses, irreversible covalent bonding becomes the primary sorption process (Parris 1980; Weber et al., 2001). Covalent bonding occurs between the amino functional group and carbonyl functionalities in natural organic matter (Schwarzenbach et al., 2003; Stevenson, 1976). Due to the irreversible nature of covalent bonding, sorption processes could effectively attenuate contaminant concentrations in the aqueous phase and eliminate later desorption from the soil matrix. However, the amount of covalent bonding is constrained by the number of available reactive bonding sites (Weber et al., 2001).

### **2.5 Remediation Approaches**

Understanding how NACs behave in the subsurface aids in designing an effective remediation treatment to reduce contaminant mass and flux. Several remediation treatments work to either physically remove contaminant mass or capitalize on biogeochemical processes, which decrease contaminant mass in the subsurface. Remediation techniques vary in the amount of human

involvement and disruption to the site. *Ex situ* techniques require transfer of the contaminants to the surface for treatment, while *in situ* techniques treat the contaminants in the subsurface.

### ***2.5.1 Ex situ Treatment Techniques***

*Ex situ* treatments, including pump and treat systems as well as excavation and disposal, physically remove contaminant mass from the subsurface. Pump and treat systems pump contaminated liquids to the surface, where the contaminated groundwater and/or NAPL are treated. Pumping also allows for hydraulic control of groundwater flow, which can be used to prevent contaminated groundwater from leaving an area. Excavation and disposal involves removing affected soil and groundwater from the contaminated area. It is then either incinerated or placed in a landfill. Both of these treatments are energy intensive and often not cost-effective.

A treatment for extracted groundwater contaminated with NACs, sequential reductive/oxidative bioreactors with a mixed consortium of microorganisms, can be used to completely mineralize NACs (Dickel et al., 1993; Berchtold et al., 1995). The first section of the reactor consists of an anaerobic environment where a consortium of microorganisms reduces the nitro group to an amine group. Since amine byproducts are recalcitrant under anaerobic conditions, transport of byproducts into aerobic conditions can lead to mineralization. Another consortium can then completely mineralize amine byproducts under aerobic conditions. While *ex situ* techniques can be quite effective, these techniques may not be feasible for sites with extensive contamination.

### ***2.5.2 In situ Treatment Techniques***

*In situ* remediation methods are often preferred for sites with widespread contamination. These techniques include both abiotic and biotic approaches. Abiotic approaches include chemical

oxidation, or chemical reduction. Chemical oxidation involves injecting a strong oxidant such as persulfate or Fenton's reagent into the subsurface. An accurate site conceptual model is needed to ensure the oxidant reaches the contaminated zone. A strong reductant such as zero-valent iron can be used to abiotically reduce the nitro group to form an amine group (Nishino et al., 2000b). However, after initial deployment, the zero-valent iron barrier may become oxidized and limit further reactivity. To further degrade the amines, the groundwater may need to be transported to an aerobic zone where the amines can be completely mineralized (Nishino et al., 2000b).

Biotic remediation strategies use native or introduced microbial communities to degrade organic contaminants with the goal of complete mineralization. Bioremediation consists of stimulating biodegradation processes that may already be occurring onsite. Biodegradation rates may be increased by injecting electron acceptors into the subsurface, bioaugmenting with a microbial species or consortia capable of degrading the contaminant, or through air sparging (Megharaj et al., 2011; An et al., 2012). As with all injection processes, it is difficult to ensure the injected materials reach the desired areas, especially when the contaminants have diffused into low permeability zones. Bioaugmenting is often not effective because introduced microorganisms do not readily adapt to their new environment and are often outcompeted by native microorganisms (Megharaj et al., 2011). Additionally, transport of microorganisms within the subsurface is limited. DeFlaun et al. (1997) found a majority of injected biomass stayed within 0.5 m of the injection well.

*In situ* techniques such as air sparging capitalize on both abiotic and biotic processes. Air sparging involves injecting air or oxygen into the subsurface. Typically air sparging is used to promote the volatilization of organic compounds from the subsurface, but it has also been shown to increase biodegradation by stimulating aerobic bacteria (Roy et al., 1996; Hall et al., 2000; Al-

Maamari et al., 2011). In a laboratory sand tank experiment, air sparging was found to remove 90% of nitrobenzene and aniline, and 99% removal efficiency was achieved when bioaugmentation was added to the system (An et al., 2012a). When investigating how air sparging affected indigenous microorganisms in the field, an increase in microbial diversity was observed, but abundance decreased (An et al., 2012b). Prior to treatment, the microbial community consisted of *Acidovorax* sp., *Flectobacillus lacus*, *Pseudomonas corrugate*, and *Rhizobium* sp. Treatment limited these species, and *Neviska* sp. and *Sphingobium* sp. were dominant after treatment. For anaerobically recalcitrant compounds like NACs, air sparging may provide a way to capitalize on aerobic processes in typically anaerobic zones. However, air sparging could eliminate populations of native obligate anaerobes, stalling further natural attenuation after the completion of the air sparging treatment.

After active remediation techniques have been employed, natural processes can be used to attenuate remaining contaminant mass. Monitored natural attenuation (MNA) utilizes biodegradation, sorption, and volatilization to decrease contaminant mass in the subsurface without direct human involvement (EPA, 1999). MNA provides a promising remediation solution for NACs in systems where aerobic conditions are prevalent (Swindoll et al., 1993; Bradley et al., 1997). While anaerobic degradation of amines may be possible if nitrate-reducing bacteria are present and an adequate supply of nitrate is available, bacteria capable of anaerobically degrading amine daughter products are not prevalent in the subsurface (Swindoll et al., 1993; Nishino et al., 2000b).

### ***2.5.3 Proposed Treatment: Thermal Enhancement***

As previously introduced, a bioremediation treatment, Sustainable Thermally Enhanced LNAPL Attenuation (STELA), has been developed to capitalize on increasing biodegradation rates with elevated temperature increases. Zeman et al. (2014) conducted a microcosm study to investigate the effect of temperature on the biodegradation of petroleum hydrocarbons. At temperatures above 22°C (~5°C higher than the natural range of groundwater temperatures experienced in the field), a substantial shift in microbial communities along with higher degradation rates were observed. A field pilot was developed for a former refinery site. Heating elements were placed into the ground and a monitoring system was developed to gather temperature, water quality, and biogas data. Irianni Renno et al. (2013) measured biogeochemical parameters at the STELA pilot site. A diverse community of Bacteria and Archaea in LNAPL contaminated areas suggested the importance of microbial processes in natural losses through methanogenesis or sulfate reduction pathways. Akhbari et al. (2013) developed a model for heat transfer in the subsurface by combining MT3DMS and MODFLOW. The model was used to design a full scale pilot and estimate infrastructure and energy costs. Estimated costs were between \$11.90 to \$14.40 per cubic meter. This value is lower than typical cost for common remedies (Akhbari et al. 2013).

## 3. FIELD STUDIES

### 3.1 Introduction

The field component of the study was conducted to resolve baseline conditions prior to a possible pilot treatment. Natural systems can be highly complex and heterogeneous. Therefore, collecting a wide variety of biogeochemical data is necessary when discerning significant natural processes. Since parameters like microbial populations, abundance of electron acceptors, and contaminant concentrations can greatly affect NAPL degradation in the subsurface, each factor needs to be considered when developing accurate site conceptual models, laboratory methods, and effective remediation treatments. Baseline data can serve as a point of comparison at the end of the remediation treatment to assess the efficacy of the technique. Additionally, field studies included a preliminary field investigation into the feasibility of using impedance as a predictive tool for tracking changes in the DNAPL body. Content of the following section includes methods employed in the field studies, associated results, and discussion.

### 3.2 Methods

Field methods consisted of carbon dioxide trap deployment, macrocore sampling, and multilevel sampling. Carbon dioxide traps were deployed to estimate carbon dioxide fluxes at the surface and assess the likelihood of biodegradation. Macrocore sampling involved a geologic analysis of the subsurface, contaminant mass determination with depth, and microbial community diversity analysis. Multilevel sampling was performed to determine how aqueous inorganic concentrations, aqueous contaminant concentrations, temperature, and impedance vary seasonally. These techniques were used to resolve baseline biogeochemical processes prior to

potential testing of thermal enhancement remediation treatment. The methodologies for field sampling and laboratory analysis are included in the following section.

### ***3.2.1 Site Description***

The field site for this study is a chemical production facility located along the Delaware River, USA. Chemical intermediates for dyes and polymers including compounds such as chloroanilines, dimethylaniline, nitroanilines, nitrobenzenes, toluidines, and nitrotoluenes were produced on the site starting in the early twentieth century. These chemicals were used in the manufacture of pharmaceuticals, agricultural chemicals, fibers, and various other chemical intermediates. While a few manufacturing processes remain in the area, most production has ceased, and buildings have been demolished. Figure 6 shows the current layout of the contaminated area and identifies prior locations of manufacturing facilities.

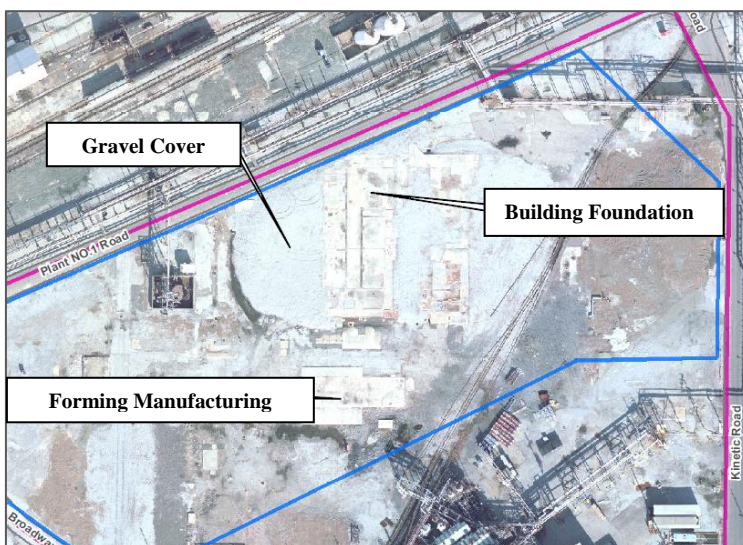


Figure 6 – Aerial view of the contaminated area (URS, 2013).

Field studies consisted of macrocore sampling, multilevel sampling, and carbon dioxide flux estimation. The location of each investigation is shown in Figure 7 on a plot of chlorobenzene

concentrations in the unsaturated zone which were determined using a passive gas sampling device called a GORE-SOBER (Stone Environmental Inc., 2011). Sampling locations were determined using chlorobenzene concentrations and NAPL detection because NAC concentrations were not available.

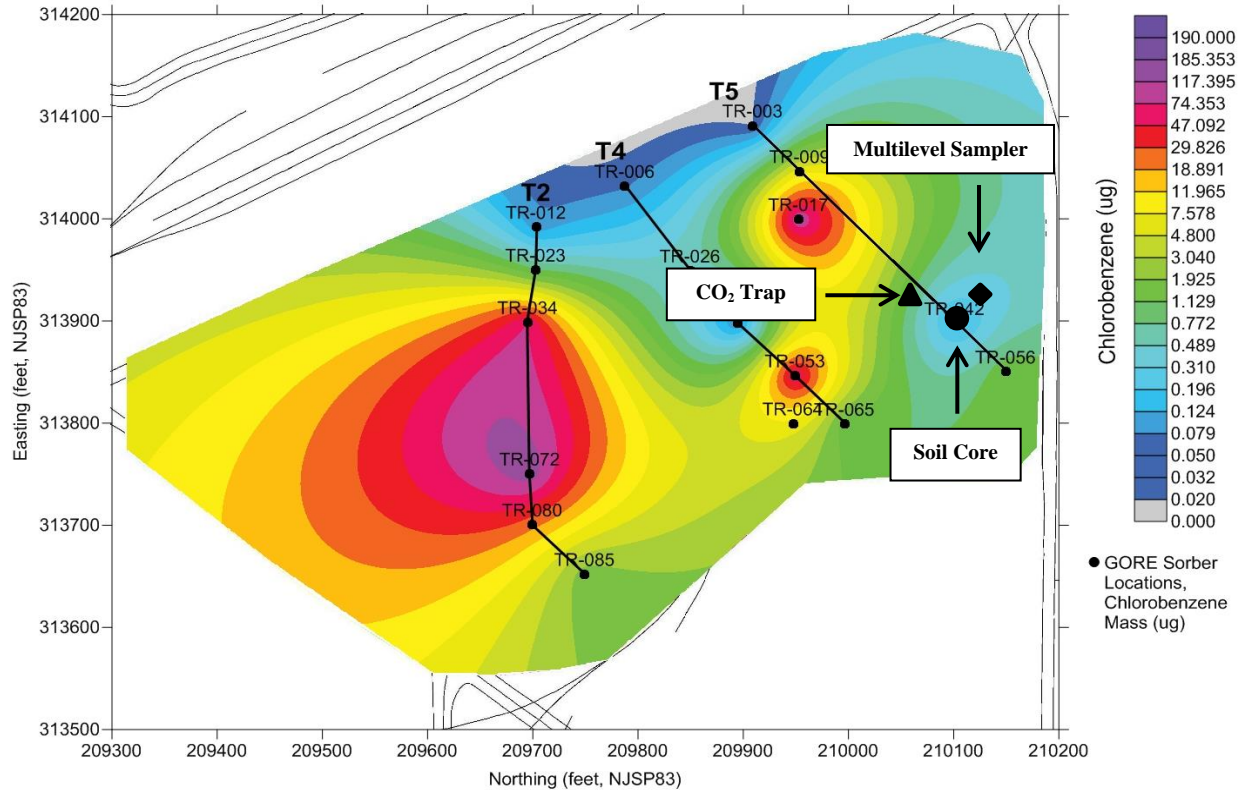


Figure 7 – Chlorobenzene total mass (Stone Environmental Inc., 2011)

Figure 8 shows chlorobenzene concentrations and NAPL sample locations with depth along transect 5 (Stone Environmental Inc., 2011). At MP-042 (TR-042 on Figure 7), NAPL was visually observed from 0 ft to -7 ft and from -11 ft to -19 ft.

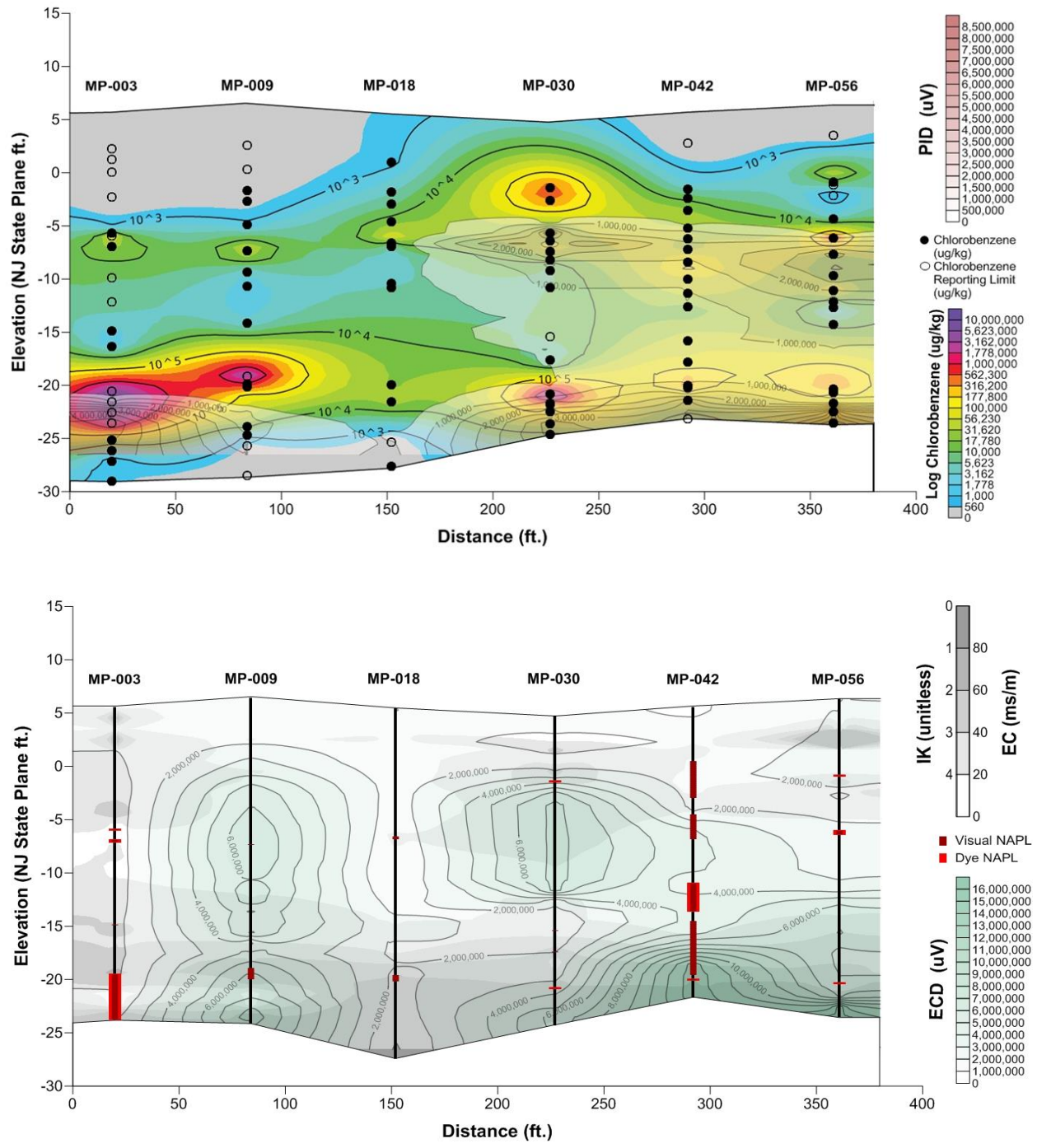


Figure 8 – Chlorobenzene concentrations (top) and observed NAPL (bottom) along Transect 5 (Stone Environmental Inc., 2011)

Stone Environmental Inc. determined site stratigraphy along transect 5 using soil cores and Index of Hydraulic Conductivity measured using the Waterloo APS<sup>TM</sup>, a groundwater sampling tool (IK) (Figure 9). IK is a continuous measurement of flow rate used to assess hydraulic conductivity. Site stratigraphy is characterized by transmissive sand layers separated by local silt/clay layers at an elevation of -5 ft to 10 ft. The upper sand layer is a fine silt/sand, while the lower transmissive zone is characterized by coarse, gravelly sand. A confining clay layer is located at -20 ft. The water table was measured in a nearby monitoring well and found to range between elevations of 1.5 - 2.1 ft (3.4 - 4 ft below ground surface, bgs).

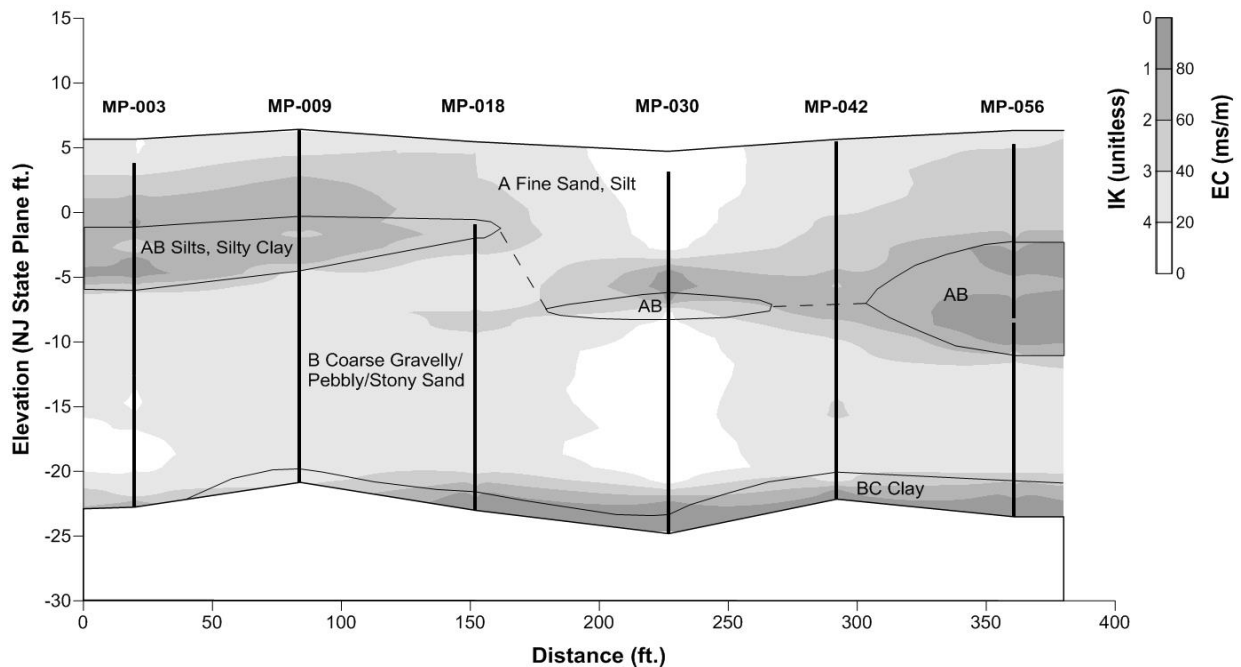


Figure 9 – Site stratigraphy (Stone Environmental Inc., 2011)

### 3.2.2 Estimating Carbon Fluxes

When contaminants are mineralized under anaerobic conditions, CO<sub>2</sub> and CH<sub>4</sub> are produced. When the CH<sub>4</sub> generated in anaerobic zones reaches aerobic zones (often in the vadose zone),

methanotrophic bacteria oxidize  $\text{CH}_4$  to  $\text{CO}_2$  in the presence of oxygen (Sihota & Mayer, 2012; Amos et al., 2005; Molins et al., 2010). When modeling gas transport and biogeochemical reactions at a site where a historical release of crude oil had occurred, Molins et al. (2010) found 98% of the carbon measured at the ground surface was in the form of  $\text{CO}_2$ . Thus,  $\text{CO}_2$  fluxes at grade can be used to estimate natural losses of organic contaminants in the subsurface (McCoy et al., 2012).

### *3.2.2.1 Carbon Dioxide Trap Design*

McCoy et al. (2012) describes a procedure to monitor  $\text{CO}_2$  fluxes at grade using  $\text{CO}_2$  traps (E-Flux, LLC, Fort Collins, CO). Traps consist of 0.1 m ID PVC pipe with two sorbent surfaces of soda lime (Sodasorb® HP-6/12, W.R. Grace, Co., a mixture of calcium and sodium hydroxides). One sorbent surface is exposed to the atmosphere, which precludes atmospheric  $\text{CO}_2$  from reaching the bottom sorbent element. The bottom sorbent element is solely exposed to  $\text{CO}_2$  from the ground surface.

### *3.2.2.2 Carbon Dioxide Trap Deployment and Analysis*

One trap was placed approximately 50 ft away from the multilevel sampling device in a contaminated area of the site. Another trap was placed in a background location on site where active manufacturing had never occurred. By placing one trap in a contaminated area and one in a nearby background location, an assessment of how the presence of contaminants effect natural loss rates of  $\text{CO}_2$  can be made.  $\text{CO}_2$  traps were deployed in December 2013, April 2014, and August 2014 to assess seasonal variation in  $\text{CO}_2$  fluxes. Each  $\text{CO}_2$  trap was left in the field for 2 weeks before being shipped back to Colorado State University, Fort Collins, CO for analysis. A third  $\text{CO}_2$  trap (travel blank) was shipped with the deployed  $\text{CO}_2$  traps in order to account for

CO<sub>2</sub> that might have gotten into the sorbent during travel. Analysis of the sorbent media was performed by E-Flux, LLC (Fort Collins, CO). The total amount of sorbed carbonate was determined and used to calculate time averaged CO<sub>2</sub> flux. Additionally, <sup>14</sup>C isotope analysis was performed on the CO<sub>2</sub> traps collected in December 2013 to estimate the amount of carbon coming from modern versus fossil fuel sources, which were used in the production of chemical intermediates for dyes and polymers.

### ***3.2.3 Macrocore Sampling***

Core samples were taken from grade to 26 ft (bgs). Samples were collected in 2 inch-diameter disposable acetate liners using a Geoprobe® rig configured for direct push drilling. The core was flash frozen on site after collection with dry ice and shipped to Colorado State University, Fort Collins, CO, where they were kept at -20°C until analysis was performed. The core was subsampled by cutting every 6 inches with a circular saw. Three samples were taken from each 6-inch subsample. The first sample, used to determine concentrations of organic contaminants with depth, was placed into a 200-mL glass jar containing 50 mL of dichloromethane as an extractant. The second sample, used for microbial analysis, was placed on dry ice and later stored at -20°C prior to analysis. The third sample was placed in a 200-mL glass jar and saved for visual characterization of the subsurface media.

#### ***3.2.3.1 Visual Characterization***

Samples were visually inspected to determine the grain size, texture, sorting, and color of the soil with depth. Fine grain soil was classified as sand or silt. Soils were then further characterized as well, moderate, or poorly sorted, and the soil components were identified as silt, fine, medium,

or coarse. In addition, samples were visually inspected to assess the amount of contamination. Contamination was classified as mobile, residual, or sheen.

### *3.2.3.2 Chemical Analysis of Contaminants in Soil*

Approximately 40 g of soil were placed into a 200-mL glass jar containing 50 mL of dichloromethane. Dichloromethane was chosen since it is not miscible in water and does not interfere with gas chromatographic analysis. The samples were hand shaken for a minute and then sonicated with an AquaWave 9376 (Bearnstead/Lab-Line, Waukegan, IL) for 15 minutes and hand shaken again for one minute. The extractant was diluted 1:5 to keep concentrations within the calibration curves. A volume of 1  $\mu$ L was injected into a gas chromatograph coupled to a mass spectrometer (Agilent Technologies 6890N Network GC system) with an Agilent 19091P-MS4 column. The injector temperature was set to 250°C. The carrier gas was helium and had a flow rate of 10 mL/min. The oven temperature was held at 50°C for 3 minutes and then ramped at a rate of 20°C/min until a temperature of 270°C was reached. Masses from 41 to 350 amu were recorded.

Calibration curves were developed for nitrobenzene, 1,2-dinitrobenzene, 1,3-dinitrobenzene, 1,2-chloronitrobenzene, 1,3-chloronitrobenzene, 1,4-chloronitrobenzene, 1,2 chlorobenzene, 1,2-dichlorobenzene, 1,4-dichlorobenzene, toluene, 2-nitrotoluene, 3-nitrotoluene, 4-nitrotoluene, 2,4-dinitrotoluene, 2,6-dinitrotoluene, 2-xylene, 4-xylene, naphthalene, 1-nitronaphthalene, aniline, 3-nitroaniline, 2-chloroaniline, and 4-chloroaniline using analytical standards (VWR, Radnor, PA; Sigma Aldrich, St. Louis, MO). Calibration curves were developed to capture all peak areas measured in aqueous and soil samples. Therefore, concentrations included in each calibration curve varied for each contaminant. Different concentrations were developed by

diluting standards in dichloromethane, and triplicates were run for each concentration. Microsoft Excel was used to develop lines of best fit. Calibration curves, lines of best fit, detection limits, and quantification limits for each contaminant are included in Appendix A.

### *3.2.3.3 Microbial Analysis*

Microbial analysis was performed in triplicate on soil core samples. Sampling depth was determined by choosing locations with unique combinations of contaminants and electron acceptors. Samples used in microbial analysis were pretreated to remove contaminants that could negatively affect DNA extraction and gene sequencing following the procedures detailed in Irianni Renno et al. (2013). The DNA was then extracted from the samples, and microbial diversity analysis was performed.

Pretreatment procedures were based on the methods developed by Whitby and Lund (2009). In a 15-mL centrifuge tube, 5 mg of soil sample were mixed with 120 ng of dehydrated skimmed milk (VWR, Radnor, PA), and 10 µg of polydeoxinocinic deoxycytidilic acid (pdldc) (Sigma-Aldrich, St. Louis, MO). Samples were vortexed for one minute on a Gennie II Vortex (Mo Bio, Carlsbad, CA). After centrifuging the sample, several wash steps were completed. These included adding 10 mL of DNA-free, sterile DI water, 500 µL of 50 mM tris-HCL (pH=8.3) (Sigma-Aldrich, St. Louis, MO), 400 µL of 200 mM NaCl (VWR, Radnor, PA), 100 µL of 5 mM Na<sub>2</sub>EDTA (Sigma-Aldrich, St. Louis, MO), and 5 µL of Triton X-100 (5% V/V) (Sigma-Aldrich, St. Louis, MO) to the sample. The sample was then vortexed for 3 minutes and centrifuged at 13,000 rpm for 5 minutes on a Sorval Legend XTR™ (Thermoscientific, Asheville, NC). Supernatant was removed. The wash procedure was repeated on the pelletized sample, but the Triton was not added in the second wash. In the third wash, 10 mL of DNA free sterile DI water,

500  $\mu\text{L}$  of 50 mM tris HCL, and 100  $\mu\text{L}$  of 5 mM  $\text{Na}_2\text{EDTA}$  were added. The sample was again vortexed for 3 minutes and centrifuged for 5 minutes at 13,000 rpm.

Powerlyser<sup>TM</sup> Powersoil<sup>®</sup> DNA Isolation Kits (MoBio, Carlsbad, CA) were used to extract DNA from the pretreated samples. To obtain high DNA yields, modifications were made to the manufacturer's instructions. These modifications included using a larger soil sample (0.5 g), combining two extractions for one Powersoil<sup>®</sup> spin filter, and limiting the volume of elution buffer to 50-60  $\mu\text{l}$ . A Gen5<sup>TM</sup> Biotek microplate reader and a Take 3<sup>TM</sup> microplate (Biotek, Winoosky, VT) were used to quantify DNA concentrations at an optical density of 260 nm. Samples were extracted in triplicate. Extracted DNA was stored at  $-20^\circ\text{C}$  until further analysis was performed.

Quantitative PCR (qPCR) was performed to determine the amount of 16S rRNA gene copies per gram of soil. Genes were quantified using SYBRgreen<sup>TM</sup> assays (Life technologies, Grand Island, NY) and an ABI 7300 real-time PCR system (Applied Biosystems, Foster City, CA). Bacterial primers were 1369F and 1541r, and archaeal primers were 931AF/1100Ar (Suzuki et al., 2000) The 25- $\mu\text{l}$  qPCR reaction consisted of Power SYBR green<sup>TM</sup>, forward and reverse primers (2.4  $\mu\text{M}$ ), magnesium acetate (10 $\mu\text{M}$ ), PCR grade water, and 1 ng of DNA template. Calibrations were performed using genomic DNA from *Thauera aromatica* (ATCC #:7002265D) and *Methanosarcina acetivorans* (ATCC #: 3595). The detection limit of the qPCR analysis was 100 copies per reaction well. Initially, qPCR reactions were held at  $95^\circ\text{C}$  for 10 min. The system then cycled from  $95^\circ\text{C}$  for 45s to  $56^\circ\text{C}$  for 30s, and then to  $60^\circ\text{C}$  for 30s. This was repeated 40 times, and fluorescence data was recorded each time. Amplicon specificity was verified with dissociation curve analysis.

Microbial diversity analysis was performed by Research and Testing Laboratory, LLC (Lubbock, TX) using a Illumina MiSeq/HiSeq Sequencer (Illumina, San Diego, CA). The eubacterial 16S rRNA assay used primers 939f and 1492r, and the archaeal assay used primers 519wf and 519r. More information can be found in the *Data Analysis Methodology* document supplied by Research and Testing Laboratory, LLC and included in Appendix D. The document also includes methodologies for sequencing, denoising, and diversity analysis. Diversity analysis classified microorganisms based on how closely their identity matched well-characterized sequences using a USEARCH algorithm and an internally maintained database. A detailed description of the algorithm and procedure is also included in the methodology document provided by Research and Testing Laboratory, LLC.

To assess changes in microbial diversity with depth, Shannon's diversity index was calculated at each depth using the equation

$$H' = - \sum_{i=1}^n p_i \ln p_i \quad [\text{Eqn. 5}]$$

where  $n$  is the number of species and  $p_i$  is the proportion of each species (Hill et al., 1973)

### ***3.2.4 Multilevel Sampling***

A multilevel sampling system was developed to collect water quality and temperature data with depth. While a monitoring well provides integrated measurements of water quality parameters, a multilevel sampler collects data at discrete intervals (Guilbeault et al., 2005). In addition to water quality and temperature sampling, electrodes also were used on the multilevel sampling device to measure impedance with depth.

### 3.2.4.1 Multilevel Sampler Materials and Design

The multilevel sampler consisted of a 2-inch ID PVC pipe. Water sampling ports, temperature sensors, and electrodes were attached to the PVC pipe.

The water sampling ports were constructed using 1/8-inch outer diameter Teflon tubing (Cole Palmer, Chicago, IL).

To prevent sand and debris from entering and clogging the sampling ports, Nitex™ (HD3-10, Tetko, Inc., Elmsford,

N.Y.) cloth was placed around the opening of the Teflon tubing. The cloth ensured particles larger than 10 µm did not enter the sampling port. Figure 10 shows a picture of the water sampling port.

Temperature sensors were built using Type K parallel construction PTFE coated thermocouple wire (TC Direct, 24 AWG). The ends of the thermocouple were spot welded and placed into a 4

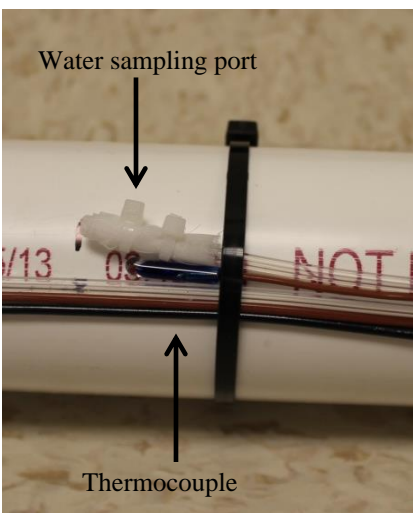


Figure 10 – Water quality sampling port and thermocouple.

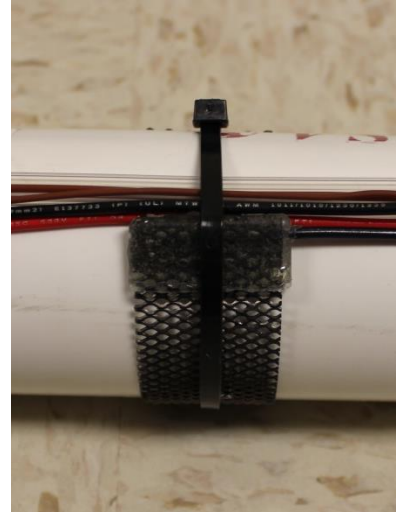


Figure 11 – Electrode for impedance measurements.

mm OD glass casing. The glass casing was then filled with epoxy (Henkel, Tra-Bond Bipax) to seal the thermocouple in place and provide protection. Figure 10 shows a picture of thermocouple.

Electrodes were added to the multilevel sampler to measure impedance changes with depth as shown in Figure 11.

Electrodes were built following the design described in Kiaalhosseini (2014). Elgard™ mesh electrodes coated with

mixed metal oxide (Corrpro, Medina, OH) were cut into 6 inch strips. The 6 inch strips were then folded onto a 20-G PVC insulated copper wire (McMaster Carr, Elmhurst, IL) to ensure a good connection between wire and titanium plate. A layer of epoxy (Lord 363, McMaster Carr, Elmhurst, IL) was placed around the connection to protect it from corrosion. Wire connectors were placed on the end of the wire to connect the wire to the banana plug. A waterproof 1040 Pelican Microcase (Torrance, CO) was used to house the banana plug and wire connectors to protect them from the weather and allow for easy data measurements with an LCR meter (BK Precision 879B). The LCR meter was used to measure inductance (L), capacitance (C), resistance (R), and impedance. However, impedance measurements were of primary interest.

Electrodes were placed 2.5 ft apart, and water quality sampling ports and thermocouples were located at the midpoint of two electrodes. Sampling points were arranged in order to obtain water quality, temperature, and impedance data at 1.75, 3.75, 6.25, 8.75, 11.25, 13.75, 16.25, 18.75, 21.25, and 23.75 ft bgs. A schematic of the multilevel sampler is provided in Figure 12.

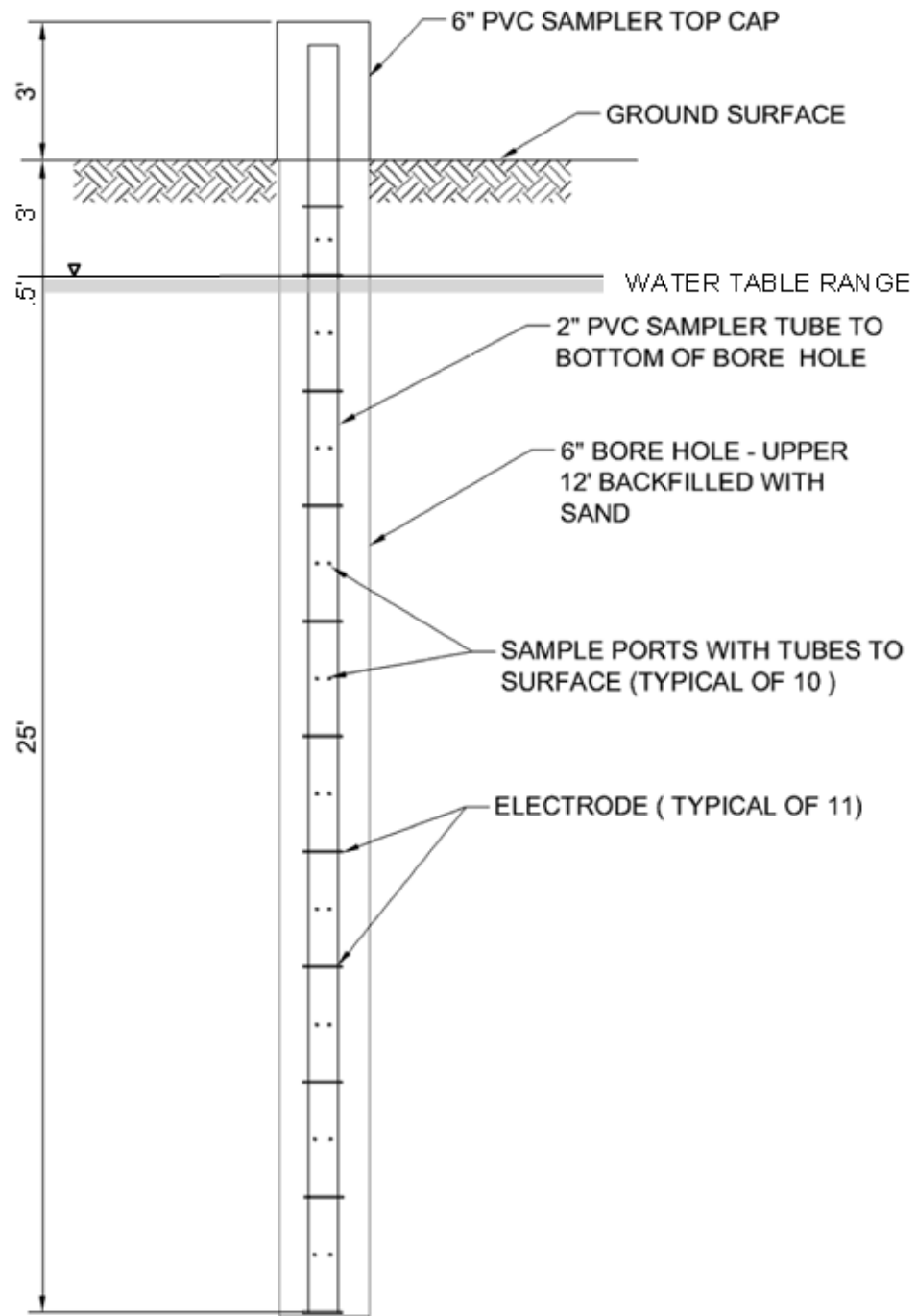


Figure 12 – Schematic of multilevel sampler.

#### *3.2.4.2 Multilevel Sampling Procedure*

Quarterly sampling was performed to measure gas composition, collect water samples, download temperature data, and take impedance measurements. To determine if methanogenesis was occurring in the subsurface, methane and carbon dioxide were measured at sampling ports above the water table using a Landtec GEM 2000 (Colton, CA). Percent carbon dioxide, methane, and oxygen found in subsurface gas were recorded.

The water quality ports were attached to a flow-through cell containing pH and ORP probes (sympHony<sup>TM</sup>, VWR, Radnor, PA). A peristaltic pump was used to pull water from the sampling ports through the flow through cell. When DNAPL was visually detected in the line, the probes were removed to prevent damage. Probe readings were stabilized and recorded prior to taking three 10-mL water samples. Each sample was capped with a Teflon crimp seal. The water samples were placed on ice and shipped overnight to Colorado State University, Fort Collins, CO. Samples were kept refrigerated at 4°C until analysis was performed.

One 10 mL sample was used to determine the organics present and their concentrations. Contaminants were extracted from the water samples into dichloromethane at a ratio of 1 mL water to 1 mL dichloromethane. The methodology outlined for extraction and analysis of the soil core was followed for the water samples.

The two remaining water samples were analyzed for water quality parameters such as major cations, anions, and elements. Analysis was performed by Colorado State University's Soil, Water, and Plant Testing Laboratory using Inductively Coupled Plasma Atomic Emission Spectroscopy. Concentrations of major elements, such as calcium, magnesium, sodium, and

potassium, were determined. The major anions measured were carbonate, bicarbonate, chloride, sulfate, and nitrate. Additionally, dissolved iron content was determined.

Temperature readings were collected every 30 minutes using Lascar USB-TC data loggers (Erie, PA). One data logger was employed per thermocouple. Data was downloaded during each quarterly sampling event. Impedance measurements were also taken quarterly to capture seasonal changes using an LCR meter (BK Precision 879B, Yorba Linda, CA).

### 3.3 Results

The following section provides detailed results from macrocore sampling and quarterly multilevel sampling.

#### 3.3.1 Estimated Carbon Fluxes

Carbon dioxide flux in the contaminated zone varied between 11.2 to 17.6  $\mu\text{mole}/\text{m}^2\cdot\text{sec}$  seasonally (Table 3). The highest observed  $\text{CO}_2$  flux was measured in April 2014.

Table 3-  $\text{CO}_2$  fluxes

CO <sub>2</sub> Trap Location	CO <sub>2</sub> Flux ( $\mu\text{mole}/\text{m}^2\cdot\text{sec}$ )			
	December 2013	April 2014	August 2014	Average
Contaminated Area	11.2	17.6	10.1	13.0
Background	2.0	2.5	7.0	3.8

The background measurement of  $\text{CO}_2$  varied between 2.0 to 2.5  $\mu\text{mole}/\text{m}^2\cdot\text{sec}$ . The  $\text{CO}_2$  flux from the contaminated zone was 4.6 and 6 times higher than the background flux for the December 2013 and April 2014 sampling events, respectively. The  $\text{CO}_2$  flux measured in August 2014 showed the flux from the contaminated area was only 44% higher than the background

location. The  $^{14}\text{C}$  analysis of the  $\text{CO}_2$  flux measured in December 2013 indicated 5.6  $\mu\text{moles}/\text{m}^2\cdot\text{sec}$  or 50% of the  $\text{CO}_2$  flux in the contaminated area came from fossil fuel-derived organic matter. Analysis of the  $\text{CO}_2$  flux from the background trap demonstrated 0.3  $\mu\text{moles}/\text{m}^2\cdot\text{sec}$  or 15% of the measured  $\text{CO}_2$  flux came from fossil fuel-derived organic matter. Using the mean  $\text{CO}_2$  flux and the  $^{14}\text{C}$  correction, the average annual  $\text{CO}_2$  flux in the study area was 6.5  $\mu\text{mole}/\text{m}^2\cdot\text{sec}$ . Following the method outlined in McCoy et al. (2014), this equates to an annual loss rate of 4,060 hydrocarbon gallon equivalents per acre per year, assuming a hydrocarbon structure of  $\text{C}_8\text{H}_{18}$  and a density of 0.77 g/mL.

### ***3.3.2 Water Table Measurements***

The water table was measured at each quarterly sampling event and was found to vary by 0.6 ft between the January 2014 and August 2014 sampling events. Table 4 contains water table measurements (bgs) from the three sampling events.

Table 4- Water table fluctuations

	January 2014	April 2014	August 2014
Depth to Water Table (ft)	4.0	3.4	3.8

### ***3.3.3 Macrocore Sampling***

Macrocore sampling involved visual characterization, contaminant analysis, and microbial analysis. The results of the soil core analysis are presented in the following sections.

### 3.3.3.1 Visual Characterization

Visual inspection of the macrocore was performed to determine geological changes with depth (Figure 13). The geology of the soil core alternated between layers of confining silt and transmissive sand deposits. Transmissive zones allow for contaminant migration, while low permeability layers prevent contaminant movement except for by diffusive processes. Additional information about soil core recovery was included in Appendix B. A silt layer was observed

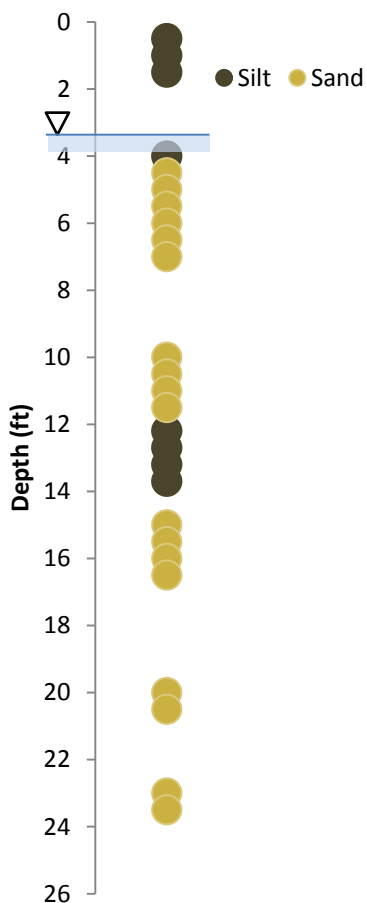


Figure 13 – Geology with depth. Each point shows where the geology was visually characterized. Silts were shown in brown, and sands were shown in yellow. Space between observation points indicates where soil core was not recovered.

from grade to 4 ft bgs followed by a transmissive sand zone from 4.5 ft to 11.5 ft bgs. A silt lens was located below the sand layer down to approximately 13.7 ft bgs. Gray sand was observed from 13.7 ft bgs to the lowest depth sample, 23.5 ft bgs. A known clay layer is located at approximately 26 ft. To prevent the spread of contaminants to lower strata, macrocore sampling was taken only to this depth.

### 3.3.3.2 Contaminant Concentrations

Contaminant species and concentrations were determined along the length of the soil core (Figure 14). Table 5 contains the contaminants quantified in the soil core, their maximum concentrations, and the depth of maximum concentration. Chlorotoluene, dichloronitrobenzene, chloronitrotoluene, ethylnitrobenzene, and chlorodinitrobenzene were

also identified using the GC-MS but were not quantified due to lack of availability of analytical standards. Contaminant concentrations were the highest in the upper transmissive zone and top of the silt layer at ~14 ft. The lower transmissive zone was less impacted and had very low concentrations of all contaminants. Compared to the NAC concentrations, the concentrations of toluene, chlorobenzene, dichlorobenzene, and naphthalene were relatively low (< 350 mg/kg) (Figure 14A). However, nitronaphthalene and 2,4-dinitrotoluene concentrations were considerably higher than the other detected contaminants. Nitronaphthalene reached concentrations of 47,500 mg/kg at 6 ft bgs, and the highest observed concentration of 2,4-dinitrotoluene was 16,000 mg/kg at 11.5 ft.

Table 5- Contaminants detected in the soil core, their maximum concentrations, and depths of maximum concentrations.

Contaminant	Maximum Concentration	Depth
	(mg/kg)	(ft)
Nitronaphthalene	47,500	6
2,4-Dinitrotoluene	16,000	11.5
1,3-Dinitrobenzene	8070	11.5
1,4-Chloronitrobenzene	5400	11.5
2,6-Dinitrotoluene	4030	11.5
1,2-Chloronitrobenzene	3810	11.5
2-Nitrotoluene	3320	11.5
4-Nitrotoluene	2090	11.5
1,2-Dinitrobenzene	1240	11.5
Naphthalene	343	11.5
Chlorobenzene	328	11.5
3-Nitrotoluene	234	11.5
Nitrobenzene	176	11.5
Toluene	154	11.5
1,2-Dicholorbenzene	153	11.5
Ethylbenzene	9	11.5
2-Xylene	9	11.5
Chlorotoluene	n.d.	n.d.
Dichloronitrobenzene	n.d.	n.d.
Chloronitrotoluene	n.d.	n.d.
Ethylnitrobenzene	n.d.	n.d.
Chlorodinitrobenzene	n.d.	n.d.

Notes:

n.d. – not determined

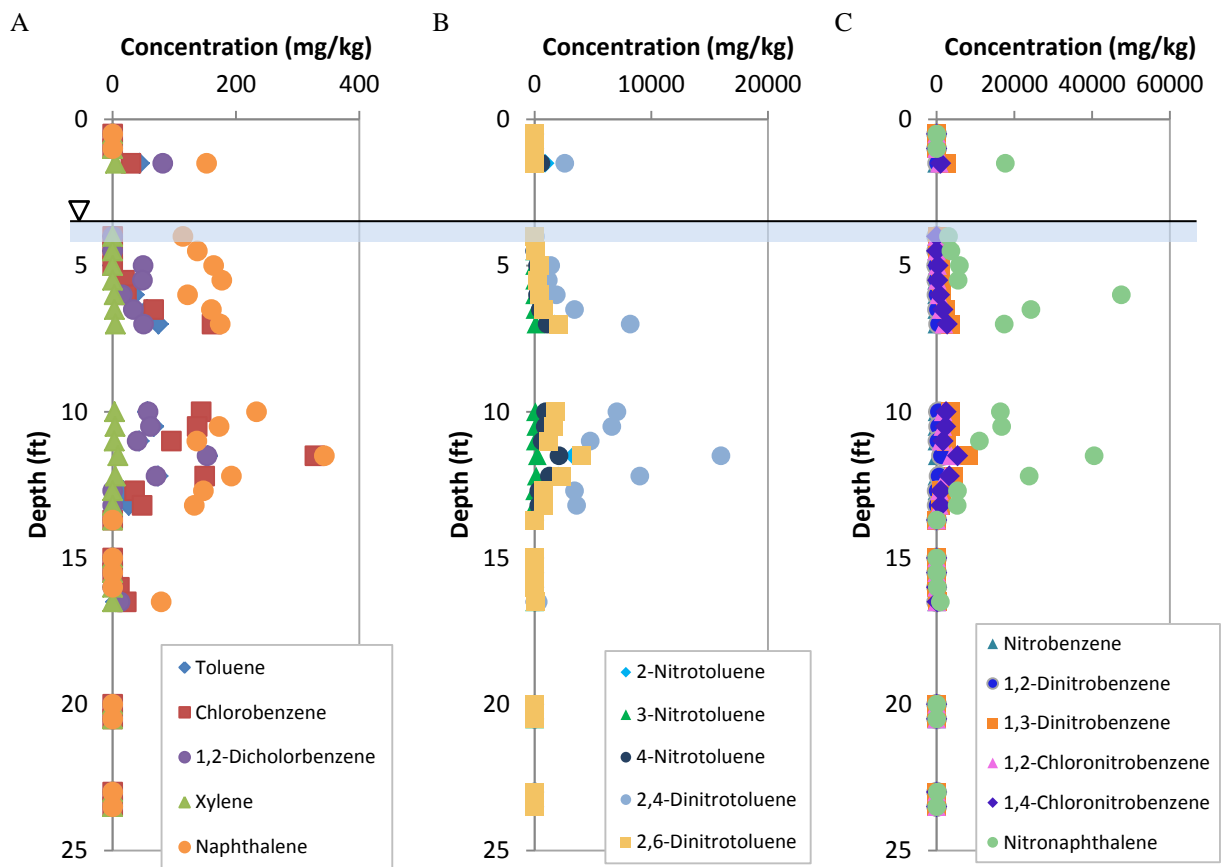


Figure 14 – Contaminant concentration in the soil core as a function of depth. All concentrations are given in mg/kg. A) Toluene, chlorobenzene, 1,2-dichlorobenzene, 2-xylene, and naphthalene concentrations, B) Nitrotoluene and dinitrotoluene concentrations, C) Nitrobenzene, dinitrobenzene, chloronitrobenzene, and nitronaphthalene concentrations

### 3.3.3.3 Microbial Variation with Depth

Microbial analysis was performed on the soil core to examine how microbial communities change with depth and the geochemistry of the subsurface. Analysis identified and quantified bacterial communities (Figure 15) and archaeal communities (Figure 16). Copies of 16S rRNA genes per gram of soil for bacteria and archaea were highest at 4.0 and 4.5 ft. At all other depths, the archaeal communities were below qPCR detection limit.

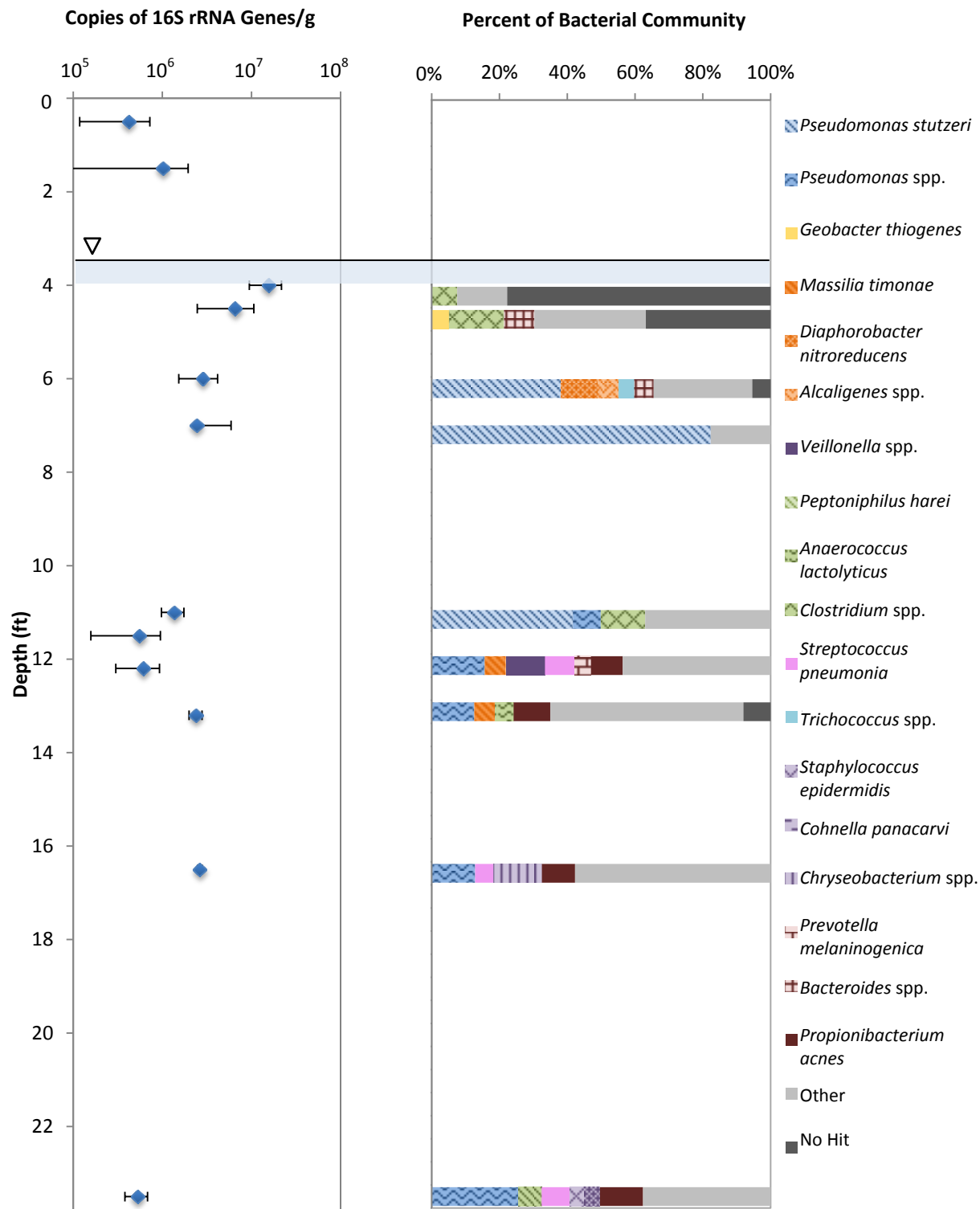


Figure 15 – Abundance of bacterial 16S rRNA genes (left) and bacterial diversity analysis (right). Other includes all species detected at less than 5%.

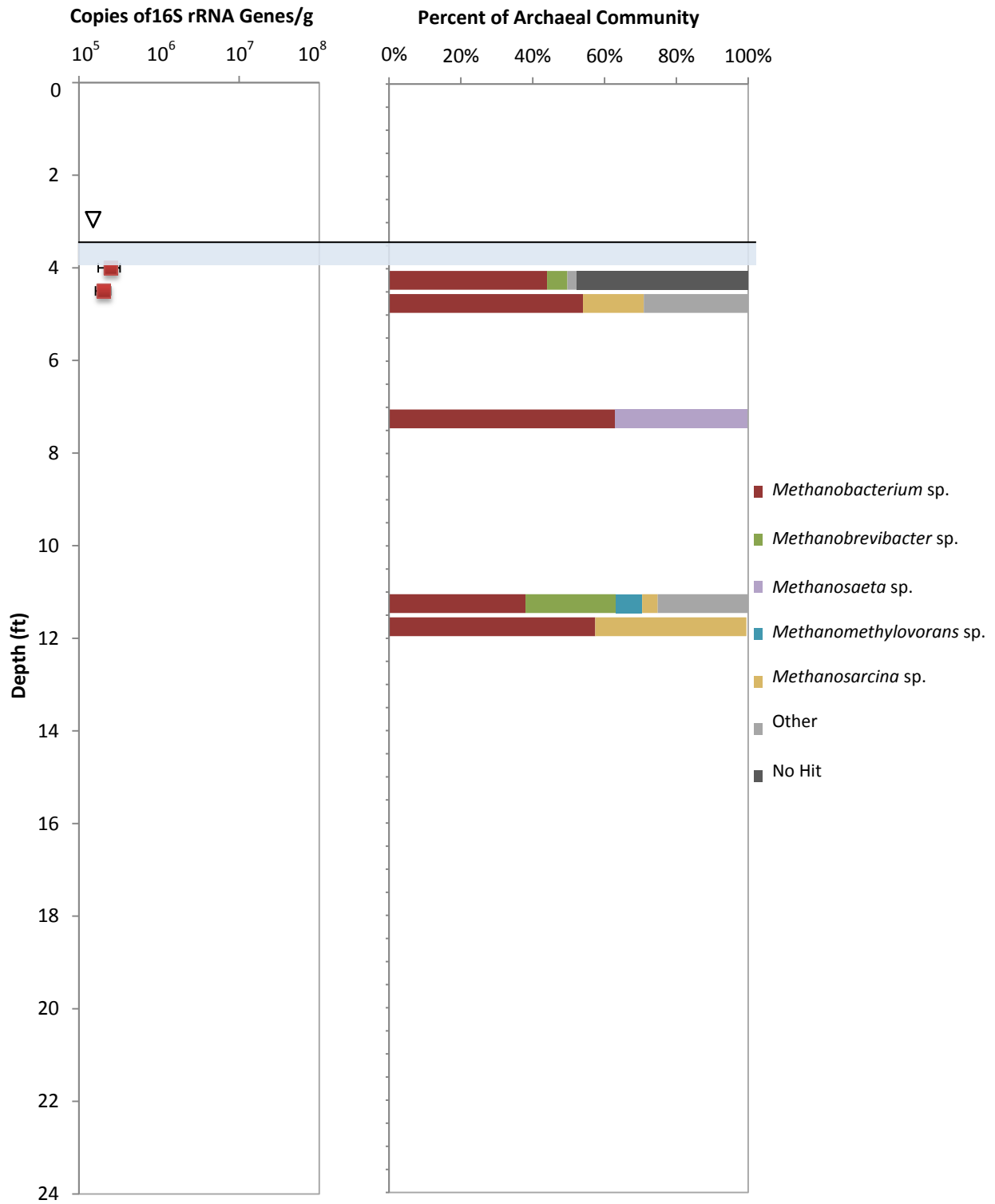


Figure 16 – Abundance of archaeal 16S rRNA genes (left) and archaeal diversity analysis (right). Other includes all species detected at less than 5%.

The bacterial community analysis revealed small percentages of *Clostridium* spp., *Bacteroides* spp., and *Geobacter thiogenes* at 4.0 ft and 4.5 ft. Shannon indices were 1.15 and 2.83 for 4.0 and 4.5 ft, respectively. Large percentages (78% for 4 ft and 37% for 4.5 ft) of microbial communities were classified as no hit, meaning the sequences could not be classified by the database used by Research and Testing Laboratory, LLC. The database includes microorganisms studied by previous researchers. Since the samples came from the environment, they most likely include microorganisms that have not yet been sequenced in the laboratory. The archaeal communities at 4.0 ft and 4.5 ft predominantly consisted of methanogens. *Methanobacterium* sp. accounted for 44% and 54% of the archaeal communities at 4 ft and 4.5 ft. *Methanobrevibacter* sp. and *Methanosarcina* sp. accounted for small percentages of the methanogens found in this zone.

Community analysis from 6.0 ft to 11.0 ft revealed less diverse communities predominately populated by *P. stutzeri*. The Shannon Index in these zones ranged from 1.01 to 2.65. At 7 ft, 83% of the bacterial community was *P. stutzeri*. While diversity analysis allowed for classification of methanogens in this zone, they were below qPCR detection limit.

From 12 ft to 23 ft, more diversity was observed in the bacterial communities with Shannon Indices ranging from 2.78 to 3.58. While other *Pseudomonas* spp. (not *P. stutzeri*) were observed, it did not account for a majority of the population. Several other species were most closely related to *Streptococcus pneumoniae*, *Staphylococcus epidermidis*, *Veillonella* spp., and *Cohnella panacarvi*, *Prevotella melaninogenica*. Methanogens populations remained below detection limit at the lower depths.

### ***3.3.4 Multilevel Sampling***

The multilevel sampling was performed on January 15, 2014, April 8, 2014, and August 6, 2014. Results from these sampling events are provided in the following sections. These sections include the analysis of aqueous inorganics, contaminant concentrations, temperature variations, and impedance measurements.

#### ***3.3.4.1 Aqueous Contaminant Concentrations***

The water table was observed at depths ranging from 3.4 to 4.0 ft bgs. NAPL was observed in the water samples between 11.0 ft and 16.0 ft. Table 6 contains the maximum concentrations of aqueous contaminants. The highest concentrations of nitrated compounds were observed at 13.75 ft. The highest concentrations of 1,3-dinitrobenzene (216 mg/L) were observed at 13.75 ft. High aqueous concentrations of 2,4 dinitrotoluene (163 mg/L) and nitronaphthalene (151 mg/L) were also observed at 13.75 ft. The highest concentrations of chlorobenzene (10 mg/L) and dichlorobenzene (5 mg/L) were in the lower transmissive zone. The maximum concentration of aniline (5 mg/L) and chloroaniline (3 mg/L) were detected in lower transmissive zone at 23.75 ft, while the maximum concentration of nitroaniline (10 mg/L) was observed in the upper transmissive zone at 3.75 ft. Toluene concentrations were low (< 6 mg/L), and xylene and ethylbenzene were not detected in the water samples. Dichloronitrobenzene, dichloronitrobenzene, chlorodinitrobenzene, and nitroxylyene isomers were also detected, but were not quantified since standards were not available. Figure 17 shows aqueous contaminant concentrations with depth from the August 6, 2014 sampling event.

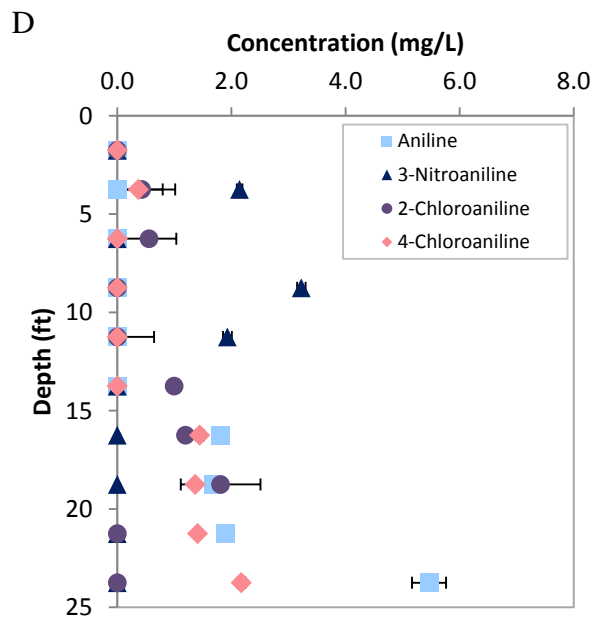
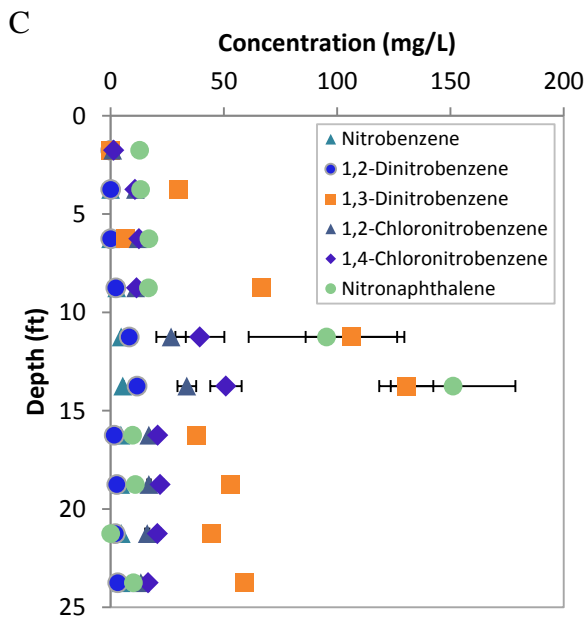
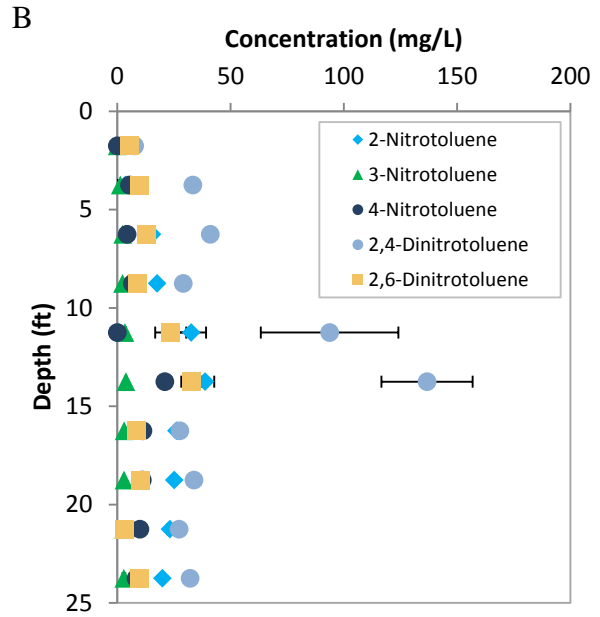
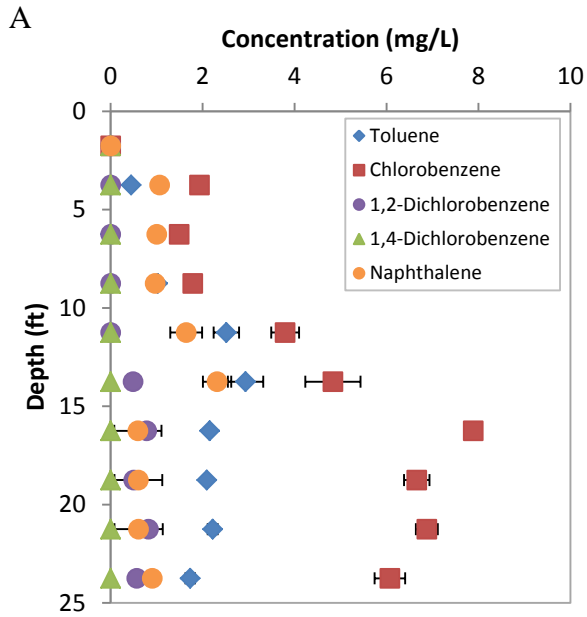
Table 6- Detected dissolved contaminants in groundwater samples, their maximum concentrations, depths of maximum concentration.

Contaminant	Maximum Concentration	Depth of Maximum Concentration	Sampling Event
	(mg/L)	(ft)	
1,3-Dinitrobenzene	216	13.75	January
2,4-Dinitrotoluene	163	13.75	January
Nitronaphthalene	151*	13.75	August
1,2-Chloronitrobenzene	91	13.75	January
1,4-Chloronitrobenzene	82	13.75	January
2-Nitrotoluene	57	13.75	January
1,2-Dinitrobenzene	53	23.75	January
2,6-Dinitrotoluene	37	13.75	January
4-Nitrotoluene	31	13.75	January
3-Nitroaniline	10	3.75	January
Chlorobenzene	10	16.25	January
Nitrobenzene	7	13.75	January
Toluene	6	13.75	January
Aniline	5	23.75	August
1,4-Dichlorobenzene	5	23.75	April
3-Nitrotoluene	4	13.75	January
2-Chloroaniline	3	23.75	April
4-Chloroaniline	2	23.75	April
Naphthalene	2	13.75	August
1,2-Dichlorobenzene	1	21.25	January
Chlorodinitrobenzene	n.d.	n.d.	n.d.
Dichloronitrobenzene	n.d.	n.d.	n.d.
Dimethylbenzylamine	n.d.	n.d.	n.d.
Nitroxylyene	n.d.	n.d.	n.d.

Notes:

n.d. – not determined

\* – concentrations were above solubility due to presence of NAPL in aqueous samples



### 3.3.4.2 Water Quality Parameters

A flow through cell was used to determine pH and ORP with depth (Figure 18). A wide pH range, 4.8 to 9.8, was observed over the entire depth of the aquifer. The pH values generally decreased with depth, showing slightly basic conditions at shallow depths and more acidic conditions at greater depths. ORP values fluctuated between sampling events. Positive values for ORP were obtained during the first two sampling events. In April, ORP decreased with depth from 700 at 3.75 ft to 240 mV at 23.75 ft (standard hydrogen electrode, SHE). However, for August, ORP increased with depth and ranged from 60 mV at 3.75 ft to 140 mV at 23.75 ft (SHE). To prevent damage to the probes, pH and ORP were not measured at depths where NAPL was observed (11 ft to 16 ft).

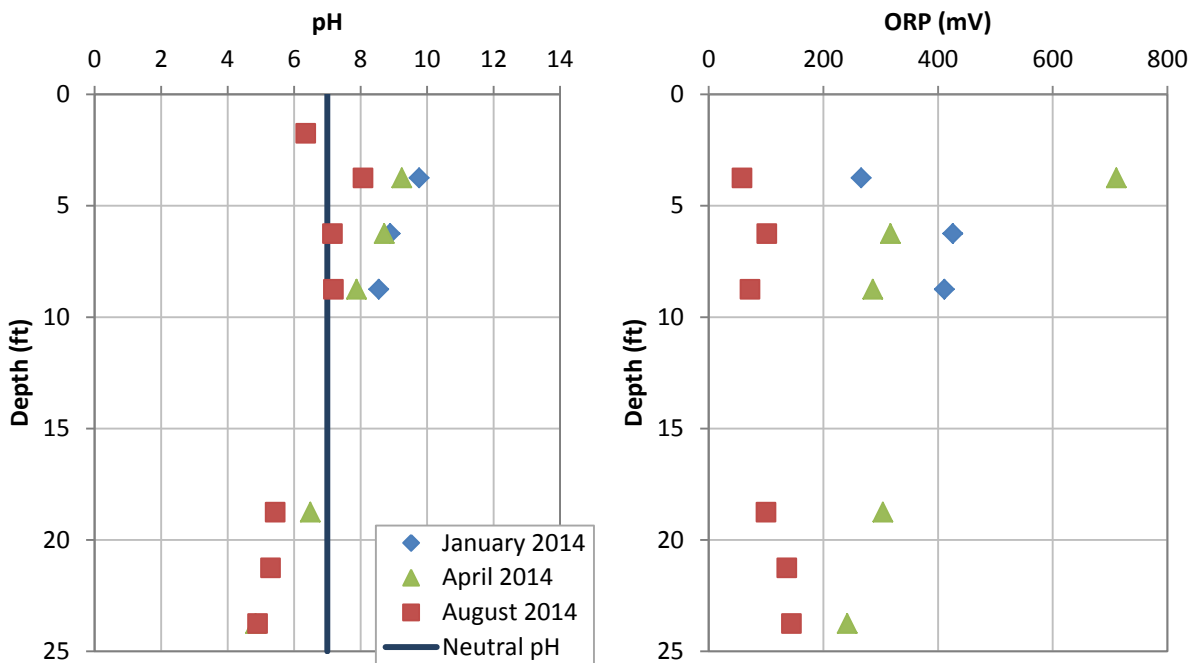


Figure 18 – pH and ORP (SHE) measurements with depth

Concentrations for electron acceptors (nitrate, dissolved iron, and sulfate) are shown in Figure 19. Nitrate concentrations were the highest during the month of August for the upper transmissive zones (up to 46.4 mg/L) and below detection in the lower transmissive region. During the previous sampling events, nitrate concentrations were below 5 mg/L. Iron concentrations were relatively low and below the detection limit in most samples. Small quantities of dissolved iron (< 0.33 mg/L) were observed during the January sampling. Most samples were below the detection limit for the April and August sampling; however, both sampling events had large dissolved iron concentrations at 23.75 ft (76 mg/L and 14.7 mg/L). High concentrations of sulfate were observed. Concentrations were lowest in the upper transmissive zone (60 - 173 mg/L for August), while the lower transmissive zone had higher concentrations (277 - 1270 mg/L for August). Additional information including conductivity, hardness, alkalinity, total dissolved solids, anions, and cations concentrations are included in Appendix B.

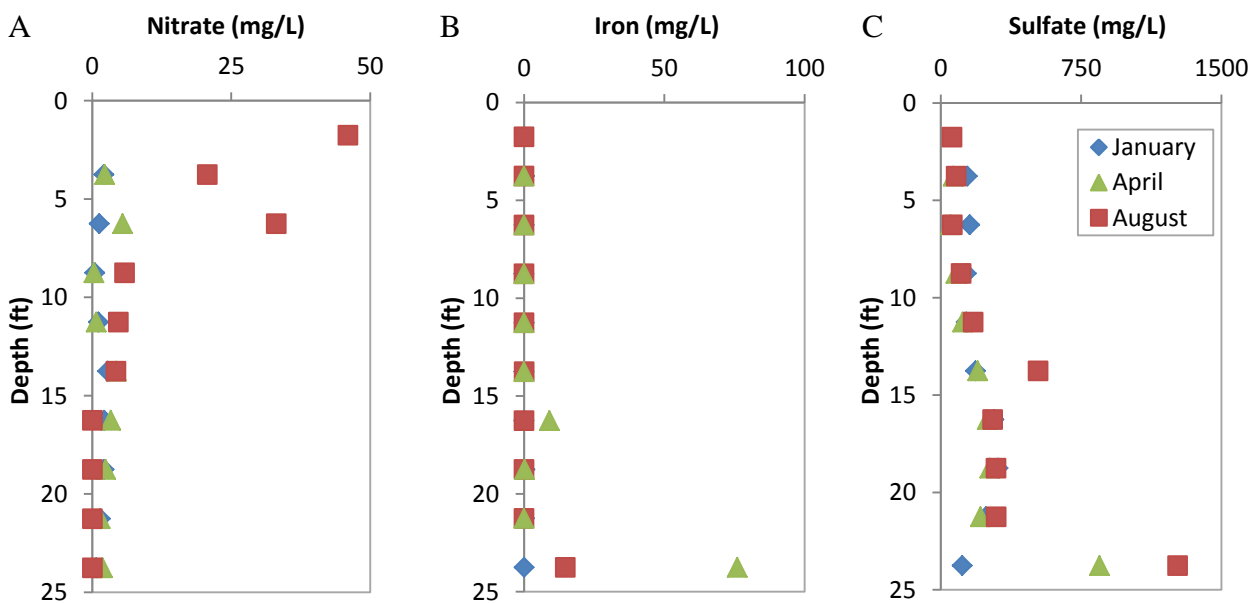


Figure 19 – Concentrations (mg/L) of electron acceptors with depth.

### 3.3.4.3 Seasonal Temperature Variation with Depth

For eight months, subsurface temperatures were recorded at ten points in the subsurface from 1.75 ft to 23.75 ft. Figure 20 shows temperature with depth over time. Subsurface temperature ranged between 2°C to 29°C at the sample location nearest to the surface, which showed the largest temperature variation. Temperature variation decreased with depth. At 23.75 ft, the temperature fluctuated between 14°C to 18°C.

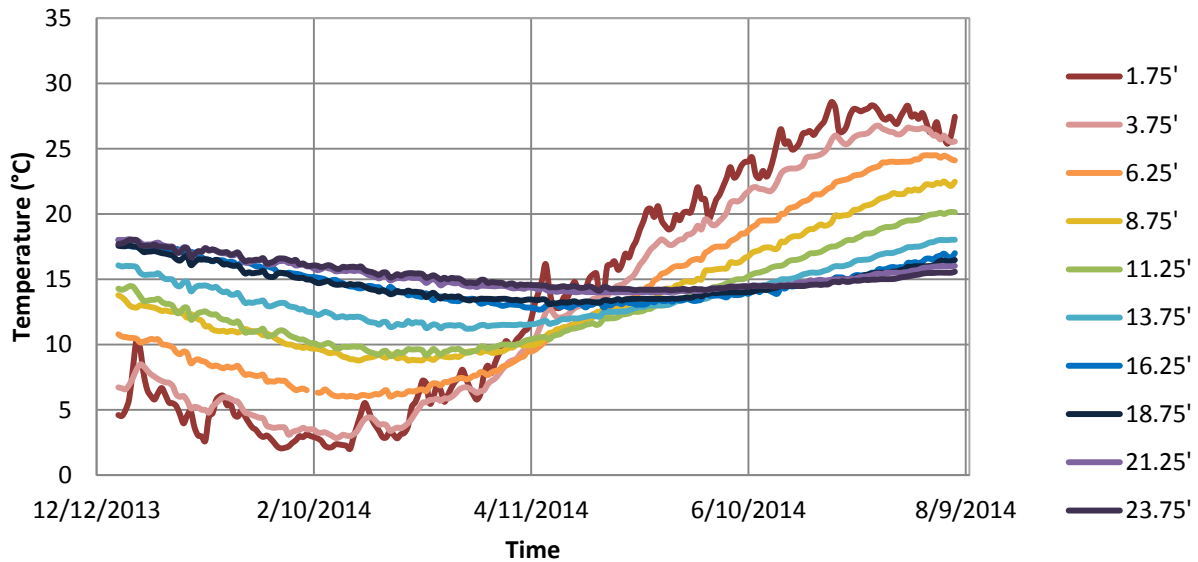


Figure 20 – Groundwater temperature with depth over 9 months.

### 3.3.4.4 Gas Sampling

The water table was below the first sampling point (1.75 ft) only on the January 15, 2014 sampling event, allowing for gas analysis. The gas at this shallow depth consisted of 3% methane, 2.5% carbon dioxide, and 21.2% oxygen. At approximately 7 ft above ground surface, methane and carbon dioxide were elevated from atmospheric conditions and each were measured

to be 0.7%. The height of the water table prevented further gas sampling during subsequent sampling events.

### 3.3.4.5 Impedance Measurements

Impedance measurements with depth were taken on three different sampling events (Figure 21). A slight decrease in impedance was observed from 2 ft to 4 ft bgs. From 3.75 - 21.25 ft, the impedance remains relatively constant until ~24 ft where resistivity increases by at least an order of magnitude depending on the sampling event. The highest impedance value of 11.2 k $\Omega$  was recorded on the January 15, 2014 at 23.75 ft. Variation between sampling events was the highest at the shallowest and deepest depths. At 23.75 ft, impedance measurements ranged from 11.2 k $\Omega$  to 5.17 k $\Omega$  for the January and August sampling events respectively.

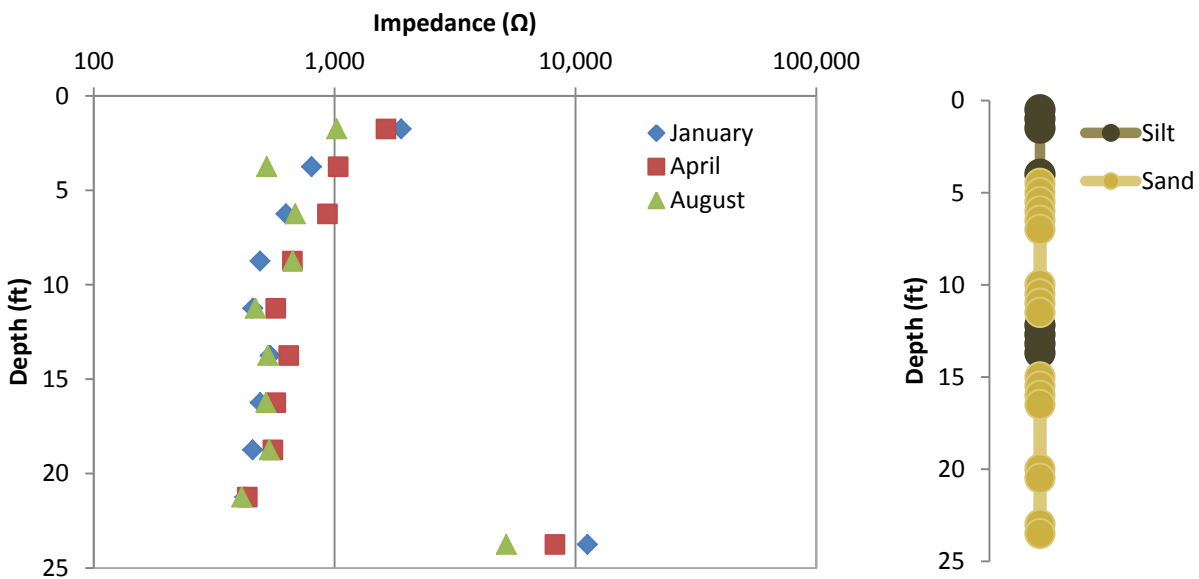


Figure 21 – Impedance measurements with depth (left). Site geology (right).

## **3.4 Discussion**

### ***3.4.1 Estimated CO<sub>2</sub> Fluxes***

Substantially increased CO<sub>2</sub> fluxes were observed in the contaminated area of the site compared to fluxes from the background area. This indicates natural degradation processes are actively occurring in the contaminated area. Moreover, <sup>14</sup>C analysis demonstrated that 50% of the carbon in the contaminated area came from fossil fuel-derived organic matter, while only 15% of the carbon in the background area came from fossil fuel-derived organic matter. This provides additional strong evidence that indigenous microorganisms are mineralizing anthropogenic contaminants under natural conditions. However, no conclusions can be advanced as to which contaminant species is/are being degraded. Nevertheless, since biodegradation is naturally occurring at the site, degradation can potentially be stimulated by increasing subsurface temperature or by other means such as supplying depleted electron acceptors (i.e., oxygen).

### ***3.4.2 Biogeochemical Characterization with Depth***

Field studies were conducted to further elucidate natural attenuation processes occurring in the subsurface. Geology, contamination, possible degradation byproducts, redox conditions, and microbial communities were analyzed to determine biogeochemical zones with depth. Microbial communities vary greatly by geology and contamination. Several studies have shown microbial community structure and abundance are affected by soil type, pH, abundance of electron acceptors and level/type of contamination (Girvan et al., 2003; Irianni Renno et al., 2013; Lauber et al., 2009; Sutton et al., 2013). Irianni Renno et al. (2013) observed variation of microbial communities between discrete zones characterized by varying redox conditions (aerobic, sulfate-reducing, or methanogenic) and levels of petroleum hydrocarbon contamination.

The following subsections discuss and classify field data into zones with similar biogeochemical characteristics. Zones were grouped based on similar microbiology, geology, and contaminant concentrations. Tables 7 and 8 contain a summary of biogeochemical parameters with depth. Table 7 summarizes geology, temperature, contaminant concentrations, and possible degradation products, and Table 8 summarizes geology, electron acceptors, and microbial characterization by depths. Other parameters such as major cations ( $\text{Ca}^{2+}$ ,  $\text{Mg}^{2+}$ ,  $\text{Na}^+$ ,  $\text{K}^+$ ) and anions ( $\text{CO}_3^{2-}$ ,  $\text{Cl}^-$ ) as well as ORP and pH also were analyzed but were not determined to be the main parameters for defining biogeochemical zones. While ORP is an important parameter for determining redox conditions, ORP readings were inconsistent, which may be due to exposure to atmospheric oxygen during sampling.

Table 7- Geology, temperature, contaminant concentrations, and possible degradation byproducts with depth.

<b>Depth Range (ft)</b>	<b>Geology</b>	<b>Subsurface Temperature Range</b>	<b>≥ 18°C (Dec-Aug)</b>	<b>Soil Core (mg/kg)</b>	<b>Aqueous (mg/L)</b>	<b>Possible Degradation Byproducts (mg/L)</b>
<b>0 – 6</b>	Silt/Sand	3-26 °C	May June July	Nitronaphthalene: 0-17,700 2,4-DNT: 0-2580	1,3-DNB <sup>1</sup> : 0-111 2,4-DNT <sup>2</sup> : 8-76 1,2-CNB <sup>3</sup> :1-46	3-Nitroaniline: 11 2-Chloroaniline : 2 4-Chloroaniline: 2
<b>6 – 11.5</b>	Sand	6-23 °C	June July	Nitronaphthalene: 11,000-47,500 2,4-DNT: 3420-16,000	1,3-DNB: 7-163 2,4-DNT: 22-110 1,2-CNB: 82	3-Nitroaniline: 7 2-Chloroaniline: 2 4-Chloroaniline: 2
<b>11.5 –16</b>	Silt/Sand	11-17 °C	----	Nitronaphthalene: 0-23,800 2,4-DNT: 0-9,010	1,3-DNB: 107-216 2,4-DNT: 81-163 1,2-CNB:6-68	3-Chloroaniline:1
<b>16 – 23.5</b>	Sand	13-18 °C	February	Nitronaphthalene: 0-940 2,4-DNT: 0-300	1,3-DNB: 38-188 2,4-DNT: 25-125 1,2-CNB:10-57	3-Nitroaniline: 4 Aniline: 6 2-Chloroaniline: 3 4-Chloroaniline: 2

<sup>1</sup>Dinitrobenzene (DNB) <sup>2</sup>Dinitrotolune (DNT) <sup>3</sup>Chloronitrobenzene (CNB)

Table 8- Electron acceptors and microbial characterization with depth.

<b>Depth Range (ft)</b>	<b>Geology</b>	<b>Electron Acceptors (mg/L)</b>	<b>Shannon Index</b>	<b>Observed Microbial Species</b>
<b>0 – 6</b>	Silt/Sand	NO <sub>3</sub> <sup>-</sup> : 2.1-46 SO <sub>4</sub> <sub>2</sub> <sup>-</sup> :60-142 Dissolved Fe: <0.01-0.2	1.2-2.8	<i>Clostridium</i> spp. (8-16%) <i>Geobacter thiogenes</i> (0-5%) <i>Bacteriodes</i> spp. (0-9%)
<b>6 – 11.5</b>	Sand	NO <sub>3</sub> <sup>-</sup> : 0.3-33.1 SO <sub>4</sub> <sub>2</sub> <sup>-</sup> :52-117 Dissolved Fe:<0.01-0.7	1.0-2.7	<i>Pseudomonas stutzeri</i> (38-82%) <i>Diaphorobacter nitroreducens</i> (0-11%)
<b>11.5 –16</b>	Silt/Sand	NO <sub>3</sub> <sup>-</sup> : 2.8-4.3 SO <sub>4</sub> <sub>2</sub> <sup>-</sup> :185-520 Dissolved Fe: <0.01-0.1	3.3-3.6	<i>Pseudomonas</i> spp. (13-16%) <i>Proponibacterium acnes</i> (9-11%) <i>Massilia timonae</i> (6%)
<b>16 – 23.5</b>	Sand	NO <sub>3</sub> <sup>-</sup> :<0.1-3.32 SO <sub>4</sub> <sub>2</sub> <sup>-</sup> :115-1270 Dissolved Fe:<0.01-76	2.8-3.3	<i>Pseudomonas</i> spp.(13-27%) <i>Proponibacterium acnes</i> (10-13%) <i>Streptococcus pneumonia</i> (5-9%) <i>Chryseobacterium</i> spp. (0-14%)

#### *3.4.1.1 Depths of 0 - 6 ft*

The first zone (0 - 6 ft) is shallow and includes the vadose zone and water table (3 - 3.5 ft below ground surface). A silt layer is at the top of the zone before it transitions into a sand transmissive zone. The temperature in this zone fluctuates between 3 - 26°C, and the most temperature variation was observed at the most shallow depth (1.75 ft). Temperatures were elevated (defined as above 18°C) in May, June, and July. Moderate levels of contamination were observed at this depth. Although nitronaphthalene had the highest concentration in the soil core (i.e., up to 17,700 mg/kg), the highest aqueous contaminant concentrations were 111 mg/L for 1,3-dinitrobenzene and 76 mg/L for 2,4-dinitrotoluene.

Comparably low concentrations of suspected degradation products of reducing pathways, 3-nitroaniline (<11 mg/L), 2-chloroaniline (<2 mg/L), and 4-chloroaniline (2 mg/L) were also detected in aqueous samples. Under reducing conditions, the electronegative nitro group in NACs can be reduced to an amine group (Hallas & Alexander, 1983; Dickel et al., 1993; Peres et al., 1998; Wang et al., 2009). The presence of 3-nitroaniline, 2-chloroaniline, and 4-chloroaniline in the aqueous phase may indicate that reductive degradation of 1,3-dinitrobenzene, 1,2-chloronitrobenzene, and 1,4-chloronitrobenzene is occurring within this zone. However, aromatic amines may have been present in (upstream) source NAPL.

Reductive degradation (i.e., dechlorination) of chlorobenzene derivatives cannot be proven based on these field data since all potential products of reductive dechlorination reactions (e.g., nitrobenzene from chloronitrobenzene) are present as parent compounds in the NAPL source. However, the presence of chlorinated anilines (given they are a biodegradation product) may be an indication that the nitro substituent is reduced more readily than the chloro substituent under

site conditions. For the major contaminant nitronaphthalene as well as for all nitrated toluene derivatives, no aminated degradation products were detected. At least for nitronaphthalene, this may be due to a lower bioavailability based on its lower aqueous solubility.

Under aerobic conditions, further biodegradation of the produced anilines would likely occur (Nishino et al., 2000b). However, the detection of *Clostridium* spp., an obligate anaerobe, suggests anaerobic conditions are present at 4 ft and further biodegradation could be impeded. Furthermore, detection of methane in the soil gas suggests that oxygen in the vadose zone above the water table may be limited. Mineralization of aniline under denitrifying and sulfate-reducing conditions has been observed previously (Schnell & Schink, 1991; Swindoll et al., 1993; De et al., 1994; Kahng et al., 2000), even though not as readily as under aerobic conditions (Nishino et al., 2000b). Substituted anilines also may irreversibly chemisorb with the soil matrix by covalently bonding to natural organic matter (Schwarzenbach et al., 2003). This will only occur as long as sorption sites are available and not saturated with contaminants.

Nitrate and sulfate concentration ranged from 2 - 46 mg/L and 60 - 142 mg/L, respectively.

Without additional analyses upstream of the MLS, the exact source of nitrate - whether present at the site or stemming from NAC degradation - cannot be identified. The nitro substituent on the NACs is released as ammonia via reducing microbial processes or as nitrite via oxidizing processes. To form nitrate, both require subsequent oxidation with O<sub>2</sub> as electron acceptor. In the August 2014 sampling, substantially higher concentrations of nitrate (21 - 46 mg/L) were detected in this top zone compared to greater depths (0 - 5.8 mg/L). Increased nitrate concentrations may be due to (temporary) aerobic biodegradation processes, which may have been stimulated by increased temperatures in shallow strata and slightly elevated water table.

Unfortunately, potential intermediates of aerobic NAC degradation were not analyzed for and can thus not support this hypothesis.

At 4 ft and 4.5 ft, the highest amount of bacterial and archaeal species were observed. Microbial communities were diverse and not greatly impacted by the transition from silt to sand.

*Clostridium* spp. accounted for 8-16% of the microbial community at 4 - 4.5 ft. Certain species of *Clostridia* have been found to degrade organic contaminants like trinitrotoluene (Kutty & Bennet, 2005; Regan & Crawford, 1994). *Geobacter thiogenes* was found at 4.5 ft and accounted for 5% of the microbial community. *Geobacter thiogenes* and its close relative *Geobacter lovley* strain SZ have been reported to reductively dechlorinate chlorinated compounds (De Wever et al., 2000). However, *Geobacter thiogenes* has not (yet) been reported in the literature to dechlorinate compounds specific to the investigated site, such as chlorobenzene, dichlorobenzene, or chloronitrobenzene. A large percent (37-78%) of the microbial community in this zone was identified as no hit, meaning the species have not been isolated and included in the analysis database. Other environmental studies also have reported large percentages (2-46%) of unclassified bacterial reads showing this is a common occurrence in environmental samples (Nacke et al., 2013; Inceoglu et al., 2011; Sutton et al., 2013). Small quantities of methanogens were also present at a depth of 4 ft, but they were less abundant than bacterial species. The methanogens in this zone are most likely the source of the methane observed during gas sampling. Methanogens were only above detection limits in this zone, suggesting methanogenesis is not a dominant biological process throughout the subsurface. Degradation processes may be linked primarily to nitrate- or sulfate-reduction in other zones.

### 3.4.1.2 Depths of 6 - 11.5 ft

Depths from to 6 to 11.5 ft are located in a sandy transmissive zone. Temperature in this zone ranged from 6 - 23°C. These depths reached 18°C in June and July. At 11 ft, NAPL was observed in the aqueous samples just above the silt layer. The maximum concentration of nitronaphthalene (47,500 mg/kg) was located at the top of this zone, and the maximum concentration of 2,4-dinitrotoluene (16,000 mg/kg) was located at 11.5 ft just above the silt layer. Maximum aqueous concentrations of 1,3-dinitrobenzene (7 - 163 mg/L), 1,2-chloronitrobenzene (82 mg/L), and 1,4-chloronitrobenzene (82 mg/L) in this zone were also located above the silt layer. Small concentrations of 3-nitroaniline (< 7 mg/L), 2-chloroaniline (< 2 mg/L), and 4-chloroaniline (< 2 mg/L) were also observed, which suggest partial reductive degradation of dinitrobenzene and chloronitrobenzene could also be occurring within this zone.

Concentrations of nitrate (< 5 mg/L) and dissolved iron (< 0.01 mg/L) were generally low, while sulfate concentrations increased with depth from (50-120 mg/L for April and 60-170 mg/L for August). Consequently, electron acceptor analyses suggest that this zone is likely sulfate-reducing, although methanogenic niches may exist (WRSC, 2006).

From 6 ft to 11.5 ft below ground surface, the microbial community is largely made up of *P. stutzeri*. Low Shannon diversity indices (1.01 to 2.65) were observed in this zone, indicating limited microbial diversity. The lowest index was observed at 7 ft, where *P. stutzeri* accounted for 83% of the microbial community, indicating that this bacterium may play a key role in biodegradation processes at the site. The high abundance of the species was in a zone of high contamination and located in a sandy transmissive zone. *P. stutzeri* was not observed in the silty clay layer, suggesting the transmissive zone is providing favorable conditions for *P. stutzeri*,

possibly by allowing increased transport of nutrients and removal of degradation products at higher rates than low permeability zones such as silts. *P. stutzeri* is a facultative aerobe, but some strains are capable of denitrification (Lalucat et al., 2006). Extensive research has been performed on the ability *P. stutzeri* to aerobically degrade aromatic compounds such as benzene, naphthalene, chloronaphthalene, chloronitrobenzene, toluene, and xylene (Baggi et al., 1987; Bertoni et al., 1996; Cafaro et al., 2004; DiLecce et al., 1997; Garcia-Valdez et al., 2003; Li et al., 2005); however, less is known about how *P. stutzeri* responds to xenophobic compounds under anoxic conditions occurring in the subsurface. *P. stutzeri* has been found to degrade pyrene, phenanthrene, naphthalene, benzoate, fluorobenzoate, and salicylate under nitrate-reducing conditions (McNally et al., 1999; Rockne et al., 2000; Vargas et al., 2000; Hirano et al., 2004). Biodegradation under nitrate-reducing conditions were found to be slower than aerobic conditions (McNally et al., 1999). Strains of *P. stutzeri* have previously been isolated from the site and have been found to degrade chlorobenzene, 1,2-dichlorobenzene, and 1,4-dichlorobenzene at anoxic/oxic interfaces (Kurt & Spain 2013). Due to the abundance of chemicals in the soil core and water samples, it is difficult to determine which contaminants may be degraded by *P. stutzeri*. Nevertheless, in contrast to the electron acceptor analysis discussed above, the presence and dominance of *P. stutzeri* suggests that biological activity in this zone is predominantly coupled to nitrate reduction, and due to low nitrate concentrations, likely limited by its availability.

#### 3.4.1.3 Depths of 11.5-16 ft

A silt/clay low permeability zone was located at the top of this zone from 12.2 - 13.7 ft. Temperature within this zone ranged from 11 - 17°C. The temperature did not exceed 18°C from December to August. In the third zone (11.5 - 16 ft), NAPL was visually observed in the water

samples, and correspondingly high contaminant concentrations were measured in the soil core. High aqueous contaminant concentrations were observed in the silt/clay layer. Maximum concentrations of 1,3-dinitrobenzene (210 mg/L), 2,4-dinitotoluene (160 mg/L), and nitronaphthalene (150 mg/L) were found at 14 ft. Possible degradation products 3-nitroaniline (4 mg/L) and 2-chloroaniline (1 mg/L) were detected in the highly contaminated area. As discussed in the previous section, amine byproducts may be degraded under sulfate and nitrate reducing condition but likely form irreversible complexes with natural organic matter. (Hallas & Alexander, 1983; Dickel et al., 1993; Peres et al., 1998; Wang et al., 2009). Nitrate ranged from below detection (0.01 mg/L) to 4.3 mg/L, while dissolved iron remained mostly low (< 0.1 mg/L) and sulfate concentrations ranged from 185 mg/L to 520 mg/L, suggesting sulfate-reducing conditions were predominant.

Microbial community analysis showed increased diversity compared to the 6 – 11.5 ft. Shannon Indices ranged from 3.3 -3.58 for 12 - 16 ft. Subsurface conditions are not providing favorable conditions for only one specific microorganism as observed in the upper transmissive zone. *Streptococcus pneumonia*, *Staphylococcus epidermidis*, and *Propionibacterium acnes* were found in the environment below 12 ft. While these bacteria species can be present in human skin flora or act as pathogens, they are also commonly found in soil systems (Wieser et al., 2000; Evstigneeva et al., 2009).

#### 3.4.1.4 Depths of 16-23.5 ft

A transmissive sand zone was observed from 16 - 23.5 ft. Temperature fluctuated between 13 - 18°C and reached the 18°C threshold temperature in February. Contaminant concentrations in the core were primarily below detection, while aqueous contaminant concentrations were still

detected. Analysis of soil core revealed low concentrations of major site contaminants, such as nitronaphthalene (0 - 940 mg/kg) and 2,4-dinitrotoluene (0 - 300 mg/kg). Aqueous concentrations of 1,3-dinitrobenzene, 2,4-dinitrotoluene, and 1,4-chloronitrobenzene were 38 - 188 mg/L, 25 - 125 mg/L, and 10 - 57 mg/L, respectively. The differences between aqueous and soil core concentrations may be attributed to site heterogeneity, since the soil core was not taken from the exact location of the multilevel sampler. Low concentrations of aniline (6 mg/L), 3-nitroaniline (< 4 mg/L), 2-chloroaniline (< 3 mg/L), and 4-chloroaniline (< 2 mg/L) indicate possible reduction of nitrobenzene, dinitrobenzene, and chloronitrobenzene.

Nitrate concentrations ranged from below detection (0.01 mg/l) to 3.2 mg/L and were below detection in the August water samples. Sulfate concentrations ranged from 115 - 1,270 mg/L. The high sulfate values suggest methanogenic conditions are not prevalent at these depths. Microbial communities were similar to those observed from 11.5 - 16 ft. Biogeochemical conditions did not appear to provide favorable conditions for one specific species of microorganisms, and high diversity was observed. Shannon indexes ranged from 2.78 to 3.30.

### ***3.4.3 Impedance with Depth***

Impedance measurements appear primarily to be influenced by site geology rather than by the presence of aqueous inorganics, DNAPL, or ionic degradation intermediates. The largest observed changes in the impedance measurements were at the shallowest and deepest depths. At shallow depths, the high measurement is occurring within the vadose zone, meaning the pore space is not completely saturated and less conductive. At the final measurement, impedance values increase drastically compared to the measurements obtained from all other depths. The electrical conductivity of the water sample taken from 24 ft increased, which is expected to

correspond to a decrease in impedance since impedance and electrical conductivity are inversely related. However, impedance drastically increases suggesting the impedance is less dependent on the pore fluid and more affected by changes in porosity. A known clay layer is located around 26 ft, due to heterogeneity in the soil, the clay layer may be higher at the location of the multilevel sampler than where the macrocore was obtained. Further statistical analysis such as principal component analysis is needed to fully assess the impact of each biogeochemical parameter on the impedance reading. This analysis was not included in the scope of the present study.

## 4. ANAEROBIC MICROCOSM STUDY

### 4.1 Introduction

A microcosm experiment using site soil was conducted to evaluate the effect of temperature on natural attenuation processes of NACs. Previous analyses of contaminant concentrations in soil cores and aqueous samples have shown maximum contaminant concentrations at ~12 ft bgs above a confining clay layer. Low nitrate concentrations ( $< 5$  mg/L) within this zone suggested oxygen was not present, and the study was performed under anaerobic conditions to represent field conditions.

### 4.2 Methods

#### 4.2.1 *Microcosm Set-up*

Soil core sampling was performed by URS. A Geoprobe® rig configured for direct push drilling was used to collect cores in 2 inch diameter disposable acetate liners from 2 ft to 12 ft below ground surface. In the field, the 5 ft acetate liners were cut in two, flushed with nitrogen, and placed into an anaerobic glove bag to maintain anoxic conditions. Samples were kept on ice or refrigerated at 4°C for two days before being shipped on ice to Colorado State University, Fort Collins, CO.

In an anaerobic chamber consisting of 98% nitrogen and 2% hydrogen, soil cores were homogenized by hand for two hours. After homogenization, 250-mL serum bottles were filled with 300 g of soil. The bottles were sealed with blue butyl stoppers (BellCo Glass, Vineland, NJ) and a crimp seal to maintain anaerobic conditions throughout the experiment.

To collect the produced biogas and prevent the buildup of gaseous byproducts, microcosms were connected with Teflon tubing to 100-mL graduated cylinders inverted in water. As gas was produced, gas traveled through the tubing to the graduated cylinder. Produced gas displaced water out of the bottom of the cylinder, and gas remained trapped in the upper portion. To allow for periodic gas sampling throughout the microcosm study, a glass T-connector was connected to the tubing running between the graduated cylinder and the soil microcosm. A schematic of the gas collection setup is shown in Figure 22. On the third microcosm for each temperature, a bottle of solvent (octanol) was added to the gas lines in an attempt to quantify volatilization losses from the microcosms. Killed controls were not available in this study due to safety concerns regarding the addition of mercuric chloride or sodium azide.

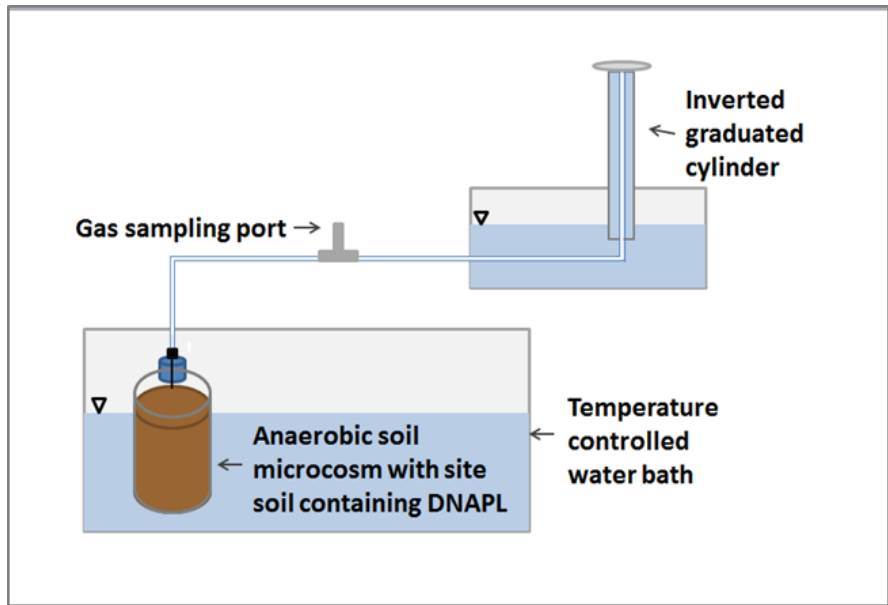


Figure 22 – Microcosm set up modeled after Zeman et al. (2012)

Microcosms were kept at temperatures of 10°C, 14°C, 18°C, 22°C, 26°C, and 30°C. The middle temperatures, 18°C and 22°C, are the upper range observed in the field, and 10°C and 14°C are the lower end of the temperatures observed in the field. Constant temperatures were maintained

using refrigeration for temperatures below ambient. Heated water baths were used for ambient temperature and above. Constant temperatures were maintained at the prescribed value for the duration of the 350 day study.

#### ***4.2.2 Contaminant Concentration Analysis***

Microcosm soil samples were analyzed in triplicate for initial and final contaminant concentrations. Contaminants were extracted using dichloromethane. Dichloromethane was added to each sample in a ratio of 1-mL dichloromethane to 1 g soil. Extractions were diluted 1:10 with dichloromethane, so concentrations would fall within the range of the calibration curves. The same analytic methods described in Chapter 3 were used to detect and quantify organic compounds. Statistical analysis was conducted on initial and final contaminant concentrations to assess if significant degradation had occurred in the microcosms. Microsoft Excel was used to perform a two-sample unequal variance t-test with two distribution tails. A 95 percent confidence interval was used to assess significance.

The total carbon (g/kg) in the measured contaminants was determined using stoichiometry. The average contaminant concentrations (mg/kg) were divided by the contaminant's molecular weight to determine the number of moles of contaminant per kg of soil.

$$\left(\frac{\text{Contaminant Mass mg}}{\text{kg of soil}}\right) \times \left(\frac{1 \text{ g}}{1000 \text{ mg}}\right) \times \left(\frac{\text{moles Contaminant}}{\text{Molecular Weight g}}\right) = \frac{\text{moles Contaminant}}{\text{kg of soil}}$$

The number of carbons per contaminant was then multiplied by the moles of each compound to determine moles of carbon per kg of soil.

The moles of carbon were then multiplied by the molecular weight of carbon to determine the grams of carbon per kg of soil.

$$\left(\frac{\text{moles Contaminant}}{\text{kg of soil}}\right) \times \left(\frac{\text{moles Carbon}}{\text{moles Contaminant}}\right) \times \left(\frac{12 \text{ g}}{\text{mole Carbon}}\right) = \frac{\text{g Carbon}}{\text{kg of soil}}$$

The grams of carbon per kg for each quantified contaminant were summed to find the total contaminant bound carbon (g/kg).

#### ***4.2.3 Microbial Analysis***

To characterize the microorganisms present in the soil core, an initial microbial analysis was performed on the homogenized site soil prior to microcosm setup. Three samples were placed in 15-mL plastic centrifuge vials and kept frozen at -20°C for a day prior to DNA extraction. Microbial analysis was performed on homogenized site soil following the procedures for pretreatment and DNA isolation detailed in Chapter 3. Pyrosequencing was performed by Research and Testing, LLC (Lubbock, TX) using a GS FLX+ 454TM Pyrosequencer (Roche, Branford, CT). The primers for eubacteria were 939f and 1492r, and the archaeal assays used primers 341f and 958r. Diversity analysis classified microorganisms based on how closely their identity matched well-characterized sequences in their database. Identity scores greater than 97% were classified to the species level, 95-97% for genus level, 90-95% for family level, 85-90% for order level, 80-85% for class level, and 77-80% phyla level.

#### ***4.2.4 Gas Sampling Procedures***

When approximately 5 mL of gas sample had accumulated in the inverted 100 mL graduated cylinder, a gas sample was removed for analysis. Gas was removed from the microcosm sample using a 5 mL gas-tight glass syringe. A 50 µL subsample was taken to measure the amount of

methane and carbon dioxide in the produced gas. The 50  $\mu$ L subsample was injected into Hewlett Packard 5890 Series II gas chromatograph with thermal conductivity detector (GC-TCD) (Wilmington, DE) with a Hayesep 8"x 1/8" Q 80/100 column with helium as the carrier gas. The GC-TCD method consisted of holding the oven temperature at 40°C for 4 minutes. Calibrations were performed using a gas standard containing 5% carbon dioxide and 4% methane (Restek, Bellefonte, PA) diluted with nitrogen gas (Airgas, Radnor, PA).

To further resolve the gas composition, additional fixed gas analysis was performed by CH2MHill (Corvallis, OR) to quantify the amount of nitrogen, oxygen, carbon dioxide, and methane in the gas samples. A vacuum was pulled on a 20mL vial. The vial was then crimped sealed with a gray PTFE/butyl rubber septum. Gas samples from microcosms were taken with a glass 5 mL syringe and injected into the 20mL vial. The bottles were then shipped to CH2M Hill in Corvallis, OR to determine the fixed gases in the biogas samples. A gas sample standard with a known amount of methane and carbon dioxide also was shipped with the samples to ensure leaks were not occurring during transport.

#### ***4.2.5 Soil Analyses***

Microcosm soils were analyzed for ammonia, nitrate, total nitrogen, sulfate as bound sulfur ( $\text{SO}_4^{2-}$ -S), total sulfur, total organic carbon, and total inorganic carbon at the beginning and end of the study. Analyses were performed by the Soil, Water, and Plant Testing Laboratory at Colorado State University, Fort Collins, CO. To analyze nitrate and ammonia, samples were treated with potassium chloride, and a flow injection analysis was performed. Total nitrogen in the samples was determined by using a Leco TruSpec CN furnace (St. Joseph, MI). Total sulfur samples were digested in nitric and perchloric acids prior to analysis, and  $\text{SO}_4^{2-}$ -S was extracted

with monocalcium phosphate. Inductively coupled plasma analysis was then performed on the digest or extract to determine total sulfur and  $\text{SO}_4^{2-}$ -S. Total inorganic carbon (TIC) was determined gravimetrically using a 6 N hydrochloric acid. Total organic carbon (TOC) was determined by subtracting total inorganic carbon from total carbon (TC) (i.e.,  $\text{TC}-\text{TIC}=\text{TOC}$ ). Total carbon in the sample was found using a Leco TruSpec CN Furnace, and TIC was measured gravimetrically using 6 N hydrochloric acid.

### **4.3 Results**

Table 9 includes the average concentrations of contaminants measured in the soil microcosms. Initial analysis of the soil core revealed high concentrations of NACs. The highest concentrations were nitronaphthalene (18,200 mg/kg) and 2,4-dinitrotoluene (10,200 mg/kg). Maximum concentrations of dinitrobenzene and chloronitrobenzene were 5,870 mg/kg and 3,190 mg/kg. Relatively low concentrations of chlorobenzene (158 mg/kg) and dichlorobenzene (63 mg/kg) were found in the soil core. Maximum concentrations of toluene, xylene, and ethylbenzene were 56 mg/kg, 8 mg/kg, and 6 mg/kg respectively. The total carbon bound in the contaminants was 24.1 g/kg. Total organic carbon in the soil (via TOC analysis) was determined to be 2.41% or also 24.1 g/kg, in agreement with GC-MS analysis.

Table 9- Average concentrations of detected contaminants in the soil core used for the microcosm study.

Contaminant	Average Concentration	Carbon
	(mg/kg)	(g/kg)
Nitronaphthalene	16,713	11.59
2,4-Dinitrotoluene	9,585	4.42
1,3-Dinitrobenzene	4,888	2.10
1,4-Chloronitrobenzene	2,895	1.32
2,6-Dinitrotoluene	2,246	1.04
1,2-Chloronitrobenzene	2,044	0.935
2-Nitrotoluene	1,889	1.160
4-Nitrotoluene	1,147	0.703
1,2-Dinitrobenzene	680	0.292
Naphthalene	248	0.232
Chlorobenzene	149	0.095
Nitrobenzene	130	0.076
3-Nitrotoluene	86	0.053
1,2-Dichlorobenzene	57	0.028
Toluene	51	0.047
1,4-Dichlorobenzene	28	0.014
2-Xylene	7	0.007
Ethylbenzene	5	0.005
	<b>Total Contaminant Bound Carbon</b>	24.1

Based on a two sample T-test analysis, initial and final concentrations indicated a statistically significant decrease in ethylbenzene (Figure 23A), xylene (Figure 23B), toluene (Figure 23C), and chlorobenzene (Figure 23D) concentrations. Significant degradation of xylene was observed at all temperatures (Figure 23B), while the other compounds experienced degradation at specific temperatures or temperature ranges. Ethylbenzene showed significant losses at 14°C, 22°C, 26°C, and 30°C. Significant losses of chlorobenzene and toluene (Figure 23C&D) were observed in microcosms at 14 - 22°C.

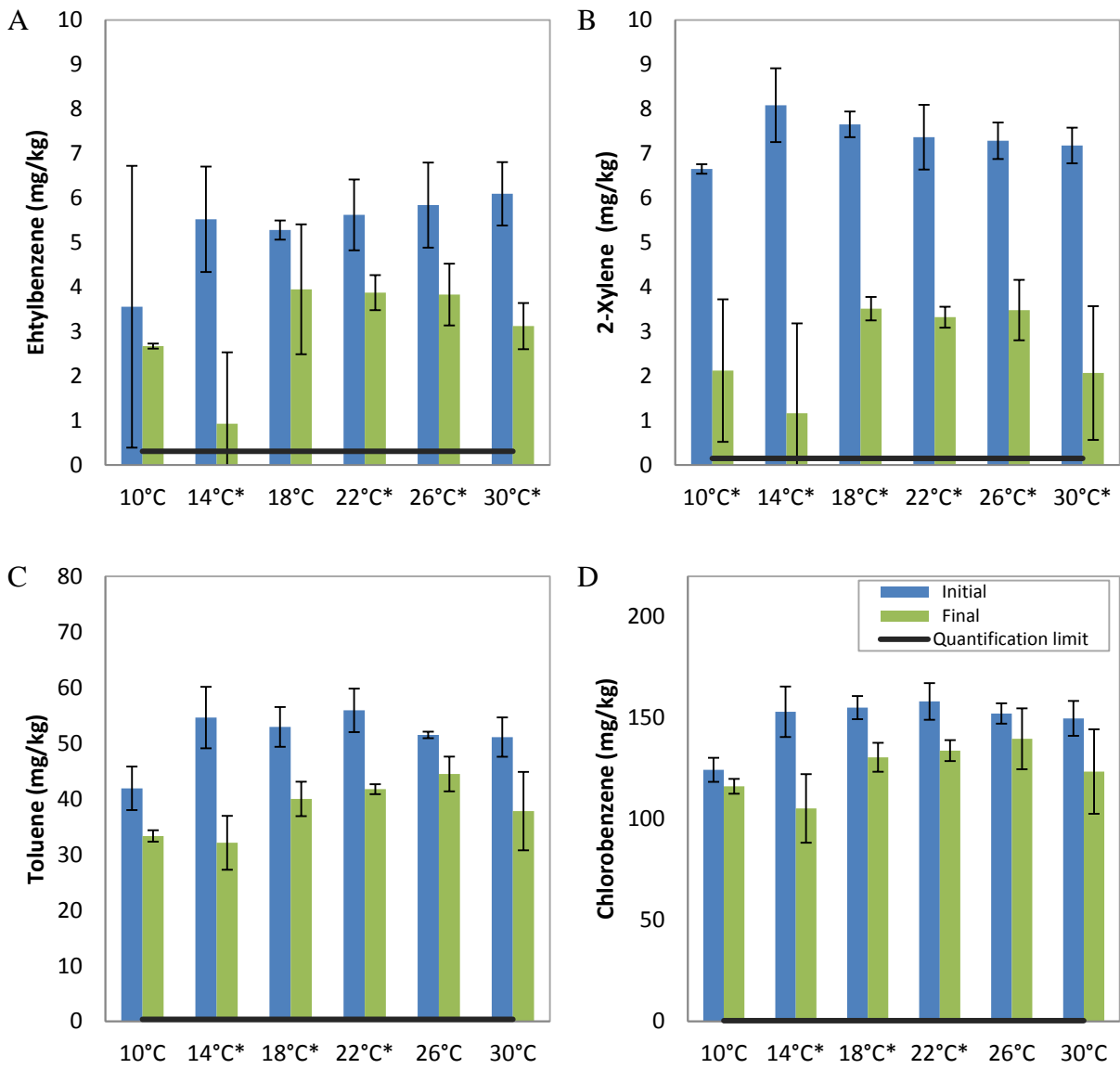


Figure 23 –Contaminant concentrations of A) ethylbenzene B) 2-xylene C) toluene and D) chlorobenzene before and after treatment. The blue bars represent initial concentration, and the green bars represent final concentration. \*Indicates a significant decrease in concentration.

Figure 24 shows initial and final concentrations of 1,4-dichlorobenzene (A), naphthalene (B), 2,4-dinitrotoluene (C), and nitronaphthalene (D). Significant degradation was not observed for these compounds.

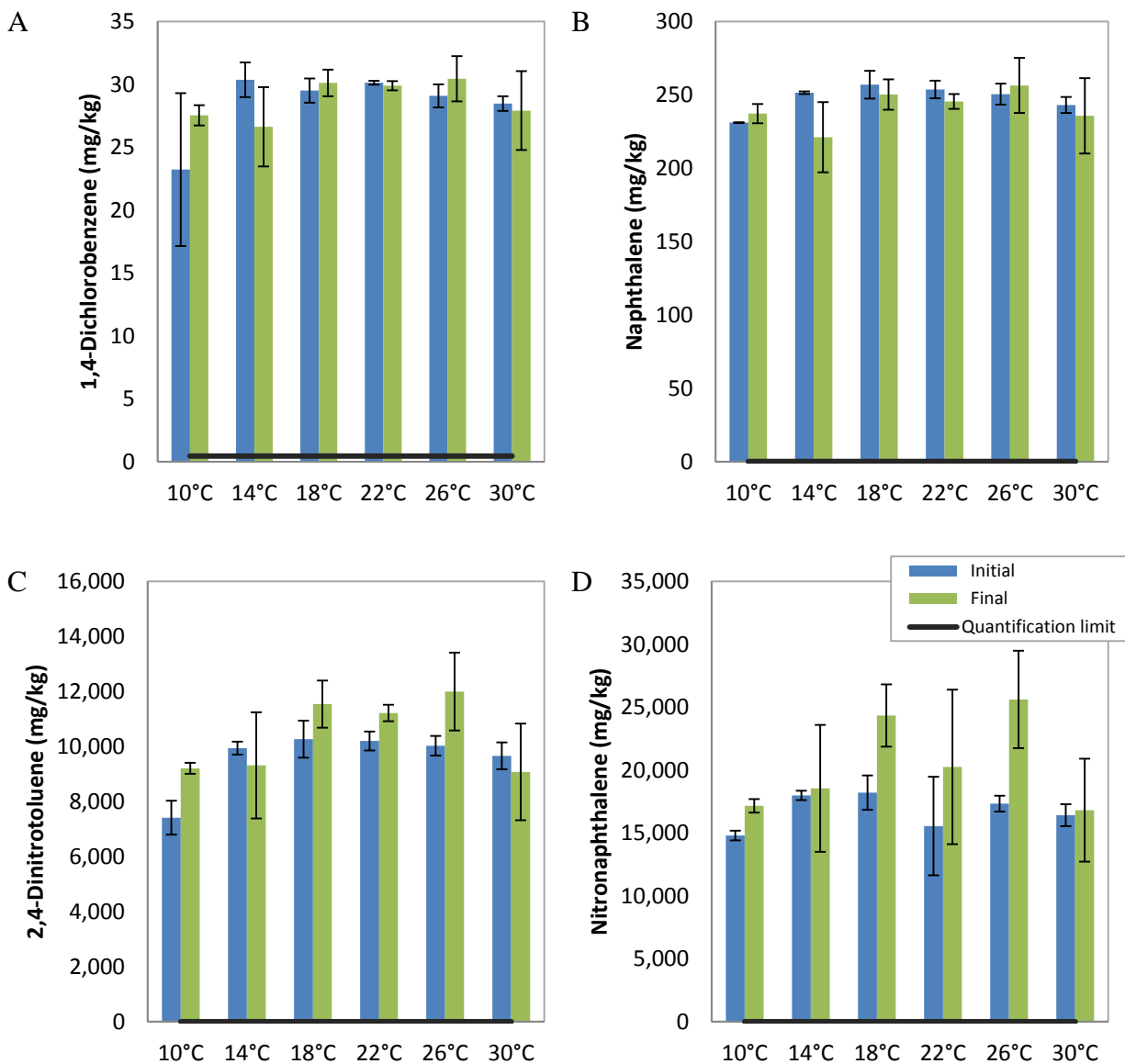


Figure 24 –Contaminant concentrations before and after treatment of A) 1,4-dichlorobenzene B) naphthalene C) 2,4-dinitrotoluene D) nitronaphthalene. The blue bars represent initial concentration, and the green bars represent final concentration.

Figure 25 shows the concentrations of 1,3-dinitrobenzene and 1,4-chloronitrobenzene.

Significant degradation was not observed. Initial and final concentrations of other detected compounds are included in Appendix C, and significant degradation was not observed.

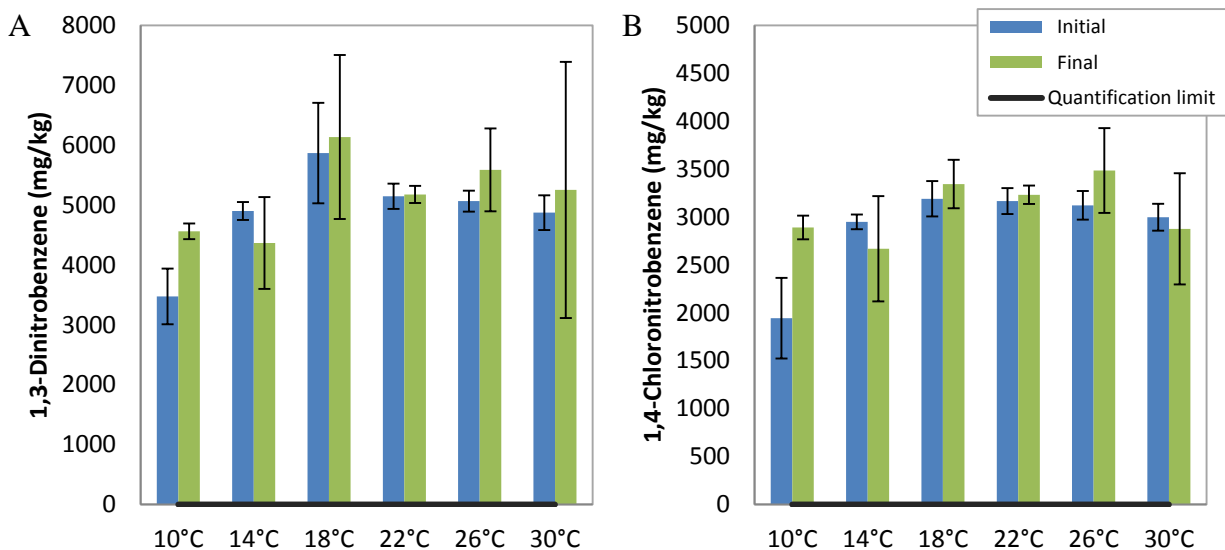


Figure 25 –Contaminant concentrations of 1,3-dinitrobenzene and 1,4-chloronitrobenzene before and after treatment . The blue bars represent initial concentration, and the green bars represent final concentration.

Further analysis was performed on the soil samples to determine the amount of ammonia (as a potential degradation product), nitrate, and sulfate (as potential electron acceptors) in the microcosm soils (Figure 26). An increase in ammonia was observed for all temperatures except for 10°C. A decrease in sulfate concentration was observed at all temperatures with the highest decrease at 18°C and 26°C. Nitrate concentrations were small and did not vary substantially from the initial concentration.

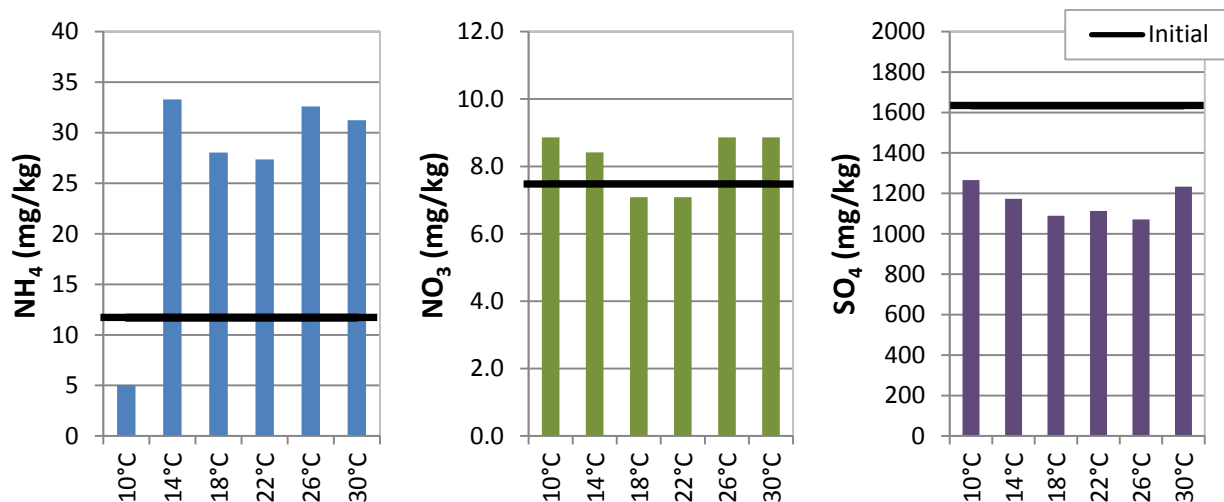


Figure 26 – Ammonia, nitrate, and sulfate concentrations in microcosms. The black line shows the concentration prior to treatment and the bars labeled by temperature show concentrations after treatment.

Small quantities (volumes < 25 mL) of gas were produced and measured throughout the microcosm experiment. The average amount of gas observed in duplicate microcosms over time is presented in Figure 27. Triplicate data was not available for the gas samples due to a change in experimental set up on the third microcosm. A bottle of solvent (octanol) was added to the gas lines on the third microcosms in an attempt to quantify potential volatilization losses. However, volatilization of octanol led to increased gas production in these microcosms. Thus, these microcosms were excluded from gas quantification. Analysis of the octanol via GC-MS did not reveal volatilization losses of the organic contaminants in the microcosms.

The order of observed gas production was 18°C > 22°C > 26°C > 14°C > 30°C > 10°C (Figure 27). The fact that more gas production was observed at median temperatures, 18°C and 22°C, than at 26°C and 30°C confirms that contaminant volatilization did not lead to gas production. Only small traces of CO<sub>2</sub> similar to atmospheric conditions were observed in the gas samples. Further fixed gas analysis was performed to determine the composition of the gas produced by

the microorganisms. Analysis of duplicate samples revealed the samples were composed of 18% oxygen and 82% nitrogen. Methane and carbon dioxide were not above the specified detection limits of 0.4% and 0.5% respectively. The analysis of the standard showed the presence of methane and carbon dioxide, which suggests that the samples did not leak during sample storage and transport.

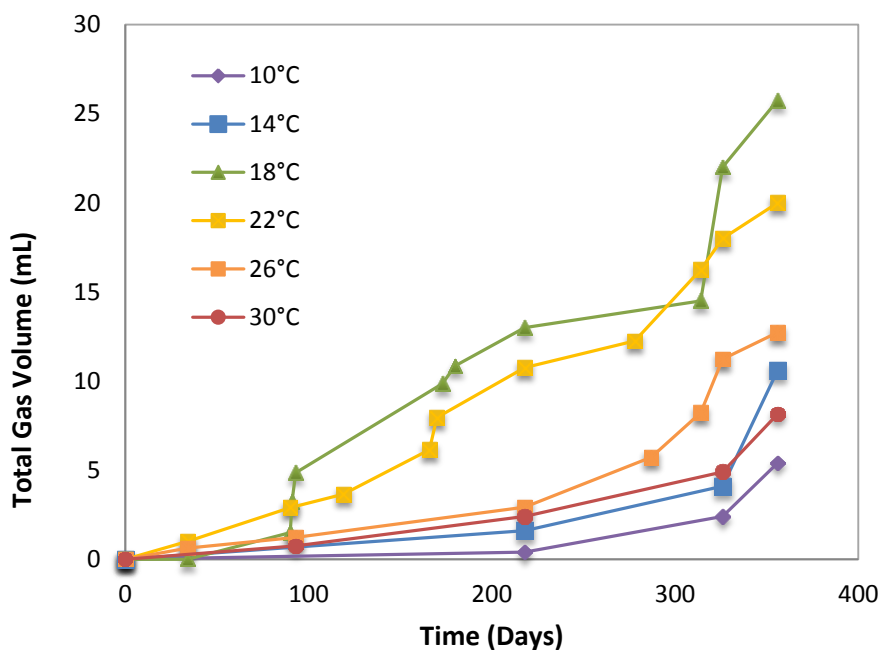


Figure 27 – Total average cumulative gas volume produced by (duplicate) soil microcosms over the duration of the experiment.

The initial microbial analysis performed on the soil found 42% of the bacterial 16S rRNA genes came from *P. stutzeri* (Figure 28). Other *Pseudomonas* species accounted for 20% of the bacterial community. *Pigmentiphaga daeguensis* and *Bacillus subtilis* species made up 6% and 4% of the bacterial community respectively. The archaea community primarily consisted of *Methanocella paludicola* (65%) and *Candidatis nitrosopumilus* spp. (28%). Species accounting for 1% or less of the bacterial or archaeal communities were included in the pie charts in gray and marked as other. Microbial analyses of microcosms at the end of the experiment were not

performed since the overall degradation performance did not justify the current high cost associated with DNA analysis.

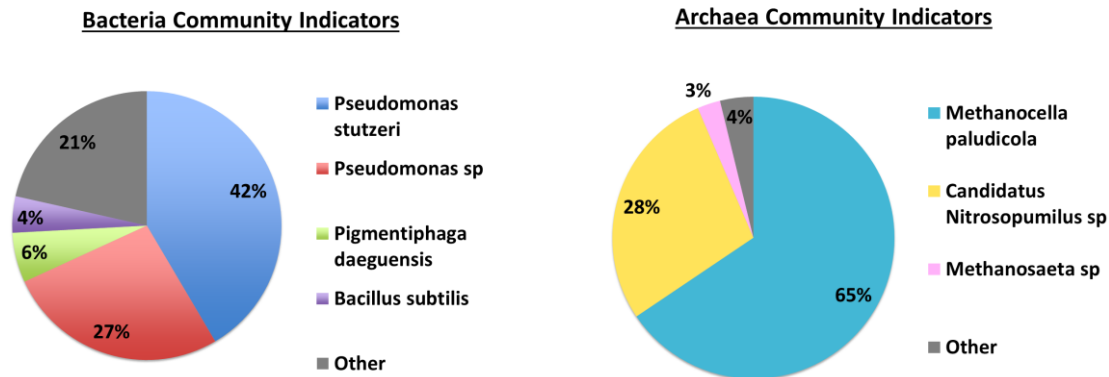


Figure 28 – Initial microbial analysis of the homogenized soil core used in microcosms.

#### 4.4 Discussion

The amount of contaminant bound carbon from GC/MS analysis of the detected contaminants were equal to the total organic carbon in the soil, indicating that the primary organic contaminants were all detected in the contaminant analysis. This leads to the conclusion that the high CO<sub>2</sub> fluxes determined at the site stemmed from mineralization of NACs under natural (anoxic) conditions.

Comparisons of concentrations before and after treatment indicate significant degradation of xylene at all temperatures. Toluene, ethylbenzene, and chlorobenzene were degraded significantly only at select temperatures with no clear trend except that no significant degradation was observed at 10°C, the lowest temperature. Thus, these results do not imply an optimal temperature for enhancing degradation processes at the site. Since killed controls were not available for this study, it cannot be determined if losses are from biodegradation or abiotic

processes, although BTEX compounds are usually persistent to abiotic degradation in the absence of a strong oxidant.

For dichlorobenzene, no significant decrease in contaminant mass was observed during the year-long experiment. The rates of reductive dechlorination are well known to decrease with decreasing number of chloro substituents (Tiehm & Schmidt, 2011). Given that chlorobenzene degradation was significant (at least at some temperatures) but dichlorobenzene degradation was not, and since benzene was not detected in the microcosms, it appears likely that chlorobenzene was degraded through an oxidative pathway leading to ring cleavage. However, other potential reductive reactions cannot be excluded such as hydrogenation of the aromatic ring, as observed for anaerobic benzene degradation (Grbic-Galic & Vogel, 1987).

Furthermore, no significant degradation was observed for any of the NACs, including dinitrobenzene and chloronitrobenzene, for which aminated products of reductive degradation had been detected in the field (Chapter 3). However, a substantial increase in ammonia was observed in all microcosms except for the microcosm held at 10°C. Ammonia release is indicative of nitrobenzene degradation by a pathway involving an initial reduction of the nitro group (Nishino & Spain, 1993). However, on a molar basis, the generated ammonia corresponds to less than 1% of the nitrogen bound in the present NACs (i.e., ~1 mmol/kg vs. >100 mmol/kg). These findings indicate that NACs were potentially degrading beyond reduction to aniline, but that rates were very slow such that mass losses were within experimental variation, not leading to statistically significant NAC depletion.

A lack of CO<sub>2</sub> production in the soil microcosms differed greatly from the CO<sub>2</sub> fluxes observed in the field. CO<sub>2</sub> fluxes ranging from 10 - 18 μmole/m<sup>2</sup>·sec were measured in the contaminated

area of the site. These fluxes were elevated 3 - 9  $\mu\text{mole}/\text{m}^2\cdot\text{sec}$  above fluxes recorded in a non-manufacturing area. Analysis of  $^{14}\text{C}$  in the  $\text{CO}_2$  flux showed 50% of the carbon came from fossil fuel-derived organic matter suggesting natural degradation of contaminants is occurring in the subsurface. Furthermore, no methane was detected in the gas generated in the microcosms, in contrast to field soil gas analyses. Despite promising indication of natural attenuation in the field, significant amounts of biologically generated gas were thus not observed in laboratory experiments. Consequently, it appears likely that soil homogenization preceding microcosm setup led to destruction of biogas producing microniches (see below) or that the high fluxes of  $\text{CO}_2$  stemmed from natural contaminant degradation processes in the (highly heterogeneous) vicinity of the soil core collected for the microcosms, possibly from the degradation of more readily degradable contaminants such as hydrocarbons.

The same conclusion of microniche destruction may apply to NAC degradation, which was not observed to a significant extent in the microcosms despite detection of aminated degradation products in the field. Microcosms were constructed by homogenizing macrocores taken from 2 - 12 ft bgs, which mixed different biogeochemical zones and may have created unfavorable conditions for site microorganisms. Microbial diversity analysis from the field demonstrated certain depths provided favorable conditions for microorganisms due to the presence of certain redox conditions, electron donors, and contaminant concentrations. For instance, DNA and electron acceptor analyses revealed that in the two shallow zones of the aquifer, from which the soil core for the microcosm study was taken, degradation processes proceeded primarily under nitrate-reducing conditions (Chapter 3). In the microcosms, however, degradation appeared to be linked to sulfate reduction, implying that the microbial community and their degradation processes and activities may have shifted away from original site conditions. Based on an

electron balance (assuming that sulfate is reduced to sulfide and organic contaminants are mineralized to CO<sub>2</sub>), the average amount of sulfate depleted (472 mg/kg) accounts for the degradation of 173 mg/kg of nitrobenzene or 102 mg/kg of benzene. For NACs at high concentrations, degradation may have been within the experimental error. Therefore, significantly decreased concentrations were not observed.

Additionally, soil homogenization may have destroyed electron acceptor gradients located in the vadose zone, which could limit mineralization rates. Previous studies have shown NACs under reducing conditions are resistant to further degradation following an initial reduction of the nitro group (Nishino et al., 2000b). Bacteria capable of degrading site contaminants may have been present in the soil microcosms, but absence of anoxic/oxic interfaces may have prevented mineralization from occurring. Kurt et al. (2012) demonstrated the ability of oxic/anoxic interfaces to prevent chlorobenzene and nitrobenzene migration using sediment from the contaminated site. Indigenous microorganisms were capable of degrading chlorobenzene at a rate of 2-4.2 g CB·m<sup>-2</sup>·d<sup>-1</sup> and nitrobenzene at a rate of 6.5 g NB·m<sup>-2</sup>·d<sup>-1</sup> when exposed to an oxic interface. Microbial analysis of the sediment exposed to nitrobenzene revealed biogeochemical conditions were favorable for *Pseudomonas* sp., *P. mendocina*, and *P. putida*, which were similar to the species detected in the initial microbial diversity analysis of the microcosm soil. *Pseudomonas stutzeri* isolated from site soil samples has been found to grow on chlorobenzene, 1,2-dichlorobenzene, and 1,4-dichlorobenzene at oxic/anoxic interfaces (Kurt & Spain, 2013). The abundance of *P. stutzeri* and other *Pseudomonas* species in the initial microbial analysis may indicate similar processes are occurring at anoxic/oxic interfaces, and dichlorobenzene and possibly other contaminants may be degrading. However, *P. stutzeri* was only found in contaminated transmissive zones where nitrate-reducing conditions predominated, and oxic

conditions even at the surface of the water table may not (permanently) exist based on the presence of methane, which was detected in the site soil gas.

Moreover, static no-flow conditions within the microcosms may have prevented higher degradation rates due to accumulation of toxic intermediates and/or prevented replenishment of electron acceptors. The dominance of nitrate-reducing bacteria in the upper zones of the aquifer, from which the microcosm soil was obtained, in combination with low nitrate-concentrations suggested that biodegradation at the site is limited by the availability/transport rate of nitrate (Chapter 3).

Finally, contamination has been found highly to influence microbial community structure. For example, a site with diesel contamination showed lower microbial diversity in contaminated areas (Sutton, 2013). In uncontaminated sites, soil type and pH have also been found to influence microbial communities (Girvan et al., 2003 Lauber et al., 2009). Irianni Renno et al. 2013 demonstrated how the presence of petroleum hydrocarbons and certain electron acceptors provided conditions where certain microorganisms thrived. When the soil core was homogenized to create the microcosms, different zones were mixed together, likely eliminating favorable environments for indigenous site microorganisms.

## 5. SUMMARY AND CONCLUSIONS

Substantially increased CO<sub>2</sub> fluxes at the land surface in the contaminated area of a former chemical manufacturing site compared to a background area suggested that natural degradation and mineralization of anthropogenic organic compounds are occurring at the site. These findings were confirmed via additional <sup>14</sup>C analyses, which revealed that more than 50% of the CO<sub>2</sub> flux was coming from fossil fuel derived organic matter, while the background flux only contained 15%. Consequently, it can be concluded that natural attenuation is occurring in the contaminated area, even though these data do not reveal which contaminants are being mineralized. Thus, there may be ways to stimulate biodegradation through increasing subsurface temperature and/or other measures.

Field investigations were performed to elucidate biogeochemical processes and establish baseline conditions for the site prior to possible development of a pilot treatment. Data obtained during the field investigations were also used to assess current biogeochemical processes occurring in the subsurface. Analysis of site soil core revealed the presence of several organic contaminants, dominated by nitroaromatic compounds (maximum concentration 47,500 mg/kg of nitronaphthalene) with minor concentrations of chloro- and alkylbenzenes. Analysis of the homogenized soil core used in the soil microcosm experiment revealed the total contaminant-bound carbon (via GC/MS) and total organic carbon (via TOC measurement) were both 24.1 g/kg, indicating that all major organic contaminants were detected, and leading to the conclusion that the elevated CO<sub>2</sub> fluxes observed in the contaminated area stemmed from mineralization of the NACs under natural conditions.

The upper zone (0 - 6 ft) contains the water table and capillary fringe. The geology shifts from silt to sand at 4 ft. Groundwater contamination is dominated by the more soluble monoaromatic and doubly nitrated compounds, with maximum concentrations reaching 111 mg/L for 1,3-dinitrobenzene and 76 mg/L for 2,4-dinitrotoluene at this depth. Microbial communities were diverse, and species such as *Clostridia* spp. (8 - 16%) and *Geobacter thiogenes* (5%) were found in this zone. Certain species of *Clostridia* have been found to degrade trinitrotoluene under anaerobic conditions. *Geobacter thiogenes* and a close relative have been found to reductively dechlorinate organic compounds. Small quantities of methanogens were found at this depth suggesting methanogenic conditions are present. However, nitrate (2 - 46 mg/L) and sulfate (60 - 142 mg/L) concentrations suggest predominantly nitrate-reducing conditions. Methanogenic conditions may not be widespread and may only be found in microniches. Nitroaniline and chloroaniline were detected in water samples, which are potential products of reductive degradation of dinitrobenzene and chloronitrobenzene, respectively. However, it cannot be excluded that there is an upstream source of anilines at the site. Anilines can be readily mineralized in the presence of oxygen, but low redox potentials and the presence of methane in the vadose zone suggest that O<sub>2</sub> may be (temporarily) limited in the shallow aquifer. However, aniline mineralization has been previously reported to occur under nitrate- and sulfate-reducing conditions, even though at substantially lower rates. Another potential permanent removal mechanism for substituted anilines is irreversible (chemi)sorption to the soil matrix by covalently bonding to natural organic matter. Potential degradation products of the less soluble nitronaphthalene and nitrated toluenes were not detected.

From 6 to 11.5 ft, contaminant concentrations increase and NAPL was observed in water samples at the bottom of this zone. Nitronaphthalene and 2,4 dinitrotoluene had the highest

contaminant mass in the soil with concentrations of 47,500 mg/kg and 16,000 mg/kg at 11.5 ft. High aqueous concentrations of 1,3-dinitrobenzene (163 mg/L) were also located above the silt/clay layer. Here, too, nitroaniline and chloroaniline were detected as potential products of reductive degradation of dinitrobenzene and chloronitrobenzene. Microbial diversity analysis revealed subsurface conditions were favorable for *Pseudomonas stutzeri* from 6 ft to 11.5 ft in the upper transmissive zone. *P. stutzeri* is a facultative aerobe that has been shown to aerobically degrade benzene, naphthalene, chloronaphthalene, chloronitrobenzene, chlorobenzene, dichlorobenzene, toluene, and xylene. Under nitrate-reducing conditions, *P. stutzeri* has been found to degrade pyrene, phenanthrene, naphthalene, benzoate, fluorobenzoate, and salicylate. The transmissive zone may provide favorable conditions for *P. stutzeri* by transporting toxic degradation byproducts out of the zone and allowing for electron acceptors (i.e., nitrate) to be transported into the zone. The abundance of nitrate-reducing microbial species in this zone indicates degradation of contaminants under nitrate-reducing conditions, likely limited by the availability of this electron acceptor since nitrate concentrations are low (5 mg/L). At abundances of up to 83%, it appears likely that *P. stutzeri* plays a key role in the biodegradation of NACs at the site.

NAPL was present in the water samples from 11 - 16 ft below ground surface, and analysis revealed high aqueous concentrations of 1,3-dinitrobenzene (216 mg/L) and 2,4-dinitrotoluene (163 mg/L) at 14 ft. From 11.5 ft to 16 ft increased microbial diversity was observed, and microbial communities did not appear to be highly dependent on site geology. A distinct change in the microbial communities was not observed between the silty clay and lower sand layer. A *Pseudomonas* spp. was detected and accounted for 13 - 16% of the microbial community. From 16 to 23.5 ft, contaminant concentrations in the soil core were generally below detection, while

low aqueous concentrations were still observed, including the potential reduced degradation products nitroaniline, chloroaniline, and aniline. Microbial communities were similar to those in the 11.5 - 16 ft range, and 27% of the community was a *Pseudomonas* spp.

An anaerobic soil microcosm study using a homogenized site soil core was conducted for 350 days to assess the effectiveness of thermal enhancement as a remediation technique. Triplicate soil batch reactors were set up at temperatures of 10°C, 14°C, 18°C, 22°C, 26°C, and 30°C. Statistically significant degradation of xylene, toluene, ethylbenzene, and chlorobenzene was observed at temperatures around 14 - 26°C, however, without a clear trend. Some gas was generated, peaking at temperatures around 18 - 22°C. The lack of benzene in combination with dichlorobenzene stability suggests an oxidative degradation pathway for chlorobenzene. The dominant microbial species identified in the homogenized soil core samples, *Pseudomonas stutzeri*, is a known chlorobenzene- and chloronitrobenzene-degrader.

Significant degradation of NACs was not observed, and in contrast to field samples, no aniline-based degradation products were detected. However, further analyses revealed ammonia concentrations increased in soil microcosms at 14°C and above. Ammonia release is indicative of a nitrobenzene degradation pathway where the nitro group is reduced. The amount of ammonia generated only accounts for less than 1% of the nitrogen bound in the NACs. Therefore, NAC degradation may have been occurring very slowly, with losses likely within experimental variation and therefore not detected as statistically significant.

CH<sub>4</sub> and CO<sub>2</sub> were not detected above atmospheric conditions, which differed from the elevated CO<sub>2</sub> fluxes observed at grade at the field site. The discrepancy may have been caused limitations in the experimental design creating unfavorable conditions for site microorganisms.

Homogenization of the soil core mixed different biogeochemical zones and anaerobic microniches may have been destroyed, creating unfavorable conditions for methanogens and other active contaminant degrading microorganisms. Additionally, anaerobic conditions were imposed on the soil microcosms and eliminated anoxic/oxic interfaces that may have been present in the field. Field studies revealed nitrate-reducing microbial species were present in transmissive zones, which may have allowed for toxic byproducts removal and the replenishment of depleted electron acceptors. The static conditions of the microcosms may have caused the accumulation of toxic byproducts or prevented the replenishment of electron acceptors.

In conclusion, degradation of anthropogenic organic contaminants at the site does occur under natural conditions, but it is unclear which contaminants are mineralized to generate the measured increased CO<sub>2</sub> fluxes. Partial reduction of the predominant NACs may lead to irreversible sorption to soil organic matter as long as sorption sites are available, but their ultimate mineralization may require the addition of oxygen. While there is no clear evidence on a temperature maximum for contaminant degradation by indigenous bacteria, some parameters suggest that only a slight increase in temperature to around 18 - 22°C may stimulate their activity. Overall, the results of this study indicate that enhancing natural attenuation processes at the site may be a promising path forward. Remaining knowledge gaps may be addressed by future work, which is proposed in the following Chapter 6.

## 6. SITE CONCEPTUAL MODEL

A site conceptual model was developed for the contaminated site to summarize key processes occurring in the subsurface and help guide future site management decisions (Figure 29). In the highly contaminated zone (yellow area in Figure 29), NACs, BTEX and chlorobenzene (CB) are mineralized to CO<sub>2</sub> and CH<sub>4</sub>. These processes, which proceed via ring opening of the aromatic compounds, occur predominantly under nitrate-reducing conditions, and *Pseudomonas stutzeri* plays a key role in ongoing biodegradation processes under natural site conditions. However, methanogenesis is still occurring, even though only in a narrow zone from 4.0 to 4.5 ft bgs. Consequently, there are substantial (biogeochemical) heterogeneities with steep redox gradients in the subsurface. It is thus likely that contaminant degradation is also linked to other processes such as sulfate-reduction and iron(III)-reduction.

At this point, it is unclear whether the detected anilines are a product of NAC reduction or if they stem from an upstream source and are transported to the contaminated zone. It appears possible, however, that reduction of the nitro substituent is driven by the oxidation of reduced iron minerals (Heijman et al., 1995) or by microbial respiration, using another (more reduced) organic carbon source as electron donor. Degradation of anilines under anoxic conditions is generally slow. They likely persist or covalently bind to soil organic matter, although it is thermodynamically favorable for them to serve as electron donors in the reductive dechlorination of chlorinated benzenes.

Since high CO<sub>2</sub> fluxes were measured within the contaminated area, it is likely that the biogas generated during contaminant degradation forms bubbles and thus causes gas ebullition. When produced gases occur next to NAPL, the NAPL forms an intermediate wetting phase between the

water and gas phases, much like a sheen between air and surface water (McLinn & Stolzenburg, 2009). With time gas bubbles coalesce and percolate up to the top of the saturated zone (capillary fringe), carrying both gas and NAPL phases. As such, ebullition has the potential to elevate NAPL to the capillary fringe, which is in close proximity to atmospheric oxygen.

In the vadose zone, CO<sub>2</sub>, CH<sub>4</sub>, BTEX, and CB are volatilized and enter the gas phase, while NACs are more hydrophilic (Table 1) and remain dissolved in groundwater. Oxygen diffuses downward into the vadose zone, but the detection of methane in this zone suggests that it is completely consumed by methanotrophic bacteria before reaching the water table. This may enable some of the less readily degradable BTEX and CB to enter the atmosphere. During times of high water table, however, oxygen may reach the capillary fringe, inducing rapid aerobic biodegradation of the organic contaminants.

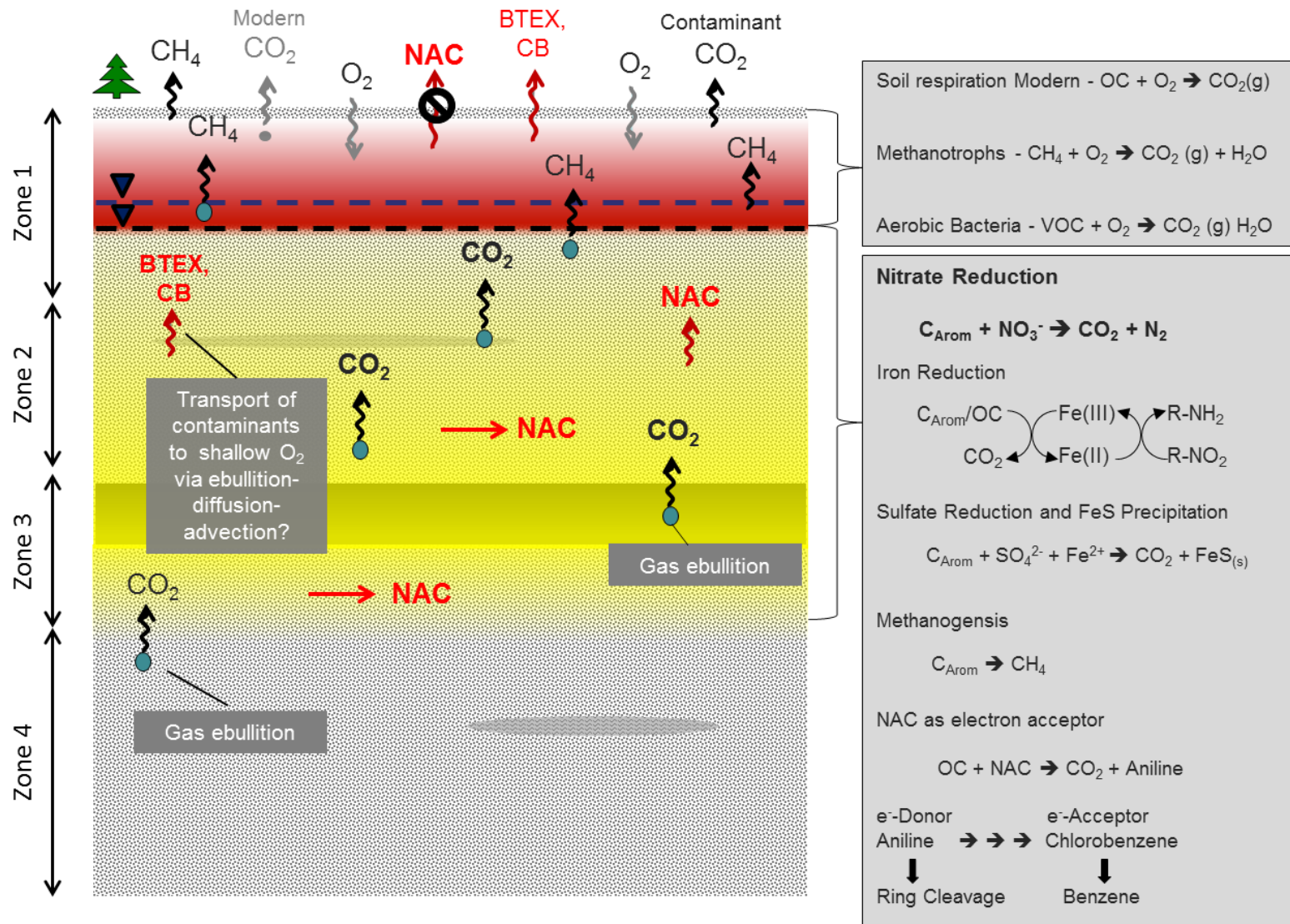


Figure 29 – Site conceptual model (not to scale). Yellow: areas of high NAC concentration. Red: area of high methane concentration in the soil gas.

## 7. FUTURE WORK

The anaerobic microcosm study did not reveal promising results for thermal enhancement of NAC degradation under anaerobic conditions, however, possibly due to experimental limitations of neglecting biogeochemical heterogeneity and dynamic flow conditions. In contrast, the field investigations - especially the analysis and quantification of CO<sub>2</sub> flux from the subsurface and detection of suspected microbial degradation products for some of the major NACs - provide clear evidence that degradation processes are occurring at the site and open up the potential for their enhancement. The literature revealed that aerobic conditions may be more suitable for biodegradation / biomineralization of NACs. Thus, further studies on the effect of oxygen delivery, potentially in combination with increasing temperature, could provide a promising path forward in designing an efficient treatment approach for the contaminants present at the site. This chapter presents and discusses potential future work and remediation approaches.

### **7.1 Additional Site Characterization**

Discrepancies between laboratory and field results encourage further field investigations. Additional field studies are needed to further elucidate biogeochemical processes and determine the activity of key microorganisms in the subsurface. Furthermore, while especially the CO<sub>2</sub> traps revealed that degradation of fossil fuel-derived organic compounds is occurring under natural conditions, they do not enable any conclusion as to which contaminant species are being degraded, or to what extent. Results suggest that alkylated benzenes, chlorobenzene, chloronitrobenzene, and dinitrobenzene are degraded, but further clarification if other NACs (the major contaminants at the site) are being degraded as well is still lacking. Furthermore, it is still unknown if the aniline intermediates from reductive degradation of chloronitrobenzene and

dinitrobenzene are completely mineralized at the site, or if they are permanently (chemi-)sorbed to natural organic matter.

Due to the difficulty of accurately simulating heterogeneous field conditions in the laboratory, *in situ* field microcosms can be used to measure degradation in the subsurface. *In situ* microcosms can be placed in monitoring wells or placed in the subsurface using direct push drilling (Bombach et al., 2010; Schurig et al., 2014). Microcosms can be placed at various depths in order to capture different biogeochemical zones; however, it may be difficult to prevent mixing of oxic and anoxic zones in monitoring wells. Mixing of oxic and anoxic zones may cause aerobic microorganisms to thrive and lead to an enrichment of aerobic organisms in the *in situ* microcosms. Using direct push drilling to place the microcosms in the subsurface can prevent mixing of biogeochemical zones and was shown to be more representative of the soil bacterial communities than *in situ* microcosms in monitoring wells, but the technology is new and has not been widely used (Schurig et al., 2014). By investigating how contaminants are degrading in each zone, actively degrading zones can be identified. Comparing actively degrading zones with zones with limited degradation can be used to determine how biogeochemical characteristics lead to high rates of biodegradation. This information may be used to design remediation systems by altering inactive zones to make them more similar to zones with high rates of biodegradation. Zones where biodegradation is limited could benefit from injection of electron acceptors or alternative carbon sources.

The most widely used *in situ* microcosms, Bio-Trap<sup>®</sup> samplers (Microbial Insights, Knoxville, TN), are made of Teflon tubing or stainless steel and filled with <sup>13</sup>C labeled contaminants and activated carbon pellets (Bombach et al., 2010). These biotrap are placed into monitoring wells, where indigenous microorganisms begin to grow on the carbon pellets and <sup>13</sup>C labeled

contaminants. Traps should be kept in place for 30 to 60 days. Various analyses should be performed to determine if microorganisms are consuming  $^{13}\text{C}$ --labeled contaminants and if the carbon is being assimilated into biomass. Biotraps can be amended with  $^{13}\text{C}$ --labeled benzene, toluene, xylene, and chlorobenzene. Compound specific isotope analysis of biomass may also provide information on degradation pathways of site microbes, and the presence of enriched metabolites in phospholipid fatty acids, amino acids, or nucleic acids may be indicative of certain pathways (Bombach et al., 2010). Also, the accumulation of  $^{13}\text{C}$ --enriched degradation products in the activated carbon pellets may provide insight into which biodegradation pathways are being followed.

## **7.2 Effect of Aerobic Conditions**

NAC degradation at the site appears to be limited by the availability of suitable electron acceptors, and especially oxygen may enable their complete mineralization. Laboratory studies can assess the feasibility of using biosparging as a site remediation technique prior to an expensive field demonstration. Additionally, the development of a biosparging treatment pilot is needed to determine if it would be an effective large-scale treatment. A series of laboratory studies investigating the impact of temperature on aerobic biodegradation rates could be helpful in determining at which temperatures microorganisms are most active. As described above (Chapter 4), enhanced contaminant degradation and gas development were observed at temperatures around 18 - 22 °C (even though still low), and thus above overall natural conditions at the site, indicating that thermal enhancement may still be a promising (additional) approach.

### ***7.2.1 Aerobic Microcosm Studies***

Field soil slurries should be placed into beakers and sealed with an Identi-plug<sup>TM</sup> Plastic Foam Stoppers (Jaece Industries, North Tonawanda, NY), which allows for air flow while preventing soil slurries from being exposed to particulates and non-native bacteria. Microcosms could be placed in temperature controlled shakers and shaken continuously at 100 rpm to maintain dissolved oxygen concentrations in the soil slurries. Microcosms should be kept at temperatures of 10°C, 14°C, 18°C, 22°C, 26°C, and 30°C to determine if temperature has a great impact on biodegradation rates under aerobic conditions. The microcosms should be sampled every 30 days. Samples should be analyzed for contaminant concentrations including potential organic intermediate products as well as for dissolved oxygen, sulfate, nitrate, ammonia, total organic and inorganic carbon, and pH. Optional microbial diversity or activity (e.g., ATP) analysis may be performed to assess changes in and degradation performance of microbial communities when exposed to aerobic conditions at different temperatures. Initial and final samples for microbial diversity analysis should be taken from each microcosm. Microbial diversity analysis and qPCR analysis would be performed to determine the abundance and types of microbial species present the microcosms. In addition, samples taken during the experiment can be tested for ATP concentration as a means of concurrent evaluation of microbial activity.

### ***7.2.2 Biosparging***

Due to successful identification of aerobic NAC degraders, biosparging appears as a promising approach to increase biodegradation rates by providing oxygen to O<sub>2</sub>-depleted zones. The success of other air sparging studies suggests this could be a promising treatment for the site (Johnson & Johnson, 2012). However, each site has its own specific microbial consortium, and it

is thus necessary to investigate how native microorganisms would respond to the introduction of oxygen into their environment.

After reviewing results from the aerobic microcosm study and determining aerobic treatment a success, a biosparging pilot could be developed to assess its feasibility at the site. To test and supply the entire depth of the aquifer, a minimum of two injection wells need to be installed so compressed oxygen can be injected into the subsurface. The first well injects air right above the silt/clay lense at ~10.5 - 11.5 ft bgs to cover the upper part of the aquifer, while a second well would be used to inject air right above the confining clay layer at ~25 - 26 ft bgs to supply lower strata. Air should be sparged in a pulsed fashion to limit contaminant volatilization while maximizing oxygen delivery. A series of multilevel samplers should be placed in a circular pattern around the injection well to take water samples at various depths and track changes in the aqueous contaminant concentration and dissolved oxygen throughout the experiment. Air quality measurements should be performed, ideally in a shallow soil vapor extraction well if water tables allow, to validate that no organic contaminants are being volatilized and to monitor for CH<sub>4</sub>. Biosparging should be performed for 3 months and water samples should be obtained every 2 weeks. Water samples should be analyzed for contaminant and electron acceptor concentrations and field parameters. Soil cores should be taken and analyzed depth-resolved at the beginning and end of the experiment. Microbial analysis should be performed on the soil cores to assess changes in microbial diversity and quantity after treatment with biosparging.

## **7.3 Temperature Modeling & Enhancement**

### ***7.3.1 Thermal Signature Modeling***

Recent research at the Center for Contaminant Hydrology at Colorado State University has shown subsurface thermal signatures may be used to monitor biodegradation in the subsurface. To determine if biodegradation is altering subsurface temperatures, thermocouples and a data logger could be deployed at a background location to monitor heat flow. The background data could then be compared to the data collected in the contaminated area to determine if there is a thermal signature corresponding to biodegradation. Elevated temperatures in the contaminated area compared to the background location would indicate that biodegradation is occurring, providing another line of evidence natural attenuation is occurring in the contaminated area.

### ***7.3.2 Temperature Enhancement with Gas Permeable Insulation***

Subsurface temperature measurements during winter months revealed values as low as 2°C. Raising the subsurface temperature could stimulate microbes especially during the cold seasons. Covering contaminated areas with Tendrain II-1010 black gas permeable insulation (Syntec, LLC, Baltimore, MD) is a sustainable way of raising the subsurface temperature by insulating against surface weather conditions and absorbing heat from the sun. Placing gas permeable insulation on the ground has been found to increase subsurface temperature by 5°C one foot below the ground surface (Akhbari et al., 2013). Deploying gas permeable insulation on the site would be a way to maintain subsurface temperatures in the highly variable top zone in a range that may stimulate microbial growth. A thermocouple and data logger should be deployed at 1.75 ft to record subsurface temperature over time. The temperature measurements should be compared to the data recorded on the multilevel sampler to assess subsurface temperature

increases from deploying the gas permeable membrane. Carbon dioxide traps should be used to assess how installation of gas permeable membrane affects CO<sub>2</sub> fluxes and biodegradation. A trap should be located in the middle of the insulated area and one should also be placed outside of the zone, providing for a comparison of CO<sub>2</sub> fluxes between insulation treatment and non-insulated treatment areas.

## 8. REFERENCES

- Akhbari, D. (2013 Fall) Thermal aspects of STELA (Sustainable Thermally Enhanced LNAPL Attenuation). In: Colorado State University Libraries.
- Al-Maamari, R.S., Hirayama, A., Shiga, T., Sueyoshi, M.N., Al-Shuely, M., Abdalla, O.A.E., and Kacimov, A.R. (2011) Fluids' dynamics in transient air sparging of a heterogeneous unconfined aquifer. *Environmental Earth Sciences* **63**: 1189-1198.
- Alisadat, S., Mohan, K.S., and Walia, S.K. (1995) A novel pathway for the biodegradation of 3-nitrotoluene in *pseudomonas-putida*. *Fems Microbiology Ecology* **17**: 169-176.
- Amos, R.T., Mayer, K.U., Bekins, B.A., Delin, G.N., and Williams, R.L. (2005) Use of dissolved and vapor-phase gases to investigate methanogenic degradation of petroleum hydrocarbon contamination in the subsurface. *Water Resources Research* **41**: 16.
- An, Y., Xiu, Z., An, Y., Liu, N., Zhang, L., and Zhou, A. (2012a) Application of air sparging and bioaugmentation for nitrobenzene and aniline remediation in shallow groundwater: a laboratory-scale study. *Fresenius Environmental Bulletin* **21**: 1802-1809.
- An, Y.-L., Zhang, L.-Y., Liu, N., Zhou, A.-X., Zhang, T.-D., and An, Y.-K. (2012b) Field scale analysis on structural changes of microbial community and its relationships with environmental factors in nitrobenzene-contaminated groundwater during air sparging remediation. *Environmental Engineering and Management Journal* **11**: 1687-1696.
- Aoki, K., Shinke, R., and Nishira, H. (1983) Microbial-metabolism of aromatic-amines .3. metabolism of aniline by *Rhodococcus-erythropolis* AN-13. *Agricultural and Biological Chemistry* **47**: 1611-1616.
- Aronson, D., and Howard, P. (1997) Anaerobic biodegradation of organic chemicals in groundwater: a summary of field and laboratory studies. In. North Syracuse, NY: Syracuse Research Center, pp. 1-263.
- Bachofer, R., Lings, F., and Schafer, W. (1975) Conversion of aniline into pyrocatechol by a nocardia sp - incorporation of Oxygen-18. *Febs Letters* **50**: 288-290.
- Baggi, G., Barbieri, P., Galli, E., and Tollari, S. (1987) Isolation of a pseudomonas-stutzeri strain that degrades ortho-xylene. *Applied and Environmental Microbiology* **53**: 2129-2132.
- Berchtold, S.R., Vanderloop, S.L., Suidan, M.T., and Maloney, S.W. (1995) Treatment of 2,4-dinitrotoluene using a 2-stage system - fluidized-bed anaerobic granular activated carbon reactors and aerobic activated-sludge reactors. *Water Environment Research* **67**: 1081-1091.
- Bertoni, G., Bolognese, F., Galli, E., and Barbieri, P. (1996) Cloning of the genes for and characterization of the early stages of toluene and o-xylene catabolism in *Pseudomonas stutzeri* OX1. *Applied and Environmental Microbiology* **62**: 3704-3711.
- Bombach, P., Richnow, H.H., Kastner, M., and Fischer, A. (2010) Current approaches for the assessment of in situ biodegradation. *Applied Microbiology and Biotechnology* **86**: 839-852.

- Boon, N., Goris, J., De Vos, P., Verstraete, W., and Top, E.M. (2000) Bioaugmentation of activated sludge by an indigenous 3-chloroaniline-degrading *Comamonas testosteroni* strain, I2gfp. *Applied and Environmental Microbiology* **66**: 2906-2913.
- Bradley, P.M., Chapelle, F.H., Landmeyer, J.E., and Schumacher, J.G. (1997) Potential for intrinsic bioremediation of a DNT-contaminated aquifer. *Ground Water* **35**: 12-17.
- Brusseau, M.L., and Rao, P.S.C. (1991) Influence of sorbate structure on nonequilibrium sorption of organic-compounds. *Environmental Science & Technology* **25**: 1501-1506.
- Cafaro, V., Izzo, V., Scognamiglio, R., Notomista, E., Capasso, P., Casbarra, A. et al. (2004) Phenol hydroxylase and toluene/o-xylene monooxygenase from *Pseudomonas stutzeri* OX1: Interplay between two enzymes. *Applied and Environmental Microbiology* **70**: 2211-2219.
- Caliman, F.A., Robu, B.M., Smaranda, C., Pavel, V.L., and Gavrilescu, M. (2011) Soil and groundwater cleanup: benefits and limits of emerging technologies. *Clean Technologies and Environmental Policy* **13**: 241-268.
- Charles, S., Teppen, B.J., Li, H., Laird, D.A., and Boyd, S.A. (2006) Exchangeable cation hydration properties strongly influence soil sorption of nitroaromatic compounds. *Soil Science Society of America Journal* **70**: 1470-1479.
- Cherry, J.A., Gillham, R.W., Anderson, E.G., and Johnson, P.E. (1983) Migration of contaminants in groundwater at a landfill - a case-study. *Journal of Hydrology* **63**: 31-49.
- Chiou, C.T., and Kile, D.E. (1998) Deviations from sorption linearity on soils of polar and nonpolar organic compounds at low relative concentrations. *Environmental Science & Technology* **32**: 338-343.
- Corporation, U. (2013) Triangle Intermediates Area Investigation Extents Map. In. Newark, DE.
- Coulon, F., Pelletier, E., Gourhant, L., and Delille, D. (2005) Effects of nutrient and temperature on degradation of petroleum hydrocarbons in contaminated sub-Antarctic soil. *Chemosphere* **58**: 1439-1448.
- Davis, J.K., Paoli, G.C., He, Z.Q., Nadeau, L.J., Somerville, C.C., and Spain, J.C. (2000) Sequence analysis and initial characterization of two isozymes of hydroxylaminobenzene mutase from *Pseudomonas pseudoalcaligenes* JS45. *Applied and Environmental Microbiology* **66**: 2965-2971.
- De, M.A., Oconnor, O.A., and Kosson, D.S. (1994) Metabolism of aniline under different anaerobic electron-accepting and nutritional conditions. *Environmental Toxicology and Chemistry* **13**: 233-239.
- De Wever, H., Cole, J.R., Fettig, M.R., Hogan, D.A., and Tiedje, J.M. (2000) Reductive dehalogenation of trichloroacetic acid by *Trichlorobacter thiogenes* gen. nov., sp nov. *Applied and Environmental Microbiology* **66**: 2297-2301.
- DeFlaun, M.F., Murray, C.J., Holben, W., Scheibe, T., Mills, A., Ginn, T. et al. (1997) Preliminary observations on bacterial transport in a coastal plain aquifer. *Fems Microbiology Reviews* **20**: 473-487.

- Delille, D., Coulon, F., and Pelletier, E. (2004) Effects of temperature warming during a bioremediation study of natural and nutrient-amended hydrocarbon-contaminated sub-Antarctic soils. *Cold Regions Science and Technology* **40**: 61-70.
- Dickel, O., Haug, W., and Knackmuss, H. (1993) Biodegradation of nitrobenzene by a sequential anaerobic-aerobic process. *Biodegradation*: 187-194.
- DiLecce, C., Accarino, M., Bolognese, F., Galli, E., and Barbieri, P. (1997) Isolation and metabolic characterization of a *Pseudomonas stutzeri* mutant able to grow on the three isomers of xylene. *Applied and Environmental Microbiology* **63**: 3279-3281.
- Dua, M., Singh, A., Sethunathan, N., and Johri, A.K. (2002) Biotechnology and bioremediation: successes and limitations. *Applied Microbiology and Biotechnology* **59**: 143-152.
- EPA Protection of Environment. In 40.
- Evstigneeva, A., Raoult, D., Karpachevskiy, L., and La Scola, B. (2009) Amoeba co-culture of soil specimens recovered 33 different bacteria, including four new species and *Streptococcus pneumoniae*. *Microbiology-Sgm* **155**: 657-664.
- Field, J.A., Stams, A.J.M., Kato, M., and Schraa, G. (1995) Enhanced biodegradation of aromatic pollutants in cocultures of anaerobic and aerobic bacterial consortia. *Antonie Van Leeuwenhoek International Journal of General and Molecular Microbiology* **67**: 47-77.
- Garcia-Valdes, E., Castillo, M.M., Bennasar, A., Guasp, C., Cladera, A.M., Bosch, R. et al. (2003) Polyphasic characterization of *Pseudomonas stutzeri* CLN100 which simultaneously degrades chloro- and methylaromatics: A new genomovar within the species. *Systematic and Applied Microbiology* **26**: 390-403.
- Gheewala, S.H., and Annachhatre, A.P. (1997) Biodegradation of aniline. *Water Science and Technology* **36**: 53-63.
- Girvan, M.S., Bullimore, J., Pretty, J.N., Osborn, A.M., and Ball, A.S. (2003) Soil type is the primary determinant of the composition of the total and active bacterial communities in arable soils. *Applied and Environmental Microbiology* **69**: 1800-1809.
- Gong, P., Hawari, J., Thiboutot, S., Ampleman, G., and Sunahara, G.I. (2001) Ecotoxicological effects of hexahydro-1,3,5-trinitro-1,3,5-triazine on soil microbial activities. *Environmental Toxicology and Chemistry* **20**: 947-951.
- Graveel, J.G., Sommers, L.E., and Nelson, D.W. (1985) Sites of benzidine, alpha-naphthylamine and para-toluidine retention in soils. *Environmental Toxicology and Chemistry* **4**: 607-613.
- Grbic-Galic, D., and Vogel, T.M. (1987) transformation of toluene and benzene by mixed methanogenic cultures. *Applied and Environmental Microbiology* **53**: 254-260.
- Guilbeault, M.A., Parker, B.L., and Cherry, J.A. (2005) Mass and flux distributions from DNAPL zones in sandy aquifers. *Ground Water* **43**: 70-86.
- Haderlein, S.B., Weissmahr, K.W., and Schwarzenbach, R.P. (1996) Specific adsorption of nitroaromatic: Explosives and pesticides to clay minerals. *Environmental Science & Technology* **30**: 612-622.

- Haigler, B.E., and Spain, J.C. (1993) Biodegradation of 4-nitrotoluene by *Pseudomonas* sp. strain 4NT. *Applied and Environmental Microbiology* **59**: 2239-2243.
- Haigler, B.E., Wallace, W.H., and Spain, J.C. (1994) Biodegradation of 2-nitrotoluene by *Pseudomonas* sp. strain JS42. *Applied and Environmental Microbiology* **60**: 3466-3469.
- Hall, B.L., Lachmar, T.E., and Dupont, R.R. (2000) Field monitoring and performance evaluation of an in situ air sparging system at a gasoline-contaminated site. *Journal of Hazardous Materials* **74**: 165-186.
- Hallas, L.E., and Alexander, M. (1983) Microbial transformation of nitroaromatic compounds in sewage effluent. *Applied and Environmental Microbiology* **45**: 1234-1241.
- Hazardous Substances Data Bank. (2014) Aniline. In: N.L.M. Toxicology Data Network.
- Hazardous Substances Data Bank. (2014) 1-Chloro-2-nitrobenzene. In: N.L.M. Toxicology Data Network.
- Hazardous Substances Data Bank. (2014) 2-4-Dinitrotoluene. In: N.L.M. Toxicology Data Network.
- Hazardous Substances Data Bank. (2014) Nitrobenzene. In: N.L.M. Toxicology Data Network.
- Hazardous Substances Data Bank. (2014) 2-Nitrotoluene. In: N.L.M. Toxicology Data Network.
- Hazardous Substances Data Bank. (2014) Nitronaphthalene. In: N.L.M. Toxicology Data Network.
- He, Z.G., and Spain, J.C. (1997) Studies of the catabolic pathway of degradation of nitrobenzene by *Pseudomonas pseudoalcaligenes* JS45: Removal of the amino group from 2-aminomuconic semialdehyde. *Applied and Environmental Microbiology* **63**: 4839-4843.
- He, Z.G., and Spain, J.C. (1998) A novel 2-Aminomuconate deaminase in the nitrobenzene degradation pathway of *Pseudomonas pseudoalcaligenes* JS45. *Journal of Bacteriology* **180**: 2502-2506.
- He, Z.Q., and Spain, J.C. (2000) Reactions involved in the lower pathway for degradation of 4-nitrotoluene by *Mycobacterium* strain HL 4-NT-1. *Applied and Environmental Microbiology* **66**: 3010-3015.
- He, Z.Q., Davis, J.K., and Spain, J.C. (1998) Purification, characterization, and sequence analysis of 2-aminomuconic 6-semialdehyde dehydrogenase from *Pseudomonas pseudoalcaligenes* JS45. *Journal of Bacteriology* **180**: 4591-4595.
- Heijman, C.G., Grieder, E., Holliger, C., and Schwarzenbach, R.P. (1995) Reduction of nitroaromatic - compounds coupled to microbial iron reduction in laboratory aquifer columns. *Environmental Science & Technology* **29**: 775-783.
- Higashioka, Y., Kojima, H., and Fukui, M. (2011) Temperature-dependent differences in community structure of bacteria involved in degradation of petroleum hydrocarbons under sulfate-reducing conditions. *Journal of Applied Microbiology* **110**: 314-322.
- Hill, M.O. (1973) Diversity and Evenness: A Unifying Notation and Its Consequences. *Ecology* **54**: 427-432.

- Hirano, S.I., Kitauchi, F., Haruki, M., Imanaka, T., Morikawa, M., and Kanaya, S. (2004) Isolation and characterization of *Xanthobacter polyaromaticivorans* sp nov 127W that degrades polycyclic and heterocyclic aromatic compounds under extremely low oxygen conditions. *Bioscience Biotechnology and Biochemistry* **68**: 557-564.
- Hsu, T.S., and Bartha, R. (1974) Biodegradation of chloroaniline-humus complexes in soil and in culture solution. *Soil Science* **118**: 213-220.
- Inceoglu, O., Abu Al-Soud, W., Salles, J.F., Semenov, A.V., and van Elsas, J.D. (2011) Comparative Analysis of Bacterial Communities in a Potato Field as Determined by Pyrosequencing. *Plos One* **6**: 11.
- Irianni Renno, M. (2013 Fall) Biogeochemical characterization of a LNAPL body in support of STELA. In *Civil and Environmental Engineering*. Fort Collins, CO: Colorado State University, p. 118.
- Jang, S.H., Kim, J., Hong, S., and Lee, C. (2012) Genome sequence of cold-adapted *Pseudomonas mandelii* Strain JR-1. *Journal of Bacteriology* **194**: 3263-3263.
- Johnson, R.L., and Johnson, P.C. (2012) In Situ Sparging for Delivery of Gases in the Subsurface. In *Delivery and Mixing in the Subsurface: Processes and Design Principles for In Situ Remediation*. Kitanidis, P.K., and McCarty, P.L. (eds). New York: Springer.
- Ju, K.S., and Parales, R.E. (2010) Nitroaromatic Compounds, from Synthesis to Biodegradation. *Microbiology and Molecular Biology Reviews* **74**: 250-+.
- Kahng, H.Y., Kukor, J.J., and Oh, K.H. (2000) Characterization of strain HY99, a novel microorganism capable of aerobic and anaerobic degradation of aniline. *Fems Microbiology Letters* **190**: 215-221.
- Kang, J.W. (2014) Removing environmental organic pollutants with bioremediation and phytoremediation. *Biotechnology Letters* **36**: 1129-1139.
- Katsivela, E., Wray, V., Pieper, D.H., and Wittich, R.M. (1999) Initial reactions in the biodegradation of 1-chloro-4-nitrobenzene by a newly isolated bacterium, strain LW1. *Applied and Environmental Microbiology* **65**: 1405-1412.
- Kiaalhosseini, S. (2014) Novel Methods for Characterization of Contaminated Sites – Electrical Resistivity Method, Magnetic Resonance Imaging, and Cryogenic Coring In. Fort Collins, CO: Colorado State University.
- Kurt, Z., and Spain, J.C. (2013) Biodegradation of Chlorobenzene, 1,2-Dichlorobenzene, and 1,4-Dichlorobenzene in the Vadose Zone. *Environmental Science & Technology* **47**: 6846-6854.
- Kurt, Z., Shin, K., and Spain, J.C. (2012) Biodegradation of Chlorobenzene and Nitrobenzene at Interfaces between Sediment and Water. *Environmental Science & Technology* **46**: 11829-11835.
- Kutty, R., and Bennett, G.N. (2005) Biochemical characterization of trinitrotoluene transforming oxygen-insensitive nitroreductases from *Clostridium acetobutylicum* ATCC 824. *Archives of Microbiology* **184**: 158-167.

- Lalucat, J., Bennasar, A., Bosch, R., Garcia-Valdes, E., and Palleroni, N.J. (2006) Biology of *Pseudomonas stutzeri*. *Microbiology and Molecular Biology Reviews* **70**: 510-+.
- Lauber, C.L., Hamady, M., Knight, R., and Fierer, N. (2009) Pyrosequencing-Based Assessment of Soil pH as a Predictor of Soil Bacterial Community Structure at the Continental Scale. *Applied and Environmental Microbiology* **75**: 5111-5120.
- Lessner, D.J., Johnson, G.R., Parales, R.E., Spain, J.C., and Gibson, D.T. (2002) Molecular characterization and substrate specificity of nitrobenzene dioxygenase from *Comamonas* sp strain JS765. *Applied and Environmental Microbiology* **68**: 634-641.
- Liu, D., Thomson, K., and Anderson, A.C. (1984) Identification of nitroso-compounds from biotransformation of 2,4-dinitrotoluene. *Applied and Environmental Microbiology* **47**: 1295-1298.
- Li, H., and Lee, L.S. (1999) Sorption and abiotic transformation of aniline and alpha-naphthylamine by surface soils. *Environmental Science & Technology* **33**: 1864-1870.
- Liu, H., Wang, S.J., and Zhou, N.Y. (2005) A new isolate of *Pseudomonas stutzeri* that degrades 2-chloronitrobenzene. *Biotechnology Letters* **27**: 275-278.
- Liu, H., Wang, S.J., Zhang, J.J., Dai, H., Tang, H.R., and Zhou, N.Y. (2011) Patchwork Assembly of nag-Like Nitroarene Dioxygenase Genes and the 3-Chlorocatechol Degradation Cluster for Evolution of the 2-Chloronitrobenzene Catabolism Pathway in *Pseudomonas stutzeri* ZWLR2-1. *Applied and Environmental Microbiology* **77**: 4547-4552.
- Liu, N., Li, H.J., Ding, F., Xiu, Z.M., Liu, P., and Yu, Y. (2013) Analysis of biodegradation by-products of nitrobenzene and aniline mixture by a cold-tolerant microbial consortium. *Journal of Hazardous Materials* **260**: 323-329.
- Ma, Y.F., Wu, J.F., Wang, S.Y., Jang, C.Y., Zhang, Y., Qi, S.W. et al. (2007) Nucleotide sequence of plasmid pCNB1 from *Comamonas* strain CNB-1 reveals novel genetic organization and evolution for 4-chloronitrobenzene degradation. *Applied and Environmental Microbiology* **73**: 4477-4483.
- Mason, R.P., and Josephy, P.D. (1985) Free radical mechanism of nitroreductase. In *Toxicity of Nitroaromatic Compounds*. Rickert, D.E. (ed). Washington, D.C.: Hemisphere Publishing Corporation, pp. 121-140.
- McCormick, N.G., Feeherry, F.E., and Levinson, H.S. (1976) Microbial transformation of 2,4,6-trinitrotoluene and other nitroaromatic compounds. *Applied and Environmental Microbiology* **31**: 949-958.
- McCoy, K.M. (2012 Fall) Resolving natural losses of LNAPL using CO traps. In: Colorado State University Libraries.
- McCoy, K., Zimbron, J., Sale, T., and Lyverse, M. (2014) Measurement of Natural Losses of LNAPL Using CO<sub>2</sub> Traps. *Groundwater*: 1745-6584.
- McLinn, E.L., and Stolzenburg, T.R. (2009) Ebullition-facilitated transport of manufactured gas plant tar from contaminated sediment. *Environmental Toxicology and Chemistry* **28**: 2298-2306.

- McNally, D.L., Mihelcic, J.R., and Lueking, D.R. (1999) Biodegradation of mixtures of polycyclic aromatic hydrocarbons under aerobic and nitrate-reducing conditions. *Chemosphere* **38**: 1313-1321.
- Megharaj, M., Ramakrishnan, B., Venkateswarlu, K., Sethunathan, N., and Naidu, R. (2011) Bioremediation approaches for organic pollutants: A critical perspective. *Environment International* **37**: 1362-1375.
- Mohn, W.W., and Stewart, G.R. (2000) Limiting factors for hydrocarbon biodegradation at low temperature in Arctic soils. *Soil Biology & Biochemistry* **32**: 1161-1172.
- Molins, S., Mayer, K.U., Amos, R.T., and Bekins, B.A. (2010) Vadose zone attenuation of organic compounds at a crude oil spill site - Interactions between biogeochemical reactions and multicomponent gas transport. *Journal of Contaminant Hydrology* **112**: 15-29.
- Nacke, H., Thurmer, A., Wollherr, A., Will, C., Hodac, L., Herold, N. et al. (2011) Pyrosequencing-Based Assessment of Bacterial Community Structure Along Different Management Types in German Forest and Grassland Soils. *Plos One* **6**: 12.
- Nedwell, D.B. (1999) Effect of low temperature on microbial growth: lowered affinity for substrates limits growth at low temperature. *Fems Microbiology Ecology* **30**: 101-111.
- Nemecekmarshall, M., Laduca, R., and Fall, R. (1993) High-level expression of ice nuclei in a pseudomonas-syringae strain is induced by nutrient limitation and low-temperature. *Journal of Bacteriology* **175**: 4062-4070.
- Nishino, S.F., and Spain, J.C. (1993) Degradation of nitrobenzene by a *Pseudomonas-pseudoalcaligenes*. *Applied and Environmental Microbiology* **59**: 2520-2525.
- Nishino, S.F., and Spain, J.C. (1995) Oxidative pathway for the biodegradation of nitrobenzene by *Comamonas* sp strain JS765. *Applied and Environmental Microbiology* **61**: 2308-2313.
- Nishino, S.F., Paoli, G.C., and Spain, J.C. (2000a) Aerobic degradation of dinitrotoluenes and pathway for bacterial degradation of 2,6-dinitrotoluene. *Applied and Environmental Microbiology* **66**: 2139-2147.
- Nishino, S.F., Spain, J.C., and He, Z. (2000b) Strategies for Aerobic Degradation of Nitroaromatic Compounds by Bacteria: Process Discovery to Field Application. In *Biodegradation of Nitroaromatic Compounds and Explosives*. Spain, J.C., Hughes, J.B., and Knackmuss, H.-J. (eds). Boca Raton, FL: CRC Press LLC, pp. 7-62.
- Pankow, J.F., and Cherry, J.A. (1996) Dense chlorinated solvents and other DNAPLs in groundwater: History, behavior, and remediation. Portland, OR: Waterloo Press.
- Parales, J.V., Kumar, A., Parales, R.E., and Gibson, D.T. (1996) Cloning and sequencing of the genes encoding 2-nitrotoluene dioxygenase from *Pseudomonas* sp. JS42. *Gene* **181**: 57-61.
- Parales, J.V., Parales, R.E., Resnick, S.M., and Gibson, D.T. (1998) Enzyme specificity of 2-nitrotoluene 2,3-dioxygenase from *Pseudomonas* sp. strain JS42 is determined by the C-terminal region of the alpha subunit of the oxygenase component. *Journal of Bacteriology* **180**: 1194-1199.

- Parales, R.E., Huang, R., Yu, C.L., Parales, J.V., Lee, F.K.N., Lessner, D.J. et al. (2005) Purification, characterization, and crystallization of the components of the nitrobenzene and 2-nitrotoluene dioxygenase enzyme systems. *Applied and Environmental Microbiology* **71**: 3806-3814.
- Park, H.S., and Kim, H.S. (2000) Identification and characterization of the nitrobenzene catabolic plasmids pNB1 and pNB2 in *Pseudomonas putida* HS12. *Journal of Bacteriology* **182**: 573-580.
- Park, H.S., Lim, S.J., Chang, Y.K., Livingston, A.G., and Kim, H.S. (1999) Degradation of chloronitrobenzenes by a coculture of *Pseudomonas putida* and a *Rhodococcus* sp. *Applied and Environmental Microbiology* **65**: 1083-1091.
- Parris, G.E. (1980) Covalent binding of aromatic-amines to humates .1. Reactions with carbonyls and quinones. *Environmental Science & Technology* **14**: 1099-1106.
- Peres, C.M., Naveau, H., and Agathos, S.N. (1998) Biodegradation of nitrobenzene by its simultaneous reduction into aniline and mineralization of the aniline formed. *Applied Microbiology and Biotechnology* **49**: 343-349.
- Research and Testing Laboratory. (2014). Data Analysis Methodology, Lubbock, TX.
- Regan, K.M., and Crawford, R.L. (1994) Characterization of *Clostridium-bifermentans* and its biotransformation of 2,4,6-trinitrotoluene (tnt) and 1,3,5-triaza-1,3,5-trinitrocyclohexane (RDX). *Biotechnology Letters* **16**: 1081-1086.
- Rhyswilliams, W., Taylor, S.C., and Williams, P.A. (1993) A novel pathway for the catabolism of 4-nitrotoluene by *Pseudomonas*. *Journal of General Microbiology* **139**: 1967-1972.
- Rieger, P.G., and Knackmuss, H.J. (1995) Basic knowledge and perspectives on biodegradation of 2,4,6-trinitrotoluene and related nitroaromatic compounds in contaminated soil. *Biodegradation of Nitroaromatic Compounds* **49**: 1-18.
- Rockne, K.J., Chee-Sanford, J.C., Sanford, R.A., Hedlund, B.P., Staley, J.T., and Strand, S.E. (2000) Anaerobic naphthalene degradation by microbial pure cultures under nitrate-reducing conditions. *Applied and Environmental Microbiology* **66**: 1595-1601.
- Roy, D., Moustafa, H., and Maillacheruvu, K. (1997) Aniline degradation in a soil slurry bioreactor. *Journal of Environmental Science and Health Part a-Environmental Science and Engineering & Toxic and Hazardous Substance Control* **32**: 2367-2377.
- Schnell, S., and Schink, B. (1991) Anaerobic aniline degradation via reductive deamination of 4-aminobenzoyl-coa in *Desulfobacterium-anilini*. *Archives of Microbiology* **155**: 183-190.
- Schurig, C., Melo, V.A., Miltner, A., and Kaestner, M. (2014) Characterisation of microbial activity in the framework of natural attenuation without groundwater monitoring well: a new Direct-Push probe. *Environmental Science and Pollution Research* **21**: 9002-9015.
- Schwarzenbach, R.P.-. (2003,1995) *Environmental organic chemistry*. New York: Wiley.
- Sheng, G.Y., Johnston, C.T., Teppen, B.J., and Boyd, S.A. (2001) Potential contributions of smectite clays and organic matter to pesticide retention in soils. *Journal of Agricultural and Food Chemistry* **49**: 2899-2907.

- Shi, X., Ji, L.L., and Zhu, D.Q. (2010) Investigating roles of organic and inorganic soil components in sorption of polar and nonpolar aromatic compounds. *Environmental Pollution* **158**: 319-324.
- Sihota, N.J., and Mayer, K.U. (2012) Characterizing Vadose Zone Hydrocarbon Biodegradation Using Carbon Dioxide Effluxes, Isotopes, and Reactive Transport Modeling. *Vadose Zone Journal* **11**: 14.
- Skoog, D.A., Holler, F.J., and Niemann, T.A. (1998) *Principles of instrumental analysis*. Philadelphia: Saunders College Pub  
Harcourt Brace College Publishers.
- Spangord, R.J., Spain, J.C., Nishino, S.F., and Mortelmans, K.E. (1991) Biodegradation of 2,4-dinitrotoluene by a *Pseudomonas* sp. *Applied and Environmental Microbiology* **57**: 3200-3205.
- Spieß, T., Desiere, F., Fischer, P., Spain, J.C., Knackmuss, H.J., and Lenke, H. (1998) A new 4-nitrotoluene degradation pathway in a *Mycobacterium* strain. *Applied and Environmental Microbiology* **64**: 446-452.
- Stevenson, F.J. (1976) Organic-matter reactions involving pesticides in soil. *Acs Symposium Series*: 180-207.
- Stone Environmental Inc. (2011) CWK Triangle Area Investigation Pilot Study Post Field Work Status.
- Suen, W.C., and Spain, J.C. (1993) Cloning and characterization of *Pseudomonas*-sp strain DNT genes for 2,4-dinitrotoluene degradation. *Journal of Bacteriology* **175**: 1831-1837.
- Sung, Y., Fletcher, K.F., Ritalaliti, K.M., Apkarian, R.P., Ramos-Hernandez, N., Sanford, R.A. et al. (2006) *Geobacter lovleyi* sp nov strain SZ, a novel metal-reducing and tetrachloroethene-dechlorinating bacterium. *Applied and Environmental Microbiology* **72**: 2775-2782.
- Sutton, N.B., Maphosa, F., Morillo, J.A., Abu Al-Soud, W., Langenhoff, A.A.M., Grotenhuis, T. et al. (2013) Impact of Long-Term Diesel Contamination on Soil Microbial Community Structure. *Applied and Environmental Microbiology* **79**: 619-630.
- Suzuki, M.T., Taylor, L.T., and DeLong, E.F. (2000) Quantitative analysis of small-subunit rRNA genes in mixed microbial populations via 5'-nuclease assays. *Applied and Environmental Microbiology* **66**: 4605-4614.
- Swindoll, C.M., Perkins, R.E., Gannon, J.T., Holmes, M., and Fisher, G.A. (1995) Assessment of Bioremediation of a Contaminated Wetland. In *Intrinsic Bioremediation*. Hinchee, R.E., Wilson, J.T., and Downey, D.C. (eds). Columbus, OH: Battelle Press, pp. 163-170.
- Takenaka, S., Murakami, S., Shinke, R., and Aoki, K. (1998) Metabolism of 2-aminophenol by *Pseudomonas* sp. AP-3: modified meta-cleavage pathway. *Archives of Microbiology* **170**: 132-137.
- Tanaka, T., Hachiyanagi, H., Yamamoto, N., Iijima, T., Kido, Y., Uyeda, M., and Takahama, K. (2009) Biodegradation of Endocrine-Disrupting Chemical Aniline by Microorganisms. *Journal of Health Science* **55**: 625-630.

- Tiehm, A., and Schmidt, K.R. (2011) Sequential anaerobic/aerobic biodegradation of chloroethenes - aspects of field application. *Current Opinion in Biotechnology* **22**: 415-421.
- Vargas, C., Song, B., Camps, M., and Haggblom, M.M. (2000) Anaerobic degradation of fluorinated aromatic compounds. *Applied Microbiology and Biotechnology* **53**: 342-347.
- Walworth, J., Woolard, C., Acomb, L., Chaobal, V., and Wallace, M. (1999) Nutrient & temperature interactions in bioremediation of petroleum-contaminated cryic soil. *In Situ Bioremediation of Petroleum Hydrocarbon and Other Organic Compounds*: 505-510.
- Wang, J., Yang, H., Lu, H., Zhou, J.T., and Zheng, C.L. (2009) Aerobic biodegradation of nitrobenzene by a defined microbial consortium immobilized in polyurethane foam. *World Journal of Microbiology & Biotechnology* **25**: 875-881.
- Weber, E.J., Colon, D., and Baughman, G.L. (2001) Sediment-associated reactions of aromatic amines. 1. Elucidation of sorption mechanisms. *Environmental Science & Technology* **35**: 2470-2475.
- Whitby, C., and Lund, S. (2009) *Applied Microbiology and Molecular Biology in Oil Field Systems*: Springer Science.
- Wieser, M., and Busse, H.J. (2000) Rapid identification of *Staphylococcus epidermidis*. *International Journal of Systematic and Evolutionary Microbiology* **50**: 1087-1093.
- WSRC (2006) Scenarios Evaluation Tool for Chlorinated Solvent MNA. In. Aiken, SC.
- Wu, H.Z., Wei, C.H., Wang, Y.Q., He, Q.C., and Liang, S.Z. (2009) Degradation of o-chloronitrobenzene as the sole carbon and nitrogen sources by *Pseudomonas putida* OCNB-1. *Journal of Environmental Sciences-China* **21**: 89-95.
- Wu, J.F., Sun, C.W., Jiang, C.Y., Liu, Z.P., and Liu, S.J. (2005) A novel 2-aminophenol 1,6-dioxygenase involved in the degradation of p-chloronitrobenzene by *Comamonas* strain CNB-1: purification, properties, genetic cloning and expression in *Escherichia coli*. *Archives of Microbiology* **183**: 1-8.
- Wu, J.F., Jiang, C.Y., Wang, B.J., Ma, Y.F., Liu, Z.P., and Liu, S.J. (2006) Novel partial reductive pathway for 4-chloronitrobenzene and nitrobenzene degradation in *Comamonas* sp strain CNB-1. *Applied and Environmental Microbiology* **72**: 1759-1765.
- Xiao, Y., Wu, J.F., Liu, H., Wang, S.J., Liu, S.J., and Zhou, N.Y. (2006) Characterization of genes involved in the initial reactions of 4-chloronitrobenzene degradation in *Pseudomonas putida* ZWL73. *Applied Microbiology and Biotechnology* **73**: 166-171.
- Ye, J., Singh, A., and Ward, O.P. (2004) Biodegradation of nitroaromatics and other nitrogen-containing xenobiotics. *World Journal of Microbiology & Biotechnology* **20**: 117-135.
- Zeman, N.R. (2013 Spring) Thermally enhanced bioremediation of LNAPL. In: Colorado State University. Libraries.
- Zeman, N.R., Renno, M.I., Olson, M.R., Wilson, L.P., Sale, T.C., and De Long, S.K. (2014) Temperature impacts on anaerobic biotransformation of LNAPL and concurrent shifts in microbial community structure. *Biodegradation* **25**: 569-585.

- Zhang, D.M., Hou, L., Zhu, D.Q., and Chen, W. (2014) Synergistic role of different soil components in slow sorption kinetics of polar organic contaminants. *Environmental Pollution* **184**: 123-130.
- Zhen, D., Liu, H., Wang, S.J., Zhang, J.J., Zhao, F., and Zhou, N.Y. (2006) Plasmid-mediated degradation of 4-chloronitrobenzene by newly isolated *Pseudomonas putida* strain ZWL73. *Applied Microbiology and Biotechnology* **72**: 797-803.
- Zheng, C.L., Zhou, J.T., Zhao, L.H., Lu, H., Qu, B.C., and Wang, J. (2007) Isolation and characterization of a nitrobenzene degrading *Streptomyces* strain from activated sludge. *Bulletin of Environmental Contamination and Toxicology* **78**: 153-157.
- Zhu, D.Q., and Pignatello, J.J. (2005) Characterization of aromatic compound sorptive interactions with black carbon (charcoal) assisted by graphite as a model. *Environmental Science & Technology* **39**: 2033-2041.
- Zhu, D.Q., Kwon, S., and Pignatello, J.J. (2005) Adsorption of single-ring organic compounds to wood charcoals prepared under different thermochemical conditions. *Environmental Science & Technology* **39**: 3990-3998.

# APPENDIX A: CALIBRATION

## A.1 Contaminant Calibration Curves

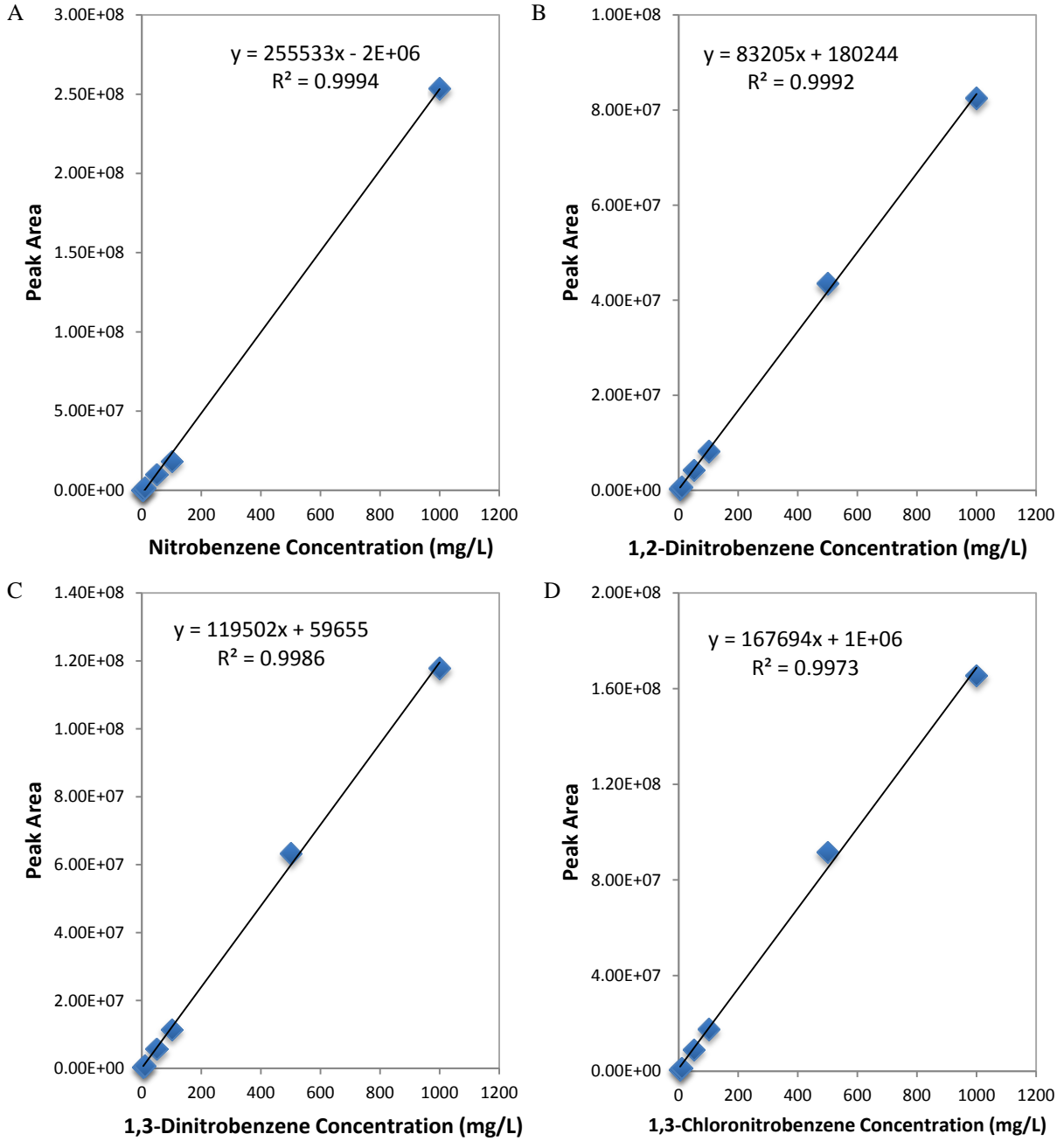


Figure 30 –Calibration curves for A) nitrobenzene B) 1,2-dinitrobenzene C) 1,3-dinitrobenzene D) 1,3-chloronitrobenzene

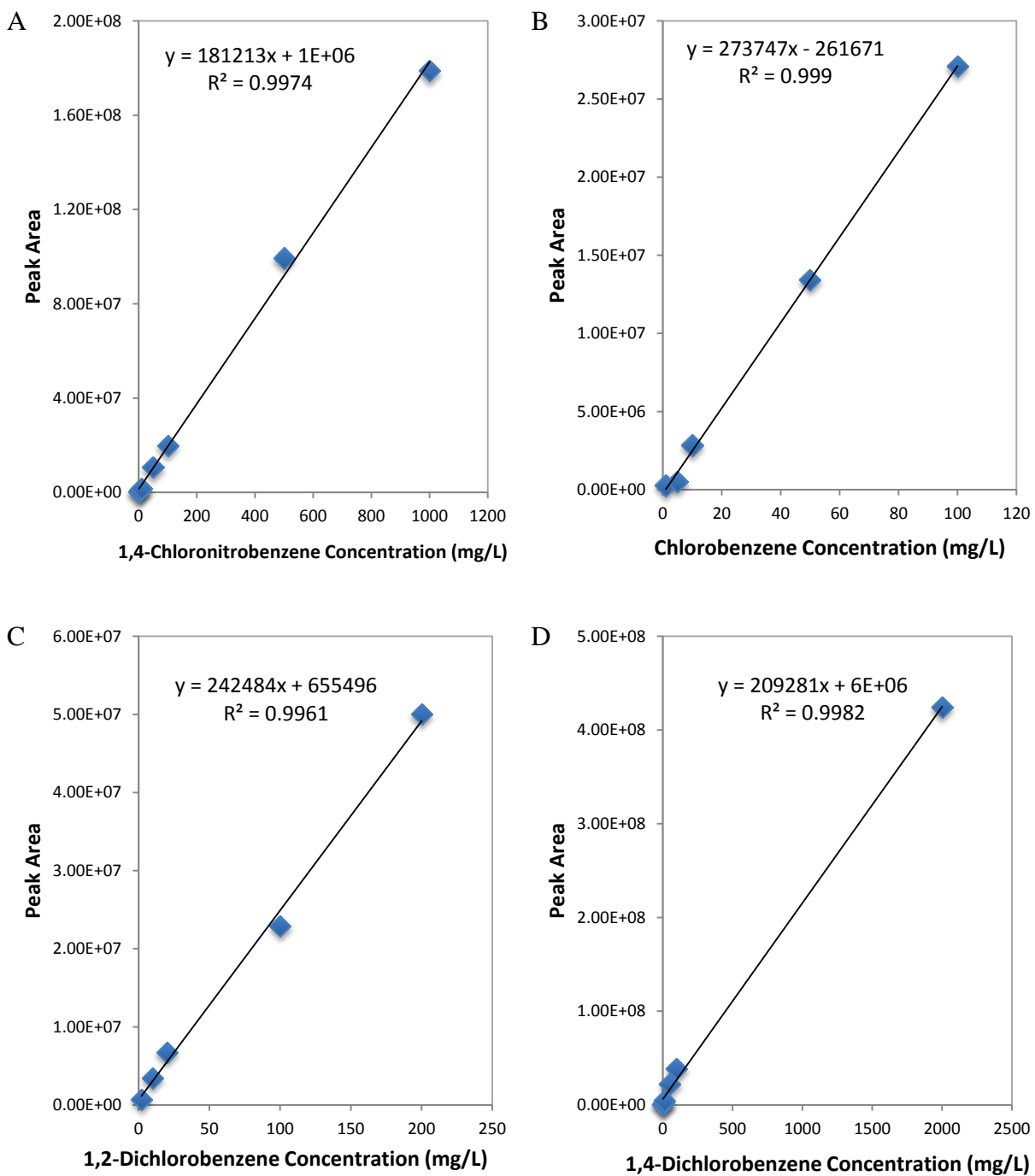


Figure 31 –Calibration curves for A) 1,4-chloronitrobenzene B) chlorobenzene C) 1,2-dichlorobenzene D) 1,4-dichlorobenzene

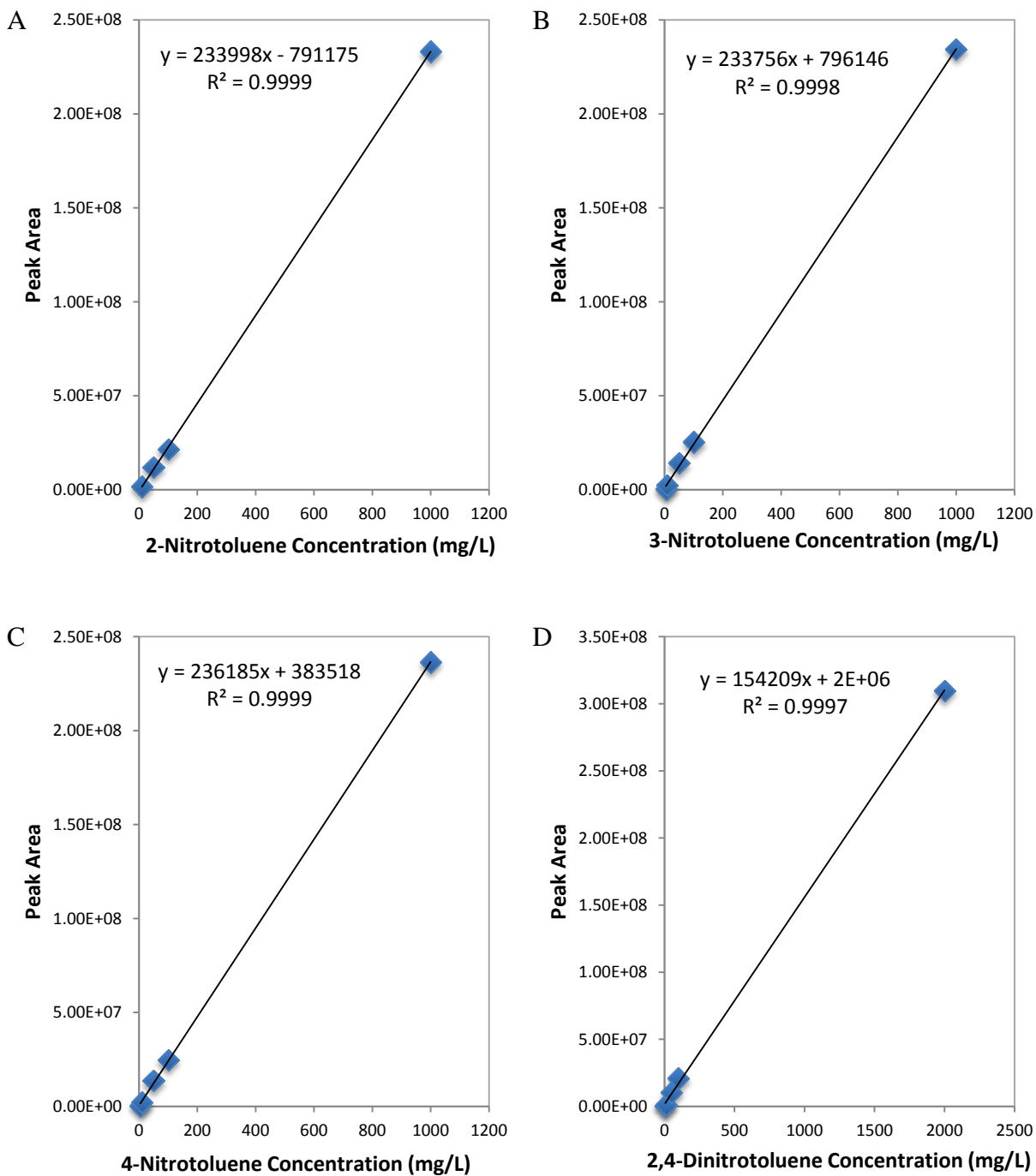


Figure 32 –Calibration curves for A) 2-nitrotoluene B) 3-nitrotoluene C) 4-nitrotoluene D) 2,4-dinitrotoluene

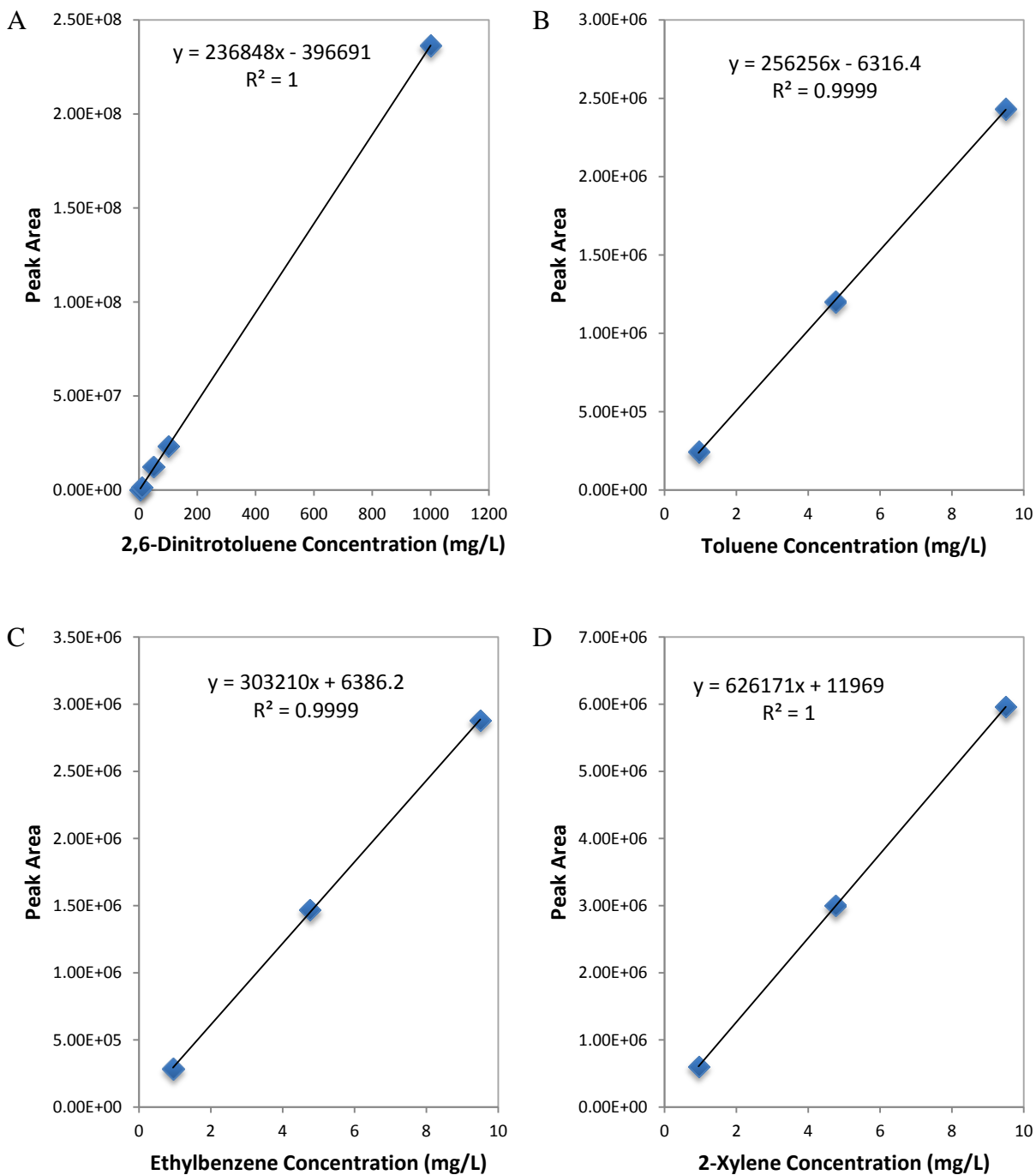


Figure 33 – Calibration curves for A) 2,6-dinitrotoluene B) toluene C) ethylbenzene D) 2-xylene

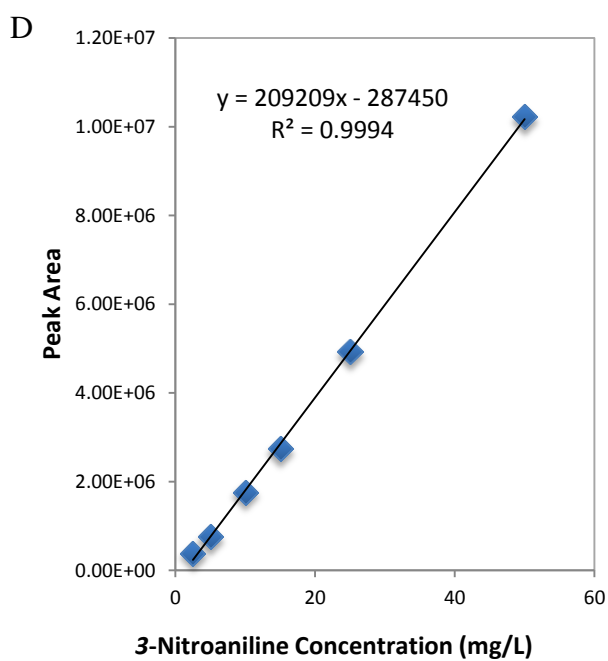
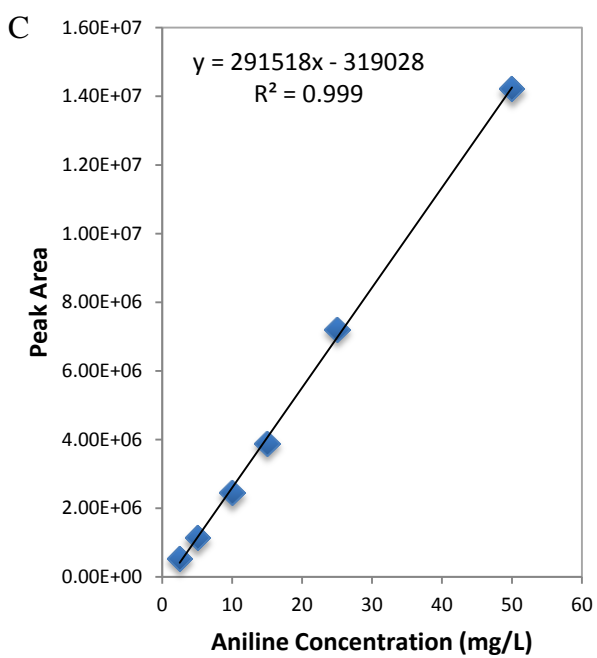
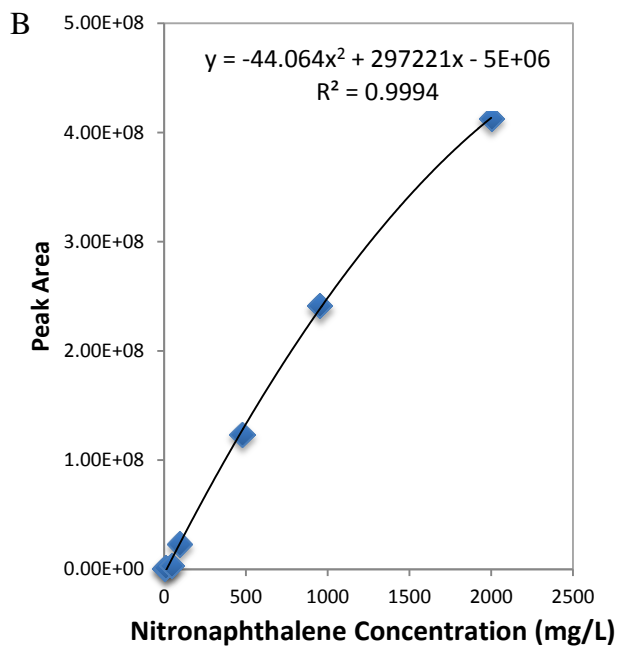
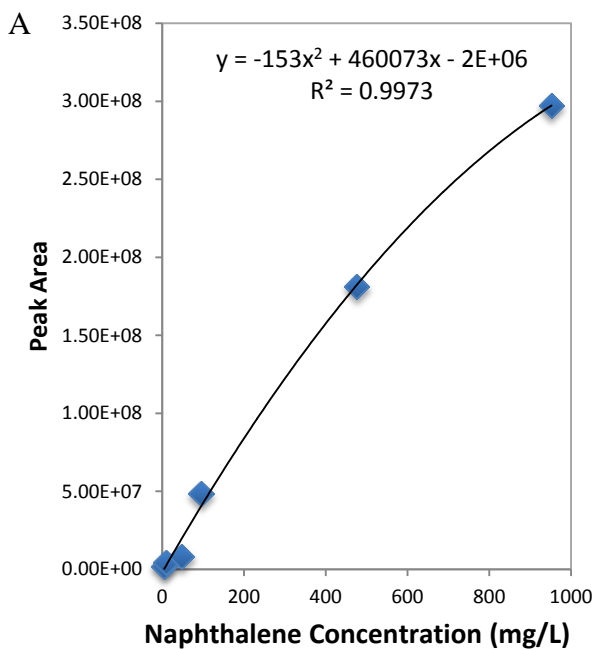


Figure 34 –Calibration curves for A) naphthalene B) nitronaphthalene C) aniline D) 3-nitroaniline

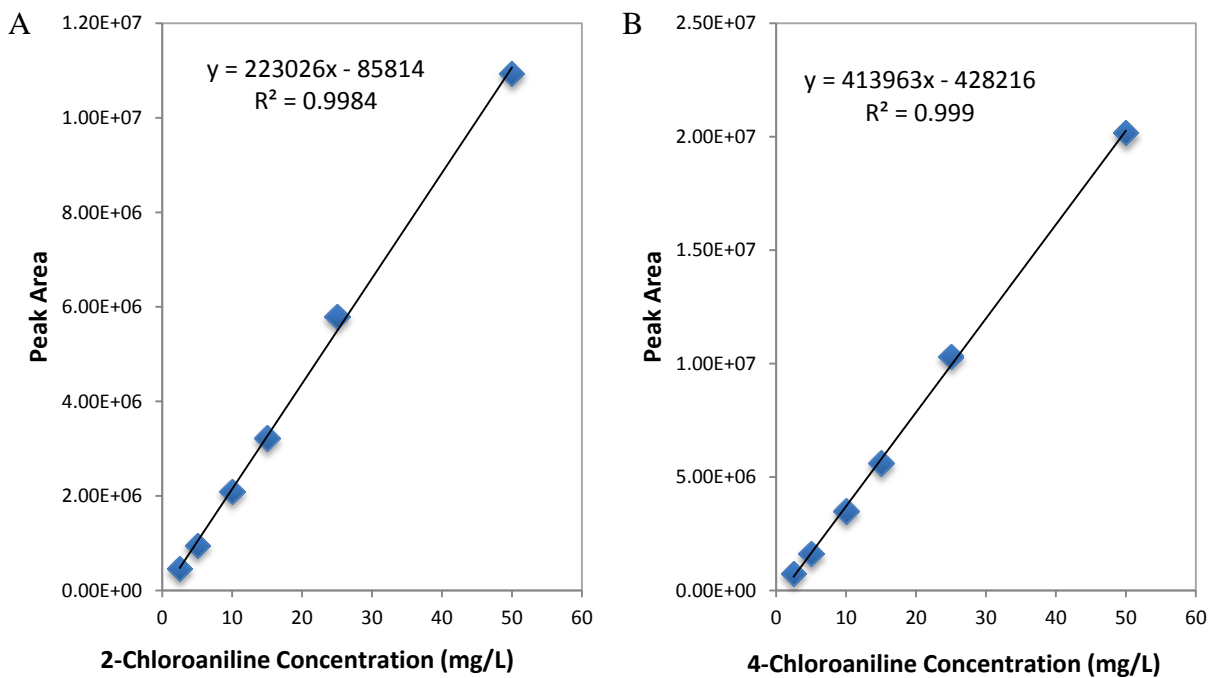


Figure 35 –Calibration curves for A) 2-chloroaniline B) 4-chloroaniline

## A.2 Determining Limit of Detection and Quantification

Detection and quantification limits were determined using procedures outlined in the *Principles of Instrumental Analysis* by Skoog, Holler, and Nieman. The limit of quantification and detection is found by first determining the minimum distinguishable analytical signal as described by the equation

$$S_m = \overline{S_{bl}} + k s_{bl} \quad [\text{Eq. 6}]$$

where  $S_m$  is the minimum distinguishable analytical signal,  $S_{bl}$  is the mean of the blank signal,  $k$  is a constant, and  $s_{bl}$  is the standard deviation of the blank signal. Limits of detection and quantification are determined using  $k$  values of 3 and 10 respectively.

The minimum distinguishable analytical signal can be used in conjunction with the equation for the calibration curve to find the minimum concentration for detection or quantification. The minimum concentration is described by the equation

$$c_m = \frac{S_m - \overline{S_{bl}}}{m} \quad [\text{Eq. 7}]$$

where  $c_m$  is the minimum concentration and  $m$  is the slope of the calibration curve.

Table 10- Limits of detection and quantification

Compound	Coefficients of Best Fit			LOD	LOQ
	ax <sup>2</sup>	bx	c	mg/L	
Nitrobenzene	0.00	2.56E+05	-2.31E+06	0.13	0.44
1,2-Dinitrobenzene	0.00	8.32E+04	1.80E+05	0.34	1.13
1,3-Dinitrobenzene	0.00	1.20E+05	5.97E+04	0.24	0.78
1,2-Chloronitrobenzene	0.00	1.65E+05	1.12E+06	0.17	0.57
1,3-Chloronitrobenzene	0.00	1.68E+05	1.10E+06	0.17	0.56
1,4-Chloronitrobenzene	0.00	1.81E+05	1.32E+06	0.16	0.52
2-Nitrotoluene	0.00	2.34E+05	-7.91E+05	0.12	0.40
3-Nitrotoluene	0.00	2.34E+05	7.96E+05	0.12	0.40
4-Nitrotoluene	0.00	2.36E+05	3.84E+05	0.12	0.40
2,4-Dinitrotoluene	0.00	1.54E+05	1.66E+06	0.18	0.61
2,6-Dinitrotoluene	0.00	2.37E+05	-3.97E+05	0.12	0.40
Benzene	0.00	1.94E+05	-1.98E+05	0.15	0.48
Toluene	0.00	2.56E+05	-6.32E+03	0.11	0.37
Ethylbenzene	0.00	3.03E+05	6.39E+03	0.09	0.31
2-Xylene	0.00	6.26E+05	1.20E+04	0.04	0.15
Aniline	0.00	2.92E+05	-3.19E+05	0.10	0.32
2-Chloroaniline	0.00	2.23E+05	-8.58E+04	0.13	0.42
4-Chloroaniline	0.00	4.14E+05	-4.28E+05	0.07	0.23
3-Nitroaniline	0.00	2.09E+05	-2.87E+05	0.13	0.45
Naphthalene	-153.00	4.60E+05	-2.01E+06	0.06	0.20
Nitronaphthalene	-44.06	2.97E+05	-4.66E+06	0.09	0.32
Chlorobenzene	0.00	2.74E+05	-2.62E+05	0.10	0.34
1,2-Dichlorobenzene	0.00	2.42E+05	6.55E+05	0.12	0.39
1,4-Dichlorobenzene	0.00	2.09E+05	6.16E+06	0.13	0.45

APPENDIX B: FIELD STUDIES SUPPLEMENTARY INFORMATION

**B.1 Soil Core Recovery**

Table 11- Recovery from macrocore sampling

Macrocore Number	Depth	Recovery	Depth Recovered
	(ft)	(ft)	(ft)
MC-1	0-4	2.0	0-2
MC-2	4-10	3.4	4-7.4
MC-3	10-15	4.4	10-14.4
MC-4	15-20	2.0	15-17
MC-5	20-23	1.0	20-21
MC-6	23-26	0.9	23-23.9

## B.2 Aqueous Contaminant Concentrations

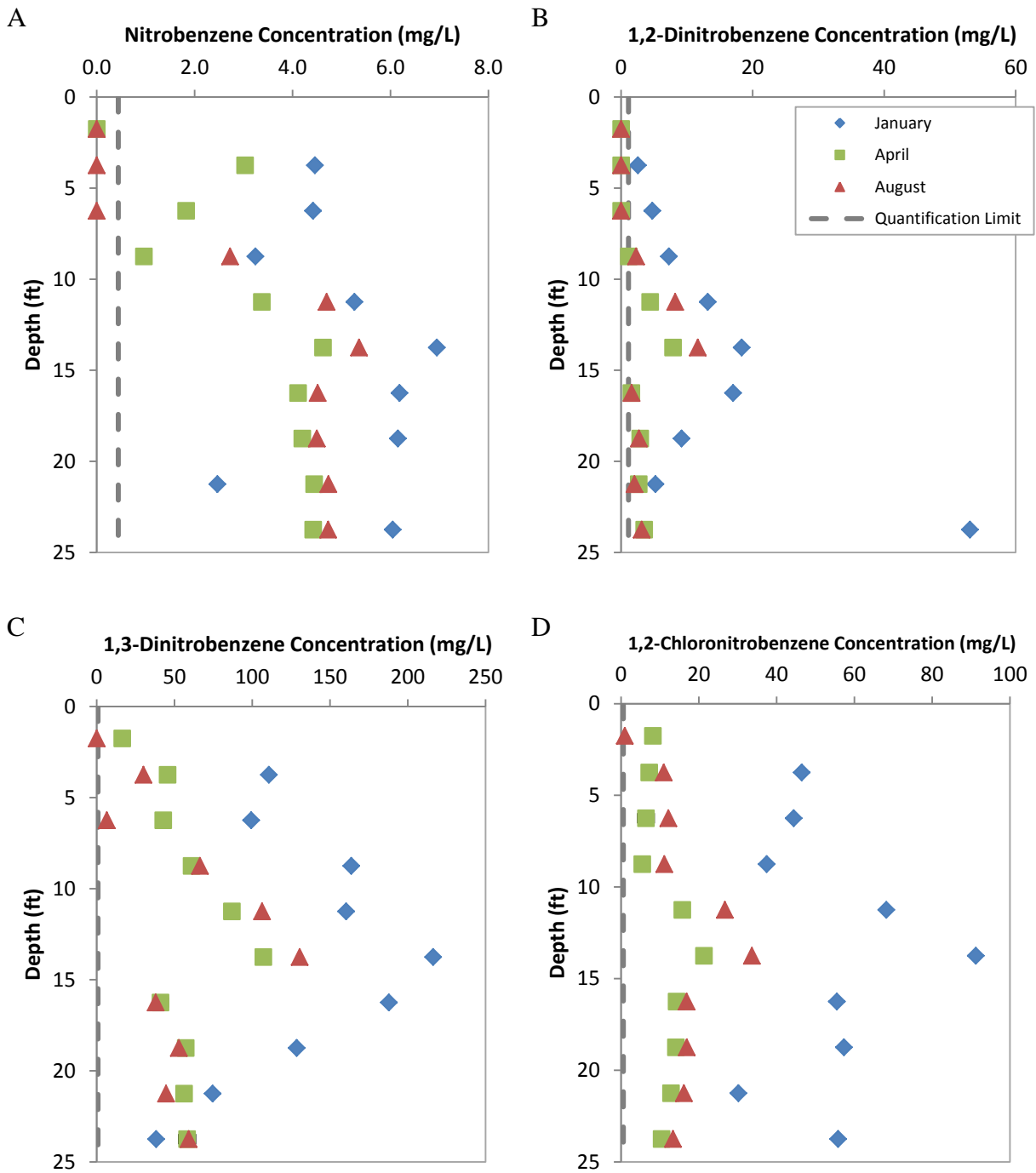


Figure 36 –Aqueous concentrations of A) nitrobenzene B) 1,2-dinitrobenzene C) 1,3-dinitrobenzene D) 1,2-chloronitrobenzene

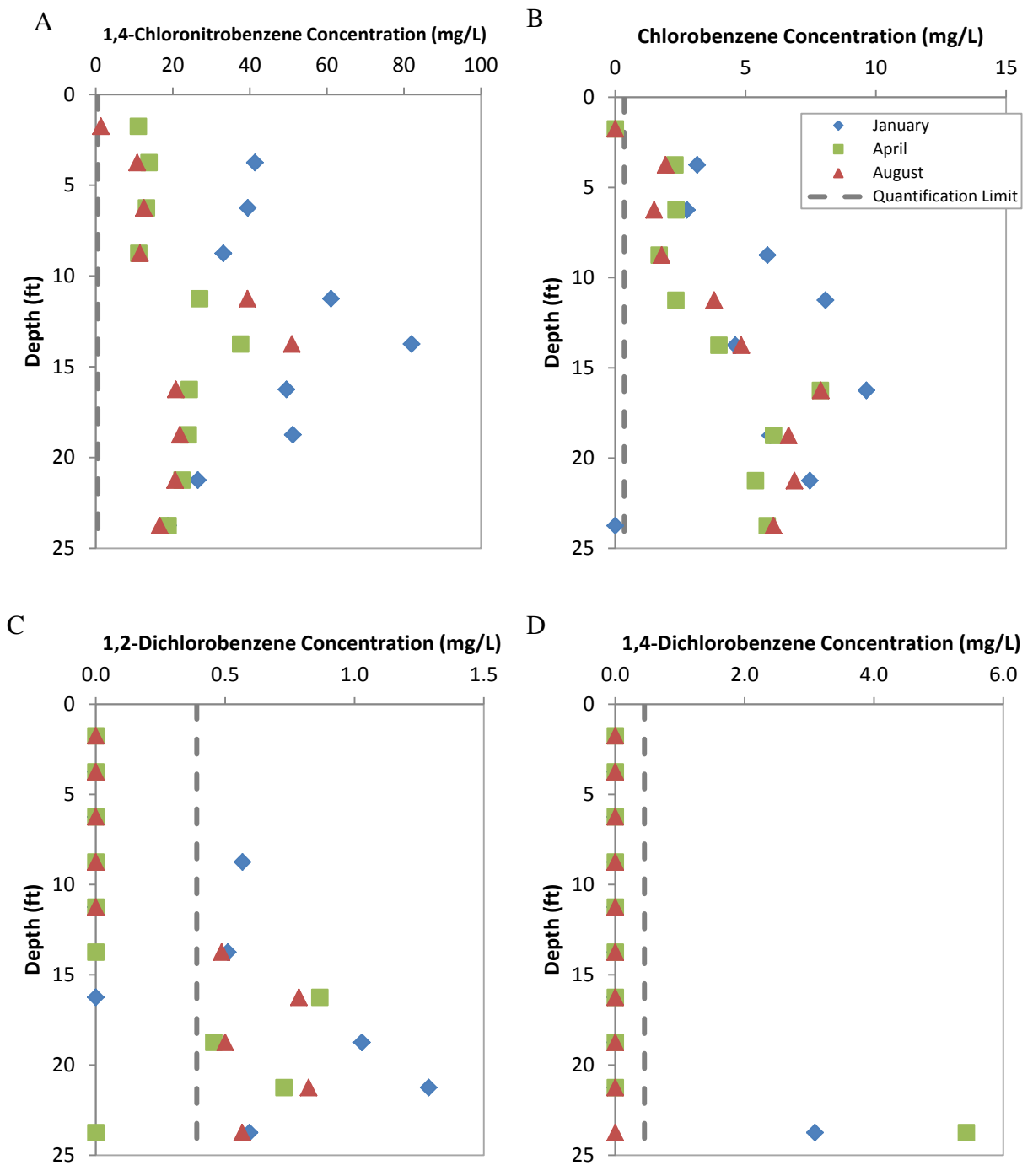


Figure 37 –Aqueous concentrations of A) 1,4-chloronitrobenzene B) chlorobenzene C) 1,2-dichlorobenzene D) 1,4-dichlorobenzene

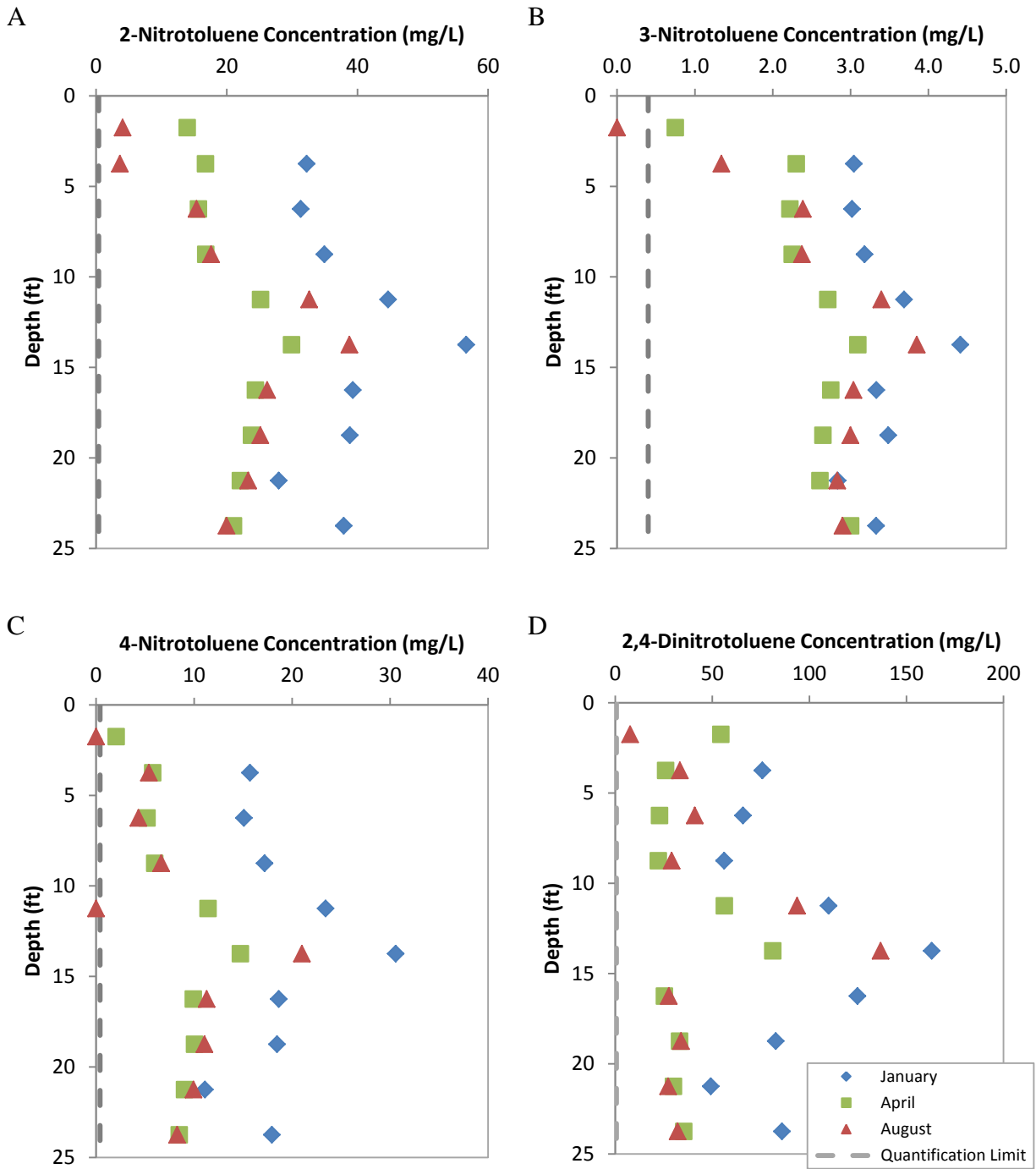


Figure 38 –Aqueous concentrations of A) 2-nitrotoluene B) 3-nitrotoluene C) 4-nitrotoluene D) 2,4-dinitrotoluene

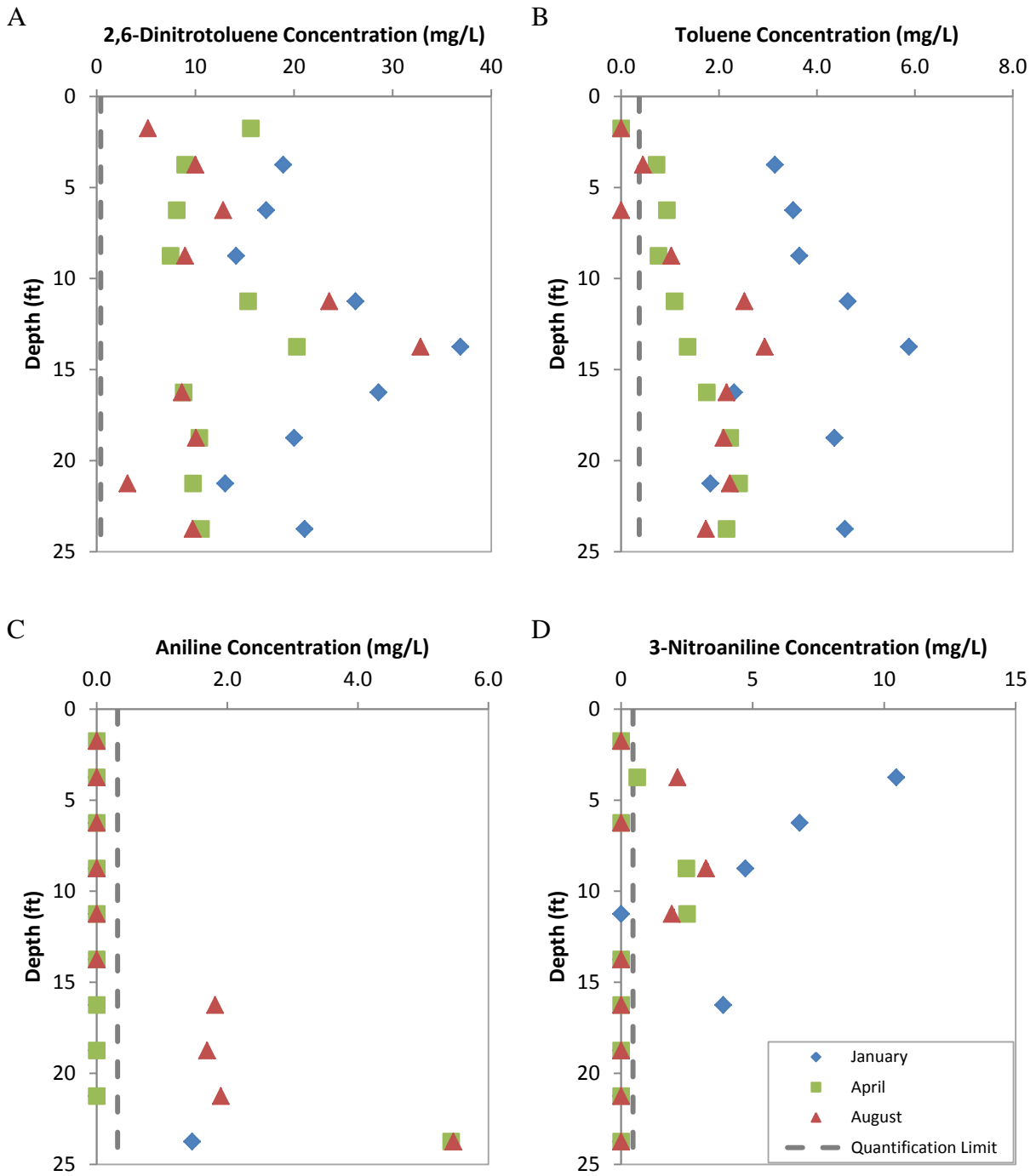


Figure 39 –Aqueous concentrations of A) 2,6-dinitrotoluene B) toluene C) aniline D) 3-nitroaniline

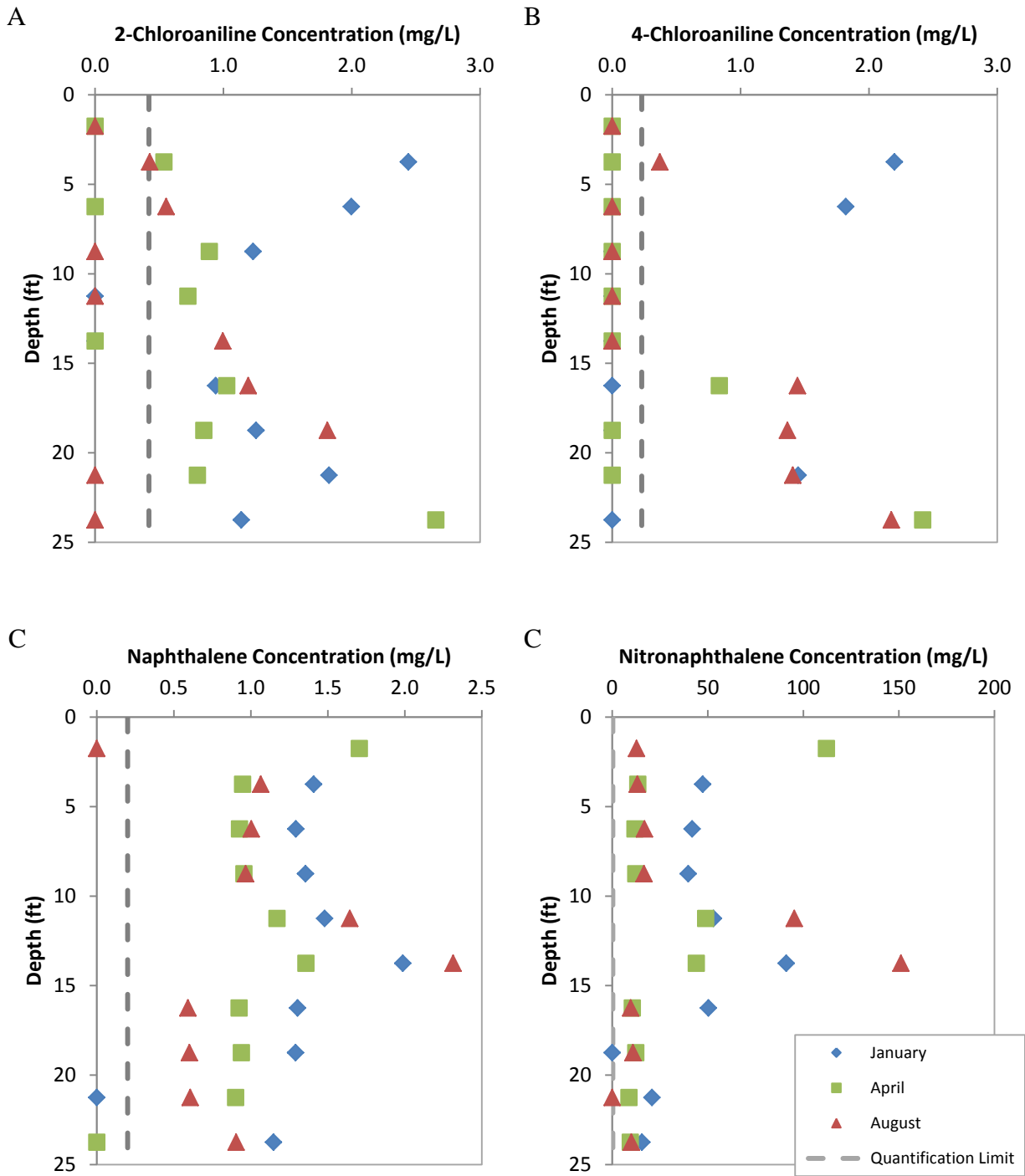
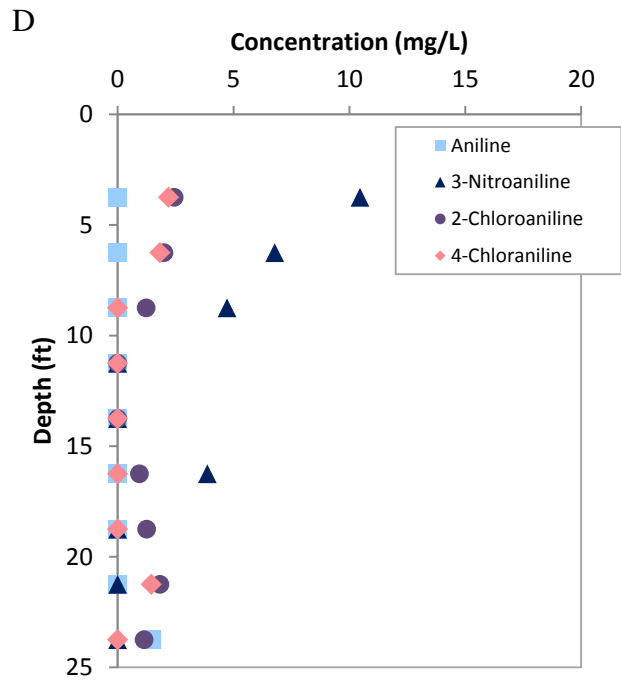
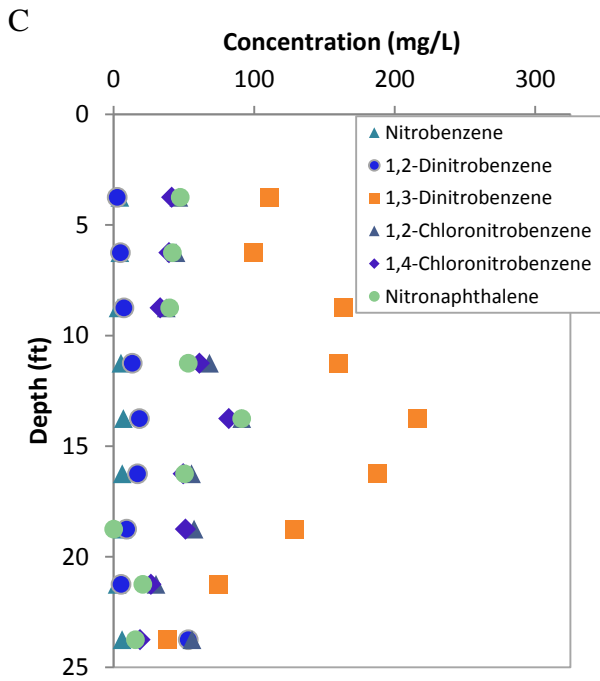
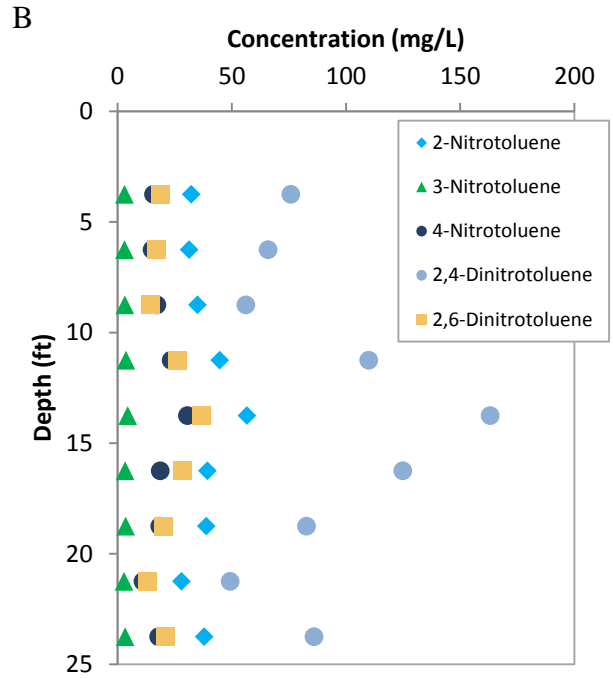
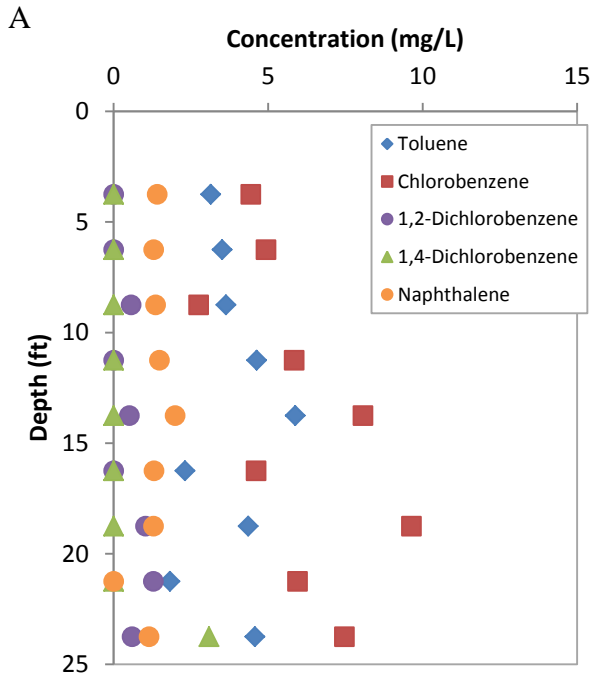
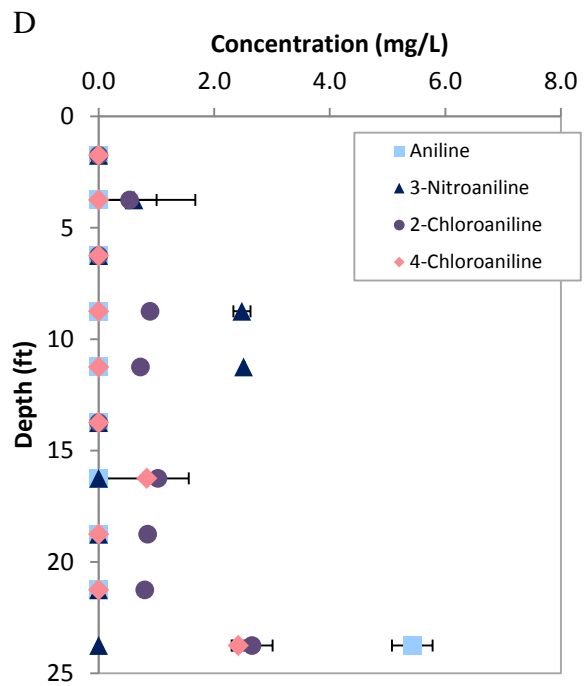
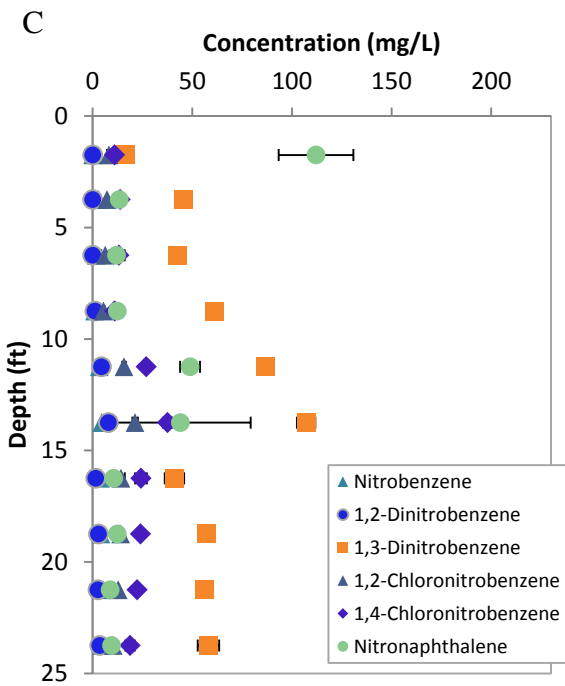
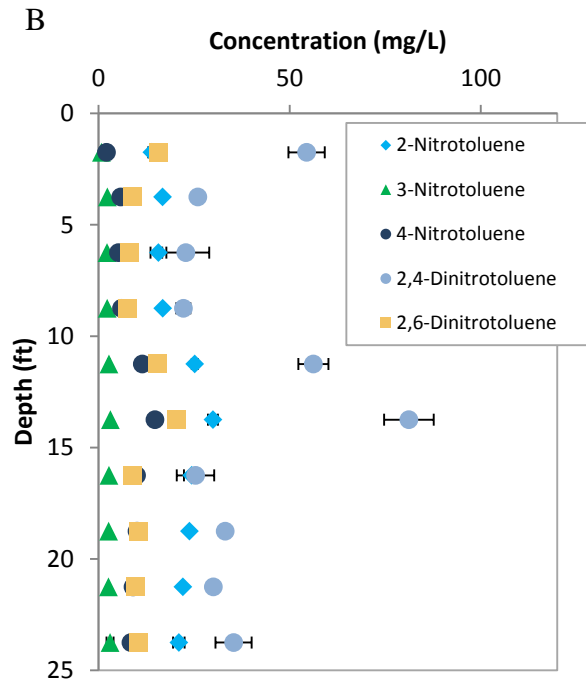
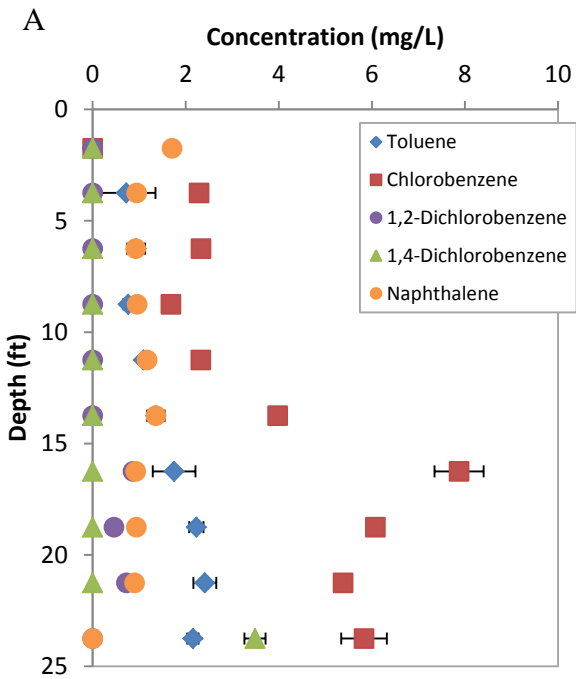


Figure 40 –Aqueous concentrations of A) 2-chloroaniline B) 4-chloroaniline C) naphthalene and D) nitronaphthalene





### B.3 Water Quality Analysis

Table 12- Water quality analysis of samples taken on January 15, 2014

Depth	pH (in situ)	pH(lab)	ORP	Conductivity	Hardness (as CaCO <sub>3</sub> )	Alkalinity (as CaCO <sub>3</sub> )	TDS
ft			mV (Ag-AgCl)	µmhos/cm	mg/L		
1.75							
3.75	9.76	6.4	30	9.9	152	57	411
6.25	8.89	7.3	190	15.83	139	126	474
8.75	8.55	7.3	175	5.16	167	62	410
11.25		8.3		5	223	224	674
13.75		7.2		4	209	223	829
16.25		6.8		4.317	221	359	1160
18.75		6.7		5.366	343	172	885
21.25		6.5		7	327	114	779
23.75		5.6		7.198	276	109	692

Table 13- Cation concentrations in water samples taken on January 15, 2014

Depth	Ca <sup>2+</sup>	Mg <sup>2+</sup>	Na <sup>+</sup>	K <sup>+</sup>	Fe
(ft)	(mg/L)				
1.75					
3.75	54	4	62	10	0.150
6.25	50	4	73	16	0.054
8.75	58	5	59	5	<0.01
11.25	55	19	112	5	0.073
13.75	58	17	169	4	<0.01
16.25	96	19	218	4	<0.01
18.75	98	25	132	5	0.325
21.25	64	20	152	7	0.160
23.75	82	29	100	7	0.034

Table 14- Anion concentrations in water samples taken on January 14, 2014

Depth	CO <sub>3</sub> <sup>2-</sup>	HCO <sub>3</sub> <sup>3-</sup>	Cl <sup>-</sup>	SO <sub>4</sub> <sup>2-</sup>	NO <sub>3</sub> <sup>-</sup>	NO <sub>3</sub> -N
(ft)	(mg/L)					
1.75						
3.75	<0.1	70	66	142	2.09	0.47
6.25	<0.1	154	21	155	1.24	0.28
8.75	<0.1	76	69	137	0.45	0.10
11.25	<0.1	273	70	136	1.11	0.25
13.75	<0.1	272	120	185	2.75	0.62
16.25	<0.1	439	98	284	2.14	0.48
18.75	<0.1	210	105	306	2.13	0.48
21.25	<0.1	140	152	241	1.47	0.33
23.75	<0.1	134	225	115	0.71	0.16

Table 15- Water quality analysis of samples taken on April 8, 2014

Depth	pH(in situ)	pH(lab)	ORP	Conductivity	Hardness (as CaCO <sub>3</sub> )	Alkalinity (as CaCO <sub>3</sub> )	TDS
ft			mV (Ag-AgCl)	μohms/cm	mg/L		
1.75							
3.75	9.24	8.4	475	263	90	161	382
6.25	8.71	7.1	81	324	83	139	325
8.75	7.88	7.3	50.3	495	175	230	497
11.25		7.7		654	171	289	656
13.75		6.3		638	191	302	803
16.25		6		790	228	139	600
18.75	6.49	5.8	68	773	267	188	699
21.25		5.7		783	235	186	625
23.75	4.84	5.2	5.6	2320	478	159	1592

Table 16- Cation concentrations in water samples taken on April 8, 2014

Depth	Ca <sup>2+</sup>	Mg <sup>2+</sup>	Na <sup>+</sup>	K <sup>+</sup>	Fe
(ft)	(mg/L)				
1.75					
3.75	31.1	3.06	47.2	32.8	<0.01
6.25	27.4	3.48	41.4	21.8	<0.01
8.75	47.4	13.9	63.1	5.92	<0.01
11.25	46.6	13.3	112	5.55	<0.01
13.75	50.2	16.1	149	6.38	<0.01
16.25	57.1	20.8	82.6	5.6	9.03
18.75	69.1	22.9	93.3	6.73	0.19
21.25	52.8	25	83.8	6.67	<0.01
23.75	83.3	65.6	279	46.4	76

Table 17- Anion concentrations in water samples taken on April 8, 2014

Depth	CO <sub>3</sub> <sup>2-</sup>	HCO <sub>3</sub> <sup>3-</sup>	Cl <sup>-</sup>	SO <sub>4</sub> <sup>2-</sup>	NO <sub>3</sub> <sup>-</sup>	NO <sub>3</sub> -N
(ft)	(mg/L)					
1.75						
3.75	<0.1	196	2.2	66.7	2.22	0.5
6.25	<0.1	169	2.5	52.2	5.45	1.23
8.75	<0.1	280	5.1	81	0.31	0.07
11.25	<0.1	352	7.9	117	0.71	0.16
13.75	<0.1	368	9.4	198	4.34	0.98
16.25	<0.1	169	10.9	249	3.32	0.75
18.75	<0.1	229	11.3	263	2.4	0.55
21.25	<0.1	227	15.1	212	1.42	0.32
23.75	<0.1	194	71.8	849	1.86	0.42

Table 18- Water quality analysis of samples taken on August 6, 2014

Depth	pH(in situ)	pH(lab)	ORP	Conductivity	Hardness (as CaCO <sub>3</sub> )	Alkalinity (as CaCO <sub>3</sub> )	TDS
ft			mV (Ag- AgCl)	µmhos/cm	mg/L		
1.75	6.35	6.3		630	245	261	261
3.75	8.07	8.2	-178	536	290	298	298
6.25	7.15	7.5	-134.8	489	294	309	309
8.75	7.18	7.6	-164	718	311	383	383
11.25		7.3		831	366	616	616
13.75		5.9		1100	438	495	495
16.25		5.8		710	282	112	112
18.75	5.43	5.9	-136	737	318	130	130
21.25	5.29	5.8	-99.8	853	383	246	246
23.75	4.9	5.4	-91.6	2360	922	198	198

Table 19- Cation concentrations in water samples taken on August 6, 2014

Depth	Ca <sup>2+</sup>	Mg <sup>2+</sup>	Na <sup>+</sup>	K <sup>+</sup>	Fe
(ft)	(mg/L)				
1.75	58.5	24.1	66.1	70.9	<0.01
3.75	90.3	15.7	61.6	36.1	<0.01
6.25	87.6	18.4	55.2	22.6	<0.01
8.75	84.6	24.2	125	44.2	<0.01
11.25	104	25.8	266	9.31	<0.01
13.75	107	41.7	361	8.92	0.07
16.25	65	29.1	121	5.25	<0.01
18.75	73.8	33	127	5.6	0.01
21.25	80.2	44	157	34.8	<0.01
23.75	162	126	544	52.5	14.7

Table 20- Anion concentrations in water samples taken on August 6, 2014

Depth	CO <sub>3</sub> <sup>2-</sup>	HCO <sub>3</sub> <sup>3-</sup>	Cl <sup>-</sup>	SO <sub>4</sub> <sup>2-</sup>	NO <sub>3</sub> <sup>-</sup>	NO <sub>3</sub> -N
(ft)	(mg/L)					
1.75	<0.1	319	84	60	46	10.4
3.75	<0.1	363	50	82.5	20.7	4.67
6.25	<0.1	377	31.3	61.9	33.1	7.47
8.75	<0.1	467	97.9	109	5.79	1.31
11.25	<0.1	752	110	173	4.67	1.05
13.75	<0.1	604	138	520	4.26	0.96
16.25	<0.1	137	107	277	<0.01	<0.01
18.75	<0.1	159	116	295	<0.01	<0.01
21.25	<0.1	300	152	296	<0.01	<0.01
23.75	<0.1	242	464	1266	<0.01	<0.01

#### B.4 Average Monthly Temperature

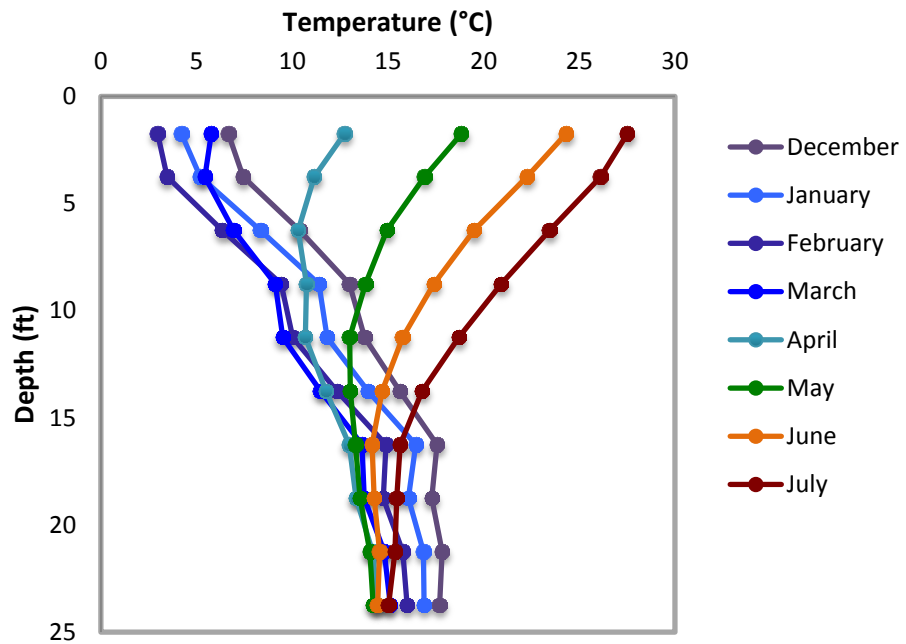


Figure 43 – Average monthly temperature with depth.

APPENDIX C: MICROCOSM STUDY SUPPLEMENTARY INFORMATION

**C.1 Microcosm Soil Analysis**

Table 21- Microcosm soil analysis

<b>Sample</b>	<b>NH<sub>4</sub></b>	<b>NH<sub>4</sub>-N</b>	<b>NO<sub>3</sub></b>	<b>NO<sub>3</sub>-N</b>	<b>Total S</b>	<b>SO<sub>4</sub>-S</b>	<b>SO<sub>4</sub></b>
	<b>mg/kg</b>						
Initial	11.7	9.0	7.5	1.7	774	543	1629
Final 10°C	5.0	2.2	8.9	2.0	569	422	1266
Final 14°C	33.3	14.6	8.4	1.9	454	391	1173
Final 18°C	28.0	12.3	7.1	1.6	539	363	1089
Final 22°C	27.4	12.0	7.1	1.6	492	371	1113
Final 26°C	32.6	14.3	8.9	2.0	588	357	1071
Final 30°C	31.2	13.7	8.9	2.0	573	411	1233

Table 22- Percent carbon and nitrogen of soil microcosm

<b>Sample</b>	<b>TOC</b>	<b>TIC</b>	<b>Total N</b>
	<b>%</b>		
Initial	2.41	0.01	0.4639
Final 10°C	2.47	0.01	0.5343
Final 14°C	2.35	0.01	0.4928
Final 18°C	2.42	0.01	0.4988
Final 22°C	2.44	0.01	0.5067
Final 26°C	2.42	0.03	0.5016
Final 30°C	2.28	0.01	0.4778

## C.2 Microcosm Concentrations

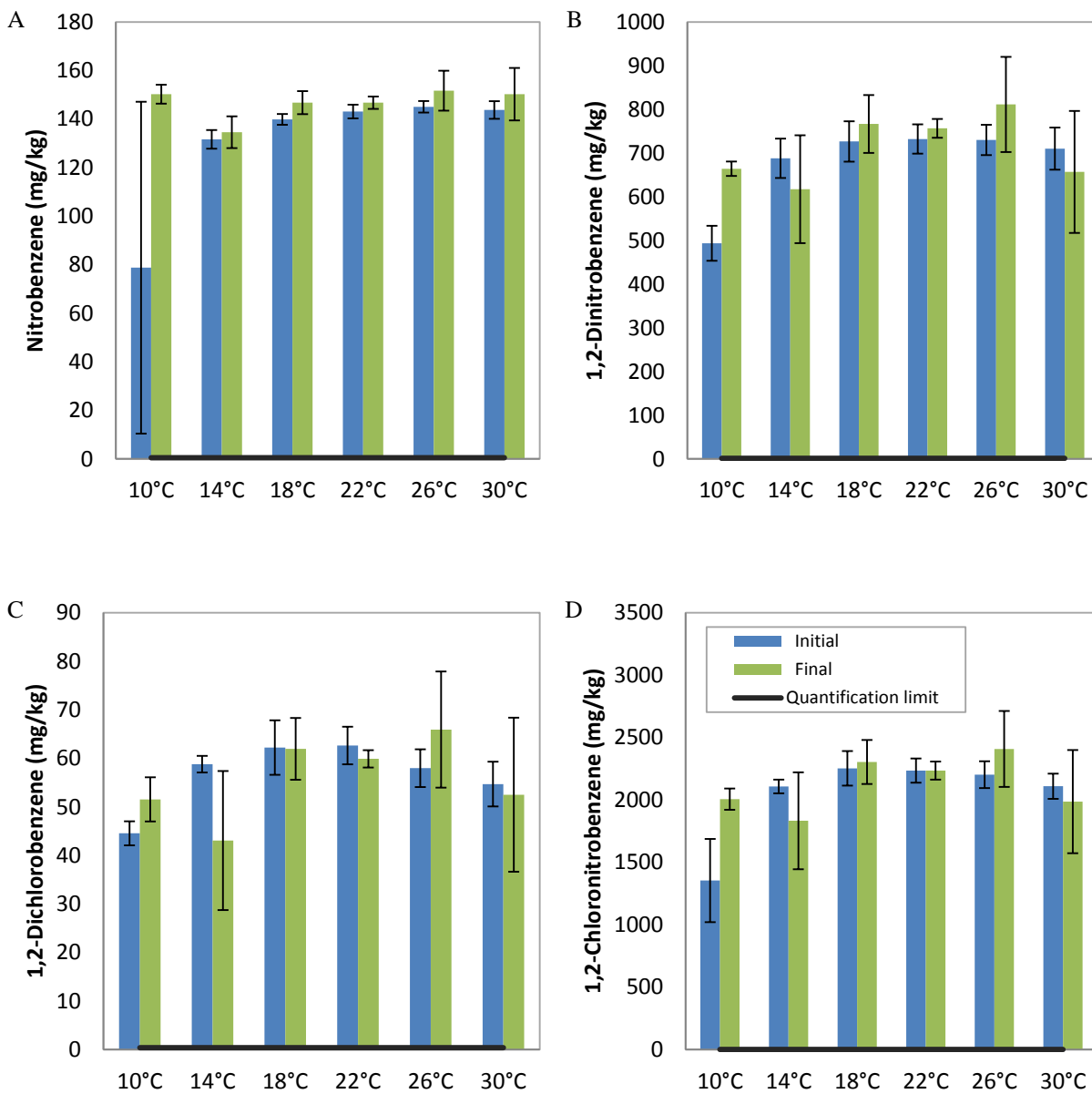


Figure 44 –Contaminant concentrations of nitrobenzene (A), 1,2-dinitrobenzene (B), 1,2-dichlorobenzene (C), and 1,2-chloronitrobenzene (D) before and after treatment. The blue bars represent initial concentration, and the green bars represent final concentration.

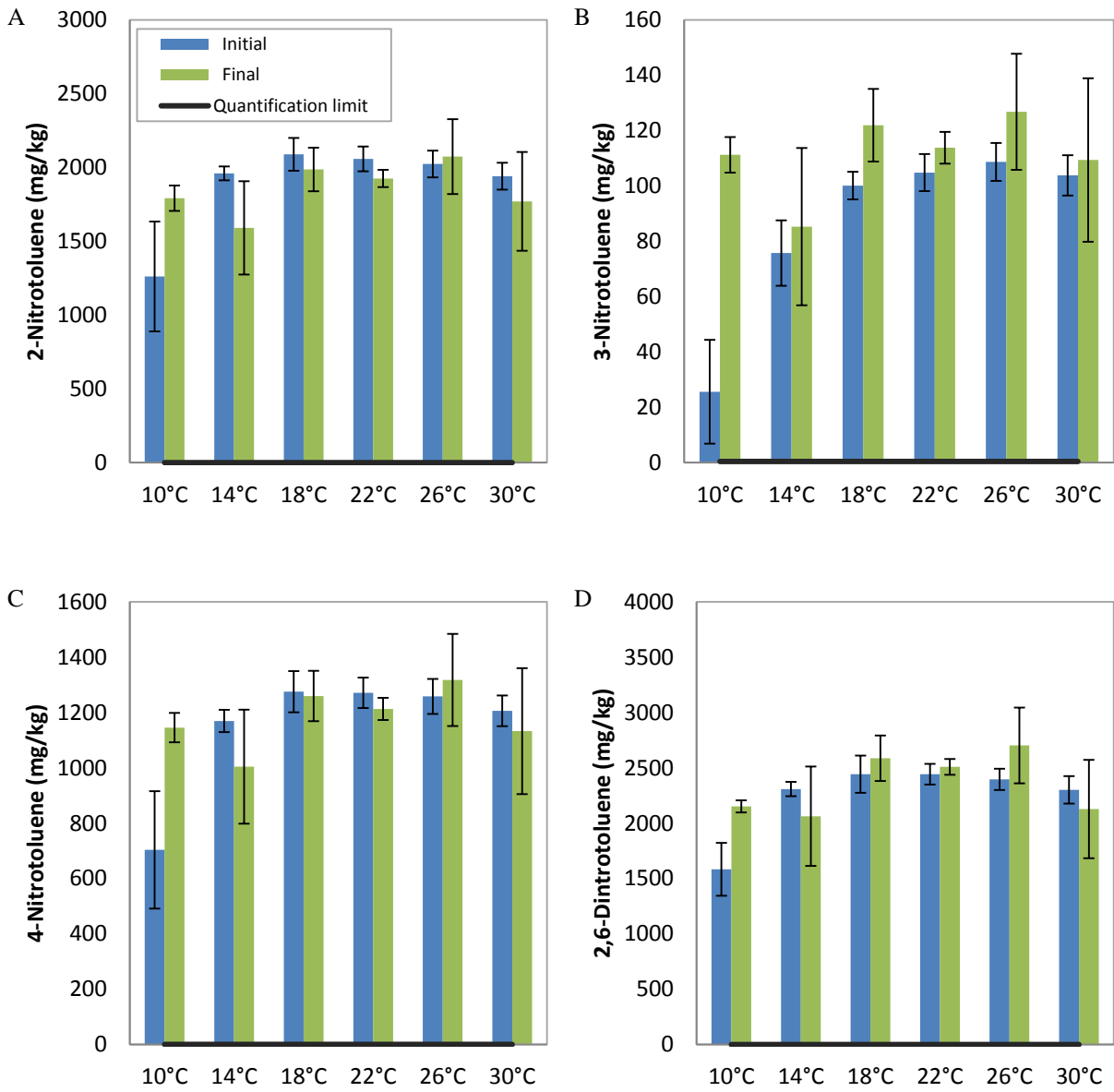


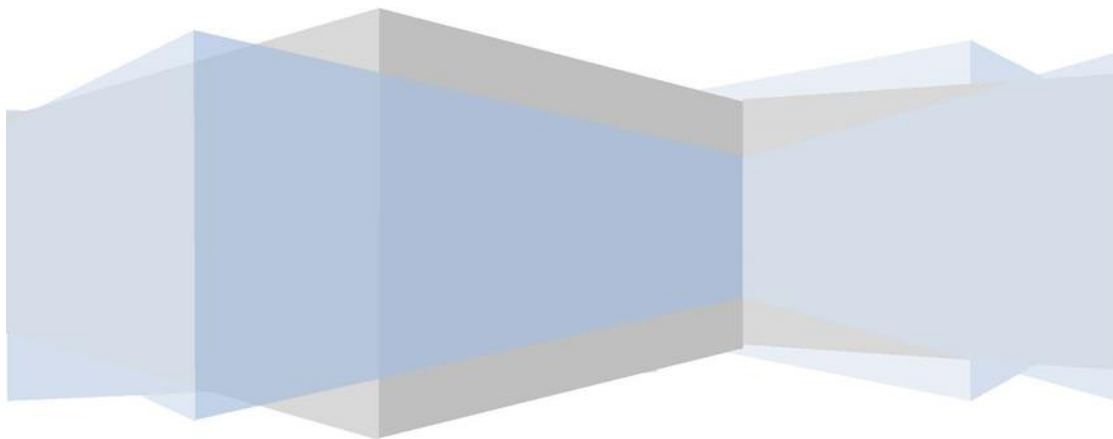
Figure 45 –Contaminant concentrations before and after treatment of 2-nitrotoluene (A), 3-nitrotoluene (B), 4-nitrotoluene (C), and 2,6-dinitrotoluene (D). The blue bars represent initial concentration, and the green bars represent final concentration.



## Data Analysis Methodology

Last Updated: 9/16/2014

The most recent version of this file can be downloaded from  
[http://www.researchandtesting.com/docs/Data\\_Analysis\\_Methodology.pdf](http://www.researchandtesting.com/docs/Data_Analysis_Methodology.pdf)





**Contents**

Version Changelog ..... 4

    Version 2.2.3 (09/16/2014)..... 4

    Version 2.2.2 (09/03/2014)..... 4

    Version 2.2.1 (08/29/2014)..... 4

    Version 2.2.0 (07/09/2014)..... 4

    Version 2.1.1 (05/20/2014)..... 4

    Version 2.1.0 (02/28/2014)..... 4

    Version 2.0.0 (01/28/2014)..... 4

Term Definitions ..... 5

Client Data Retention Policy ..... 5

Data Analysis Methodology ..... 6

    Visual Overview of the Data Analysis Process ..... 6

    Overview of the Data Analysis Process..... 6

    Denoising and Chimera Checking ..... 7

        Denoising ..... 7

        Chimera Checking ..... 9

Raw Sequence Data File Formats.....10

    SFF File Generation (454 Only).....10

    FASTQ File Generation .....10

Microbial Diversity Analysis .....12

    Quality Checking and FASTA Formatted Sequence/Quality File Generation.....12

    Sequence Clustering.....13

    Tree Building .....14

    Taxonomic Identification .....14

    Diversity Analysis .....15

Analysis description .....16



## Data Analysis Methodology

Zip Archives.....	19
Zip Archive Names .....	19
Split Zip Archives.....	19
Windows .....	19
Linux / Mac.....	20
References .....	21



## Version Changelog

### Version 2.2.3 (09/16/2014)

- Updated the data archive to split files too large to fit on our webserver.
- Included instructions for how to handle split zip archives.

### Version 2.2.2 (09/03/2014)

- Added the OTUs folder to the Analysis archive.
- Moved OTUmap.txt from Analysis/OTUMap.txt to Analysis/OTUs/OTUMap.txt
- Added OTUs.fas to the Analysis/OTUs archive.
- Corrected the otus.tre file. All ';' within sequence definitions have been changed to '\_ '.

### Version 2.2.1 (08/29/2014)

- Added the customer data retention policy.

### Version 2.2.0 (07/09/2014)

- Added phylogenetic tree construction using MUSCLE and FastTree.
- Added Krona visualization to the Taxonomic Analysis pipeline.
- Added phylogenetic tree, multiple sequence alignment, and Krona visualizations to the analysis zip archive.
- Updated 454 and Ion Torrent PGM processing to run using the same workflow as MiSeq.
- Added description for the OTUMap.txt file in the Analysis Folder.

### Version 2.1.1 (05/20/2014)

- Updated OTU Selection. Trimming to shortest sequence now performed before UPARSE OTU Selection.

### Version 2.1.0 (02/28/2014)

- Updated denoiser to use PEAR for paired-end read merging in place of USEARCH.

### Version 2.0.0 (01/28/2014)

- Updated denoiser to use USEARCH 7, replacing USEARCH 5.
- Methodology now accounts for processing of 454, Ion Torrent PGM and Illumina MiSeq data.



## Term Definitions

Terms used within this guide are defined as follows:

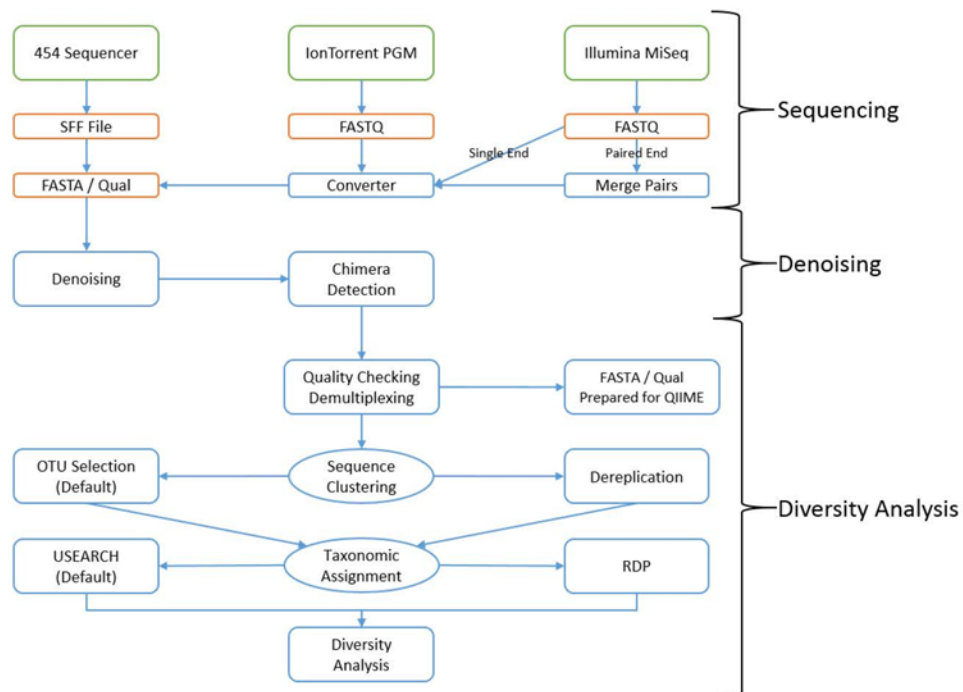
- Tag
  - The term tag refers to the 8-10 bp sequence at the 5' end of the sequence read.
  - The tag is also known as the barcode in some programs.
- ASCII value
  - ASCII (American Standard Code for Information Interchange) is a character encoding scheme based on the English alphabet to encode the following: the numbers 0-9, the letters a-z, the letters A-Z, basic punctuation, control codes (such as new line), and the blank space.
  - Each letter, number and punctuation mark on a keyboard is assigned a numeric value (mostly between 0 and 127) using the ASCII table in order to create a way of encoding/decoding character symbols into computer readable digital bit patterns.

## Client Data Retention Policy

Data will be made available for download (typically via a 12 month temporary link) upon completion of your project. RTL will make every reasonable effort to store all electronic data for your project for a period of 24 months from the date of notification that the project has been completed. If you have any questions regarding your data or if you need to discuss longer term storage, please contact us.

## Data Analysis Methodology

### Visual Overview of the Data Analysis Process



### Overview of the Data Analysis Process

Once sequencing of your data has completed, the data analysis pipeline will begin processing the data. The data analysis pipeline consists of two major stages, the denoising and chimera detection stage and the microbial diversity analysis stage. During the denoising and chimera detection stage, denoising is performed using various techniques to remove short sequences, singleton sequences, and noisy reads. With the bad reads removed, chimera detection is performed to aid in the removal of chimeric sequences. Lastly, remaining sequences are then corrected base by base to help remove noise from within each sequence. During the diversity analysis stage, each sample is run through our analysis

pipeline to determine the taxonomic information for each constituent read and then this information is collected for each sample. This stage is performed for all customers whose data is sequenced using primers targeting the 16S, 18S, 23S, ITS or SSU regions. Analysis can be performed on other regions but may require additional charges.

The data analysis pipeline is broken down into the following steps, each of which is discussed more thoroughly in the sections below:

- Denoising and Chimera Checking
  1. Denoising
  2. Chimera Checking
  3. SFF File Generation (454 only) – FASTQ File Generation (Ion Torrent & Illumina)
  
- Microbial Diversity Analysis
  1. Quality Checking and FASTA Formatted Sequence/Quality File Generation
  2. Sequence Clustering
  3. Taxonomic Identification
  4. Data Analysis

## Denoising and Chimera Checking

### Denoising

The process of denoising is used to correct errors in reads from next-generation sequencing technologies. According to the paper “Accuracy and quality of massively parallel DNA pyrosequencing” by Susan Huse, et al. and “Removing noise from pyrosequenced amplicons” by Christopher Quince, et al. the per base error rates from 454 pyrosequencing attain an accuracy rate of 99.5% [1] [2]. The paper “A tale of three next generation sequencing platforms: comparison of Ion Torrent, Pacific Biosciences and Illumina MiSeq sequencers” by Michael Quail, et al. states that the observed error rates generated by the Illumina MiSeq is less than .4% while the Ion Torrent PGM has an error rate of 1.78% [3]. Due to the large number of reads and even higher number of base calls per sequencing run, the total number of noisy reads can be quite substantial. In order to determine true diversity it becomes critical to determine which reads are good and which reads contain noise introduced by the experimental procedure. The Research and Testing Laboratory analysis pipeline attempts to correct this issue by denoising entire regions of data prior to performing any other steps of the pipeline.

The Research and Testing Laboratory analysis pipeline performs denoising by performing the following steps on each region:

1. The forward and reverse reads are taken in FASTQ format and are merged together using the PEAR Illumina paired-end read merger [4]. (Illumina MiSeq Paired End Sequencing Only)
2. The FASTQ (Illumina MiSeq and Ion Torrent PGM Only) and SFF (454 Only) formatted files are converted into FASTA formatted sequence and quality files.
3. Reads are run through an internally developed quality trimming algorithm. During this stage each read has a running average taken across the sequence and is trimmed back at the last base where the total average is greater than 25.
4. Sequence reads are then sorted by length from longest to shortest.
5. Prefix dereplication is performed using the USEARCH [5] algorithm. Prefix dereplication groups reads into clusters such that each sequence of equal or shorter length to the centroid sequence must be a 100% match to the centroid sequence for the length of the sequence. Each cluster is marked with the total number of member sequences. Sequences < 100bp in length are not written to the output file, however no minimum cluster size restriction is applied which will allow singleton clusters to exist in the output.
6. Clustering at a 4% divergence (454 & Illumina) or 6% divergence (IonTorrent) is performed using the USEARCH [5] clustering algorithm. The result of this stage is the consensus sequence from each new cluster, with each tagged to show their total number of member sequences (dereplicated + clustered). Clusters that contain <2 members (singleton clusters) are not added to the output file, thus removing them from the data set.
7. OTU Selection is performed using the UPARSE OTU selection algorithm [6] to classify the large number of clusters into OTUs.
8. Chimera checking, which is explained in more detail below in the section entitled “Chimera Checking”, is performed on the selected OTUs using the UCHIME chimera detection software executed in *de novo* mode [7].
9. Each clustered centroid from step 6 listed above is then mapped to their corresponding OTUs and then marked as either Chimeric or Non-Chimeric. All Chimeric sequences are then removed.
10. Each read from step 3 is then mapped to their corresponding nonchimeric cluster using the USEARCH global alignment algorithm [5].
11. Using the consensus sequence for each centroid as a guide, each sequence in a cluster is then aligned to the consensus sequence and each base is then corrected using the following rules where C is the consensus sequence and S if the aligned sequence:
  - a. If the current base pair in S is marked to be deleted, then the base is removed from the sequence if the quality score for that base is less than 30.

- b. If the current position in S is marked to have a base from C inserted, then the base is inserted into the sequence if the mean quality score from all sequences that mark the base as existing is greater than 30.
  - c. If the current position in S is marked as a match to C but the bases are different, then the base in S is changed if the quality score for that base is less than 30.
  - d. If a base was inserted or changed, the quality score for that position is updated. If the base was deleted the quality score for that position is removed.
  - e. Otherwise, leave the base in S alone and move to the next position.
12. The corrected sequences are then written to the output file.

### Chimera Checking

As discussed in the paper “Chimeric 16S rRNA sequence formation and detection in Sanger and 454-pyrosequenced PCR amplicons” by Brian Haas, et al. the formation of chimeric sequences occurs when an aborted sequence extension is misidentified as a primer and is extended upon incorrectly in subsequent PCR cycles [8]. This can be seen in Figure 1, shown below.

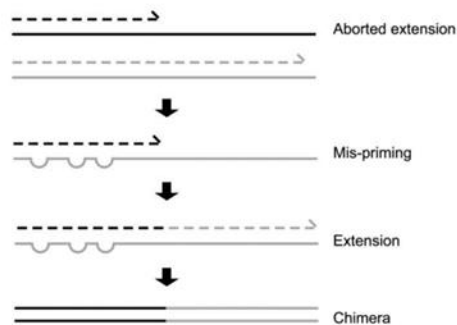


Figure 1.

Formation of chimeric sequences during PCR. An aborted extension product from an earlier cycle of PCR can function as a primer in a subsequent PCR cycle. If this aborted extension product anneals to and primes DNA synthesis from an improper template, a chimeric molecule is formed. Figure and description taken directly from “Chimeric 16S rRNA sequence formation and detection in Sanger and 454-pyrosequenced PCR amplicons” by Brian Haas, et al. [8].

Because amplification produces chimeric sequences that stem from the combination of two or more original sequences [7], we will perform chimera detection using the *de novo* method built into UCHIME.

The Research and Testing Laboratory analysis pipeline performs chimera detection and removal by executing UCHIME [7] in *de novo* mode on the clustered data that was output by our denoising methods. By using this method we can determine chimeras across entire region of data even after accounting for noise and removing low quality sequences.

## Raw Sequence Data File Formats

### SFF File Generation (454 Only)

A sff file is a binary file containing detailed information regarding each read in a single file. For each read, the sff contains a flowgram, quality score and sequence with defined lengths from QC measures performed by the machine. The sff represents the raw data and includes many reads that may have been excluded due to length or chimera detection or any other filter requested for custom processing. Since the files are binary, they cannot be opened with standard text editors. Special programs like Mothur [9] or BioPython [10] are able to load their data into human readable formats and output fasta, qual, flowgram or text (sff.txt) versions. Sff files or their derivatives can then be used for further processing of the data. Sff files provided may be of two forms. In the case of an entire region containing a single investigator's samples, the entire region plus mapping file is provided. In cases where multiple investigators had samples on a single region, each sample is demultiplexed from the sff file using the Roche sffinfo tool by providing its barcode, effectively eliminating it from any read extracted. The split sff can then be used for raw data or submitted directly to archives like the NCBI's SRA. In cases where a single sff for all samples is desired but an entire quadrant is not used, an investigator may request a single sff for a nominal charge. Alternatively, it is possible to use the provided split sff files for denoising/chimera removal by modifying the mapping files. Additional instructions are available if you wish to do so.

### FASTQ File Generation

FASTQ files are text based formatted data files that store the nucleotide sequences generated by the sequencer and their corresponding quality scores encoded as ASCII characters. A FASTQ file contains 4 lines per read that contain the following information:

- Line 1 contains the sequence ID (read definition) and is prepended with an at symbol, '@'.
- Line 2 contains the sequence data.
- Line 3 acts as a separator line between the sequence data and the quality score, it contains a single plus sign, '+'.
- Line 4 encodes the quality values for the sequence in line 2 with each quality score being represented by a single character. As such Line 2 and Line 4 must be the same length.

Decoding of the quality scores requires you to know the phred score offset that was used when the file was generated. Once you know the offset, you can take the ASCII value for the given character and subtract the offset value to obtain the quality score. For example, if the phred offset is +33 and the character 'B' is encountered, then the quality score for that position would be 33 as 'B' is represented by

the ASCII value 66 and the offset is 33 ( $66 - 33 = 33$ ). Using the same logic, 'A' (represented by the value 65) would be  $65 - 33 = 32$  meaning the 'A' character represents a quality score of 32. A free to view ASCII table can be found here: <http://www.ascii-code.com/>.

### *Illumina MiSeq*

The Illumina MiSeq produces FASTQ files with a phred offset of +33. While the FASTQ file(s) generated by a MiSeq do contain all of the raw sequence data generated by the sequencer, they **do not** contain any information regarding the primer (forward or reverse). Unlike other next generation sequencing technologies, the MiSeq does not sequence the primer, instead it begins sequencing at the first base pair following the forward or reverse primer. This can make processing of your data difficult if the post processing program you decide to use requires it be able to see the primer on the sequence, however most modern programs have removed this restriction due to the prevalence of Illumina data. FASTQ files generated by the Illumina MiSeq come in two forms depending on the sequencing – either paired end or single end. Single end reads are stored in a single FASTQ file with each read in the file representing a read from the sequencer. Paired end reads, however, are slightly more complex and are covered in following section. Reads from the Illumina MiSeq are stored per sequence and are demultiplexed by the Illumina Software, thus your raw data will be missing all barcode information.

### Paired End FASTQ Files

Paired end reads are stored in two FASTQ files with the first file storing the forward “half” of the read and the second file which stores the reverse “half” of the read. It should be noted that both reads are provided in forward order, meaning if you wish to link the two reads together you will first need to take the reverse complement of the reads in the second file. Depending on the insertion size and sequencing read length, the forward and reverse reads may or may not overlap at some point. Unlike other FASTQ files, the order of reads within these files must be kept in a specific order to avoid issues with most post processing programs. The reads within these two files must stay the same between the two files, meaning if you remove or move a sequence in one file, you must remove it or move it to same place in the other file to preserve the same order in both files.

Because the insert size for a paired end sequence matters, we provide two examples of how your sequences may, or may not, line up. In both examples it is assumed that you have already taken the reverse complement of the reverse reads.

**Example 1** – Insert Size approx. 500bp using a 2x300 kit.



**Example 2** – Insert Size approx. 800bp using a 2x300 kit.



#### *IonTorrent PGM*

The IonTorrent PGM produces FASTQ files with a phred offset of +33. FASTQ files generated by the IonTorrent contain all of the raw reads stored in a single FASTQ file with barcode information available for demultiplexing. FASTQ files you receive from us from an IonTorrent will be merged into as few files as possible given the number of barcodes available if your samples were run on multiple IonTorrent chips.

#### Microbial Diversity Analysis

In order to determine the identity of each remaining sequence, the sequences must first be quality checked and demultiplexed using the denoised data generated previously. These sequences are then clustered into OTUs using the UPARSE [6] algorithm. The centroid sequence from each cluster is then run against either the USEARCH global alignment algorithm or the RDP Classifier against a database of high quality sequences derived from the NCBI database. The output is then analyzed using an internally developed python program that assigns taxonomic information to each sequence and then computes and writes the final analysis files.

#### Quality Checking and FASTA Formatted Sequence/Quality File Generation

The denoised and chimera checked reads generated during sequencing are condensed into a single FASTA formatted file such that each read contains a one line descriptor and one to many lines of sequence/quality scores. The Research and Testing Laboratory analysis pipeline takes the FASTA formatted sequence and quality files and removes any sequence which fails to meet the following quality control requirements:

1. Sequences must be at least ½ the expected length given the primer sets used.
2. Sequences must contain a valid error free barcode.

Sequences that pass the quality control screening are condensed into a single FASTA formatted sequence and quality file such that each read has a one line descriptor followed by a single line of

sequence/quality data. The descriptor line in both files has been altered to contain the samples name followed by the original descriptor line, separated with a unique delimiter (::).

This stage of the pipeline creates the FASTA reads archive which contains the following files:

1. The sequence reads from all samples concatenated into a single sequence file. The original tags have been removed from each sequence and an “artificial tag” has been added in its place. The title of the file will be <name>\_<order ID>.fas.
2. The quality scores from all samples concatenated into a single quality file. The scores are labeled with the corresponding sample name and will have a matching line in the .fas file. Since the original tags were removed from the sequence and an “artificial tag” was put into its place, the quality scores have been similarly altered such that the original scores for the tag have been removed and an “artificial quality tag” has been added in its place. The artificial quality tag consists of Q30s for the length of the tag. This file will be labeled <name>\_<order ID>.qual.
3. A mapping file consisting of sample names included in the analysis. This file contains the information for each sample such that each line has the sample name, tag and primer used for the sample. This file will be labeled as: <name>\_<order ID>.txt

### Sequence Clustering

OTU selection clusters sequences into clusters using either an OTU selection program or dereplication depending on the needs of the customer. By default, the OTU selection method is used to determine OTUs and uses the centroid sequence for each OTU to determine taxonomic information. However, if the customer requests that we use the dereplication method, then the clusters will instead represent 100% identity clusters and taxonomic information will be assigned to each of these cluster’s centroid sequence instead.

#### *OTU Selection (Default)*

OTU selection is performed using the guidelines discussed in the paper “UPARSE: Highly accurate OTU sequences from microbial amplicon reads” by Robert Edgar [6]. In that paper, the following methodology is laid out in order to select OTUs:

1. Perform dereplication on the sequences.
2. Remove all singleton clusters from the data set and sort the data by abundance.
3. Trim all sequences to the same length.
4. Perform OTU clustering using UPARSE.

#### 5. Map original reads to the OTUs

Dereplication of sequences is performed using the USEARCH prefix dereplication method [5]. Once complete we removed all singleton clusters and sorted the remaining sequences by cluster size from largest to smallest. The sequences are then run through a trimming algorithm that trims each sequence down to the same size. It should be noted that the sequences are only trimmed for UPARSE and the final taxonomic analysis is based upon the full length sequences. Next we use the UPARSE algorithm to select OTUs [6]. Using the USEARCH global alignment algorithm [5] we then assign each of the original reads back to their OTUs and write the mapping data to an OTU map and OTU table file.

#### *Dereplication*

Some customers would prefer to not have their data go through UPARSE if they are interested in the taxonomic information of the singleton sequences. For these customers we have the pipeline replace the OTU selection stage with a dereplication step using the USEARCH prefix dereplication algorithm [5]. Once the dereplication is complete a dereplication mapping table and dereplication table (same format as the OTU table) are both created and the centroid sequences are written to a file for taxonomic assignment.

#### *Tree Building*

Once OTU selection has been performed, a phylogenetic tree in Newick format is constructed. In order to construct the phylogenetic tree, multiple sequence alignment must be done on the OTU sequences in order to generate equal length aligned sequences. The multiple sequence aligner MUSCLE [11] [12], developed by Robert Edgar, is used with a maximum of 2 iterations in order to perform the alignment of the OTU data. The finished multiple sequence alignment is then passed into FastTree [13] [14], developed by Morgan Price at the Lawrence Berkeley National Lab, a program used to infer approximately-maximum-likelihood phylogenetic trees from aligned sequence data. If you would like to learn more about how FastTree works, please visit the following link:

<http://www.microbesonline.org/fasttree/#How>.

#### *Taxonomic Identification*

In order to determine the taxonomic information for each remaining sequence, the sequences must be run through either the USEARCH global alignment program or the RDP classifier. By default the USEARCH based method is employed however the RDP classifier can be substituted if a customer has requested that we use the RDP classifier instead. In either case the data is identified using a database of



high quality sequences derived from NCBI that is maintained in house. If a customer would prefer we classify their data using a different database such as GreenGenes then we can substitute that database in place of our own. If a non-standard database is requested that requires Research and Testing Laboratory to spend time converting or creating, then a small fee may be charged.

### *USEARCH Global Search (Default)*

The global search method uses a mixture of the USEARCH global search algorithm along with a python program to then determine the actual taxonomic assignment that is assigned to each read. This method is described in the paper "An extensible framework for optimizing classification enhances short-amplicon taxonomic assignments" by Nicholas Bokulich, et al. [15]. The paper describes a methodology in which a high quality database is used in pair with USEARCH rapidly find the top 6 matches in the database for a given sequence. From these 6 sequences you then assign a confidence value to each taxonomic level (kingdom, phylum, class, order, family, genus and species) by taking the number of taxonomic matches that agree with the top match and then divide by the number of total matches, e.g. Bacteria is the top kingdom match and 5 hits state Bacteria and 1 hit shows another kingdom, this would assign a confidence of  $5/6 = .83$ . Once confidence values are assigned for each sequence an RDP formatted output file is generated to be used by our final analysis program.

### *RDP Classifier*

The RDP Classifier is naïve Bayesian classifier than can rapidly determine taxonomic information for sequences while automatically determining the confidence it has at each taxonomic level [16]. The RDP classifier is run against an internally maintained database or a customer requested database along with a taxonomic file to help determine confidence values by giving the classifier a taxonomic tree.

### *Diversity Analysis*

Regardless of the classifier that was used, the data next enters the diversity analysis program. This program takes the OTU/Derep table output from sequence clustering along with the output generated during taxonomic identification and begins the process of generating a new OTU table with the taxonomic information tied to each cluster. This updated OTU table is then written to the output analysis folder with both the trimmed and full taxonomic information for each cluster. For each taxonomic level (kingdom, phylum, class, order, family, genus and species) four files are generated which contain the number of sequences per full taxonomic match per sample, the percentage per full taxonomic match per sample, the number of sequences per trimmed taxonomic match per sample and the percentage per trimmed taxonomic match per sample. These files are all described in more detail below.

## Analysis description

The analysis archive you receive with your data will contain the following files:

- For each taxonomic level (<level>) where level is Kingdom, Phylum, Class, Order, Genus or Species.
  - FullTaxa.<level>.counts.txt
    - This file contains a table with the columns representing each sample in your order and the rows representing each unique taxonomic information for the top hit listed down to <level>, e.g. if <level> is Phylum then it will give each unique Kingdom/Phylum combination.
    - Each row/column intersection defines the number of sequences in the sample that matched that particular unique taxonomic information.
    - Keep in mind that the Full Taxa data shows only the taxonomic information for the top hit, regardless of what the confidence values were.
  - FullTaxa.<level>.percent.txt
    - This file contains a table with the columns representing each sample in your order and the rows representing each unique taxonomic information for the top hit listed down to <level>, e.g. if <level> is Phylum then it will give each unique Kingdom/Phylum combination.
    - Each row/column intersection defines the percent of sequences in the sample that matched that particular unique taxonomic information.
    - Keep in mind that the Full Taxa data shows only the taxonomic information for the top hit, regardless of what the confidence values were.
  - TrimmedTaxa.<level>.counts.txt
    - This file contains a table with the columns representing each sample in your order and the rows representing each unique taxonomic information for the top hit listed down to <level>, e.g. if <level> is Phylum then it will give each unique Kingdom/Phylum combination.
    - Each row/column intersection defines the number of sequences in the sample that matched that particular unique taxonomic information.
    - Keep in mind that the Trimmed Taxa data shows the taxonomic information after the confidence values are taken into account. The USEARCH method rejects the taxonomic information at a level if the confidence is below 51% while the RDPClassifier uses a minimum confidence of 80%.
  - TrimmedTaxa.<level>.percent.txt
    - This file contains a table with the columns representing each sample in your order and the rows representing each unique taxonomic information for the top

- hit listed down to <level>, e.g. if <level> is Phylum then it will give each unique Kingdom/Phylum combination.
    - Each row/column intersection defines the percent of sequences in the sample that matched that particular unique taxonomic information.
    - Keep in mind that the Trimmed Taxa data shows the taxonomic information after the confidence values are taken into account. The USEARCH method rejects the taxonomic information at a level if the confidence is below 51% while the RDPClassifier uses a minimum confidence of 80%.
- OTU/Derep tables
  - FullTaxa.otu\_table.txt
    - This file contains a table with the columns representing each sample in your order and the rows representing each unique OTU or Dereplication Cluster. The final column contains the taxonomic information for that particular OTU/Cluster listed down to the Species level.
    - Keep in mind that the Full Taxa data shows only the taxonomic information for the top hit, regardless of what the confidence values were.
  - TrimmedTaxa.otu\_table.txt
    - This file contains a table with the columns representing each sample in your order and the rows representing each unique OTU or Dereplication Cluster. The final column contains the taxonomic information for that particular OTU/Cluster listed down to the Species level.
    - Keep in mind that the Trimmed Taxa data shows the taxonomic information after the confidence values are taken into account. The USEARCH method rejects the taxonomic information at a level if the confidence is below 51% while the RDPClassifier uses a minimum confidence of 80%.
- Krona Folder
  - Raw Data Folder
    - This folder contains the raw data files that were passed to Krona in order to generate the FullTaxa and TrimmedTaxa Krona HTML files. These files were derived directly from the FullTaxa.species.counts.txt and TrimmedTaxa.species.counts.txt files described above. These files are provided for transparency purposes regarding how your visualization data was created.
  - FullTaxa.krona.html
    - This file contains the Krona visualization of the FullTaxa.species.count.txt file discussed above. The visualization file is a standard HTML file and should be accessible using any web browser. This visualization was generated using the FullTaxa.species.counts.txt file described before and contains data on all



- This file contains the phylogenetic tree in Newick tree format created using the otus.msa file described above. This file was generated using FastTree as described in the section titled Tree Building on page 14.

While each file is listed a .txt file, the files are actually tab separated variable files (tsv) and can be opened using any text editor (we suggest using Notepad++ for large file manipulation - <http://notepad-plus-plus.org>) or any spreadsheet editor such as Excel or OpenOffice Calc. Each file can be dragged and dropped into Excel or you may choose to right click on the file name, select “Open With” and choose Excel as the program. Each file contains information about all the samples. Sample names span the first row with the taxonomic designations at each respective taxonomic level listed in the first column.

## Zip Archives

### Zip Archive Names

The following archives will be passed along to you upon completion of your order:

- <Name>\_<OrderNumber>Raw<SequencingDate>.zip
  - This archive will contain the raw FASTQ (Illumina MiSeq) or raw SFF (Roche 454 and IonTorrent PGM).
- <Name>\_<OrderNumber>Fasta<SequencingDate>.zip
  - This archive will contain the denoised sequence data for your entire order in FASTA/Qual format.
- <Name>\_<OrderNumber>Analysis<SequencingDate>.zip
  - This archive contains the data described in the “Analysis description” section found on page 16.
  - This archive will only be sent if you used a standard primer set that we have a working database for. Custom assays will likely not be analyzed.

### Split Zip Archives

If any zip archive is larger than 10GB in size, we will be unable to upload the file to our file server without breaking the file into smaller chunks. In order for you to open these files you will need to download each file in the archives set (denoted with <ArchiveName>.zip.XXX where XXX is a number starting at 001 and counting upwards) and then stitch them back together prior to unzipping the archive. The following commands can be used to rebuild the zip file prior to unzipping.

### Windows

Stitching the files together in Windows requires you to do the following:



- Open a command/DOS prompt
  - In most versions of windows go to “Start menu” then type in cmd and run cmd.exe.
- Navigate to the folder you downloaded the files into.
- Type in the following: `copy /B ArchiveName.zip.* ArchiveName.zip`
- Unzip the ArchiveName.zip file as you normally would.

#### Linux / Mac

Stitching the files together in Linux or Mac requires you to do the following:

- Open a command terminal.
- Navigate to the folder you downloaded the files into.
- Type in the following: `cat ArchiveName.zip.* > ArchiveName.zip`
- Unzip the ArchiveName.zip file as you normally would.

## References

- [1] S. M. Huse, J. A. Huber, H. G. Morrison, M. L. Sogin and D. M. Welch, "Accuracy and quality of massively parallel DNA pyrosequencing.," *Genome Biology*, vol. 8, no. 7, 2007.
- [2] C. Quince, A. Lanzen, R. J. Davenport and P. J. Turnbaugh, "Removing Noise From Pyrosequenced Amplicons," *BMC Bioinformatics*, vol. 12, no. 38, 2011.
- [3] M. A. Quail, M. Smith, P. Coupland, T. D. Otto, S. R. Harris, T. R. Connor, A. Bertoni, H. P. Swerdlow and Y. Gu, "A tale of three next generation sequencing platforms: comparison of Ion Torrent, Pacific Biosciences and Illumina MiSeq sequencers," *BMC Genomics*, 2012.
- [4] J. Zhang, K. Kobert, T. Flouri and A. Stamatakis, "PEAR: A fast and accurate Illumina Paired-End reAd mergeR," *Bioinformatics*, 2013.
- [5] R. C. Edgar, "Search and clustering orders of magnitude faster than BLAST," *Bioinformatics*, pp. 1-3, 12 August 2010.
- [6] R. C. Edgar, "UPARSE: highly accurate OTU sequences from microbial amplicon reads," *Nature Methods*, vol. 10, pp. 996-998, 2013.
- [7] R. C. Edgar, B. J. Haas, J. C. Clemente, C. Quince and R. Knight, "UCHIME improves sensitivity and speed of chimera detection," *Oxford Journal of Bioinformatics*, vol. 27, no. 16, pp. 2194-2200, 2011.
- [8] B. J. Haas, D. Gevers, A. M. Earl, M. Feldgarden, D. V. Ward, G. Giannoukos, D. Ciulla, D. Tabbaa, S. K. Highlander, E. Sodergren, B. Methé, T. Z. DeSantis, The Human Microbiome Consortium, J. F. Petrosino, R. Knight and B. W. Birren, "Chimeric 16S rRNA sequence formation and detection in Sanger and 454-pyrosequenced PCR amplicons," *Genome Research*, 2011.
- [9] P. Schloss, S. L. Westcott, T. Ryabin, J. R. Hall, M. Hartmann, E. B. Hollister, R. A. Lesniewski, B. B. Oakley, D. H. Parks, C. J. Robinson, J. W. Sahl, B. Stres, G. G. Thallinger, D. J. V. Horn and C. F. Weber, "Introducing mothur: Open-source, platform-independent, community-supported software for describing and comparing microbial communities," *Appl Environ Microbiol*, vol. 75, no. 23, pp. 7537-41, 2009.

- [10] P. J. A. Cock, T. Antao, J. T. Chang, B. A. Chapman, C. J. Cox, A. Dalke, I. Friedberg, T. Hamelryck, F. Kauff, B. Wilczynski and M. J. L. d. Hoon, "Biopython: freely available Python tools for computational molecular biology and bioinformatics," *Bioinformatics*, vol. 25, no. 11, 2009.
- [11] R. C. Edgar, "MUSCLE: multiple sequence alignment with high accuracy and high throughput," *Nucleic Acids Research*, vol. 32, no. 5, pp. 1792-1797, 2004.
- [12] R. C. Edgar, "MUSCLE: a multiple sequence alignment method with reduced time and space complexity," *BMC Bioinformatics*, 2004.
- [13] M. N. Price, P. S. Dehal and A. P. Arkin, "FastTree: computing large minimum evolution trees with profiles instead of a distance matrix.," *Molecular biology and evolution*, vol. 26, no. 7, pp. 1641-1650, 2009.
- [14] M. N. Price, P. S. Dehal and A. P. Arkin, "FastTree 2 – Approximately Maximum-Likelihood Trees for Large Alignments," *PLOS One*, 2010.
- [15] N. A. Bokulich, J. R. Rideout, K. Patnode, Z. Ellett, D. McDonald, B. Wolfe, C. F. Maurice, R. J. Dutton, P. J. Turnbaugh, R. Knight and J. G. Caporaso, "An extensible framework for optimizing classification enhances short-amplicon taxonomic assignments," *Not Yet Published*, 2014.
- [16] Q. Wang, G. M. Garrity, J. M. Tiedje and J. R. Cole, "Naive Bayesian classifier for rapid assignment of rRNA sequences into the new bacterial taxonomy.," *Applied and Environmental Microbiology*, vol. 73, no. 16, pp. 5261-5267, 2007.